Introduction to PLASMA PHYSICS

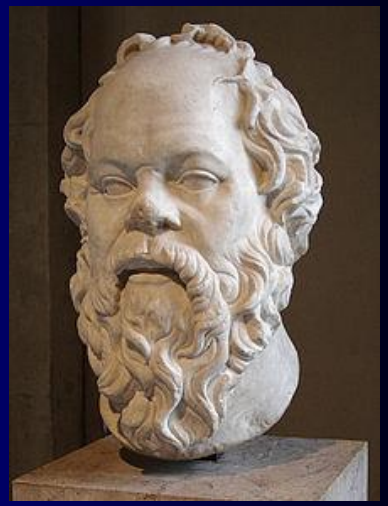

Scio me nihil scire

(„Vím, že nic nevím.“ I know that I know nothing)

Consistency of the universe

Socrates (470–399 BC)

Introduction to PLASMA PHYSICS

UFP 1A ZS 2024

Prof. J. Glosík
KFPP MFF UK

Burning Match Stick

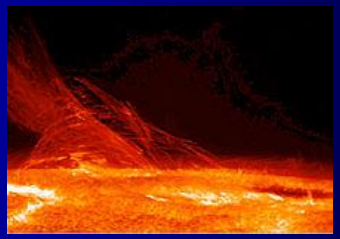

Sun

Andromeda composite

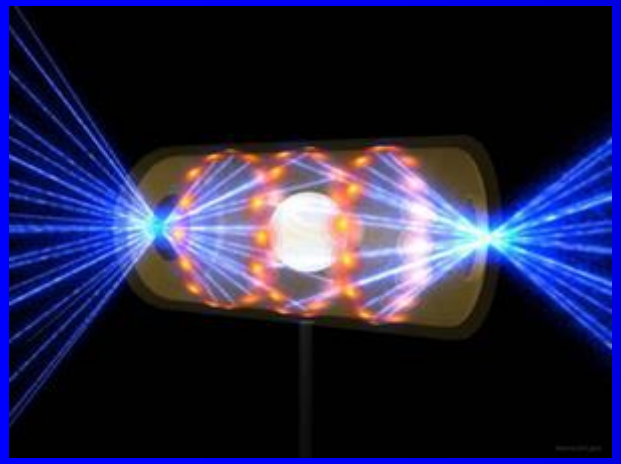

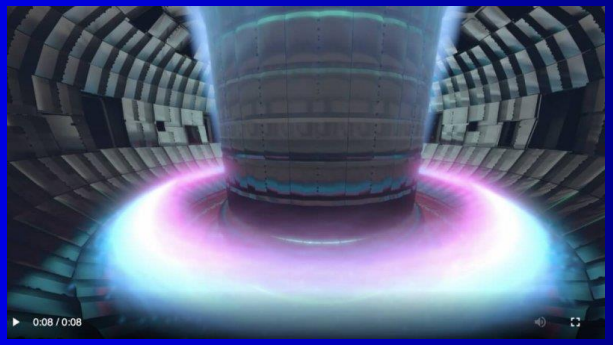

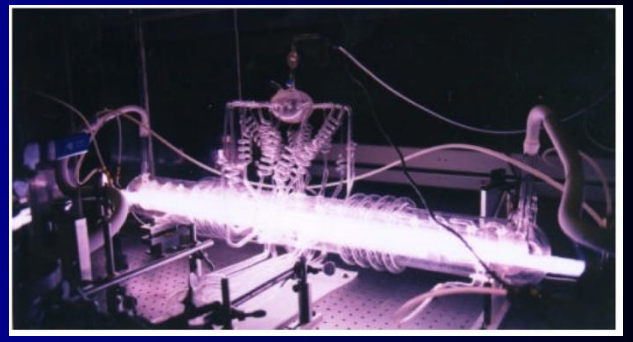

Fusion in a flash. At the National Ignition Facility (NIF) at Lawrence Livermore National Lab, 192 powerful lasers blast a BB-sized fuel pellet inside a metallic cylinder to generate nuclear fusion.

Ultra cold Plasma
Experiment: $T \sim 6$ mK

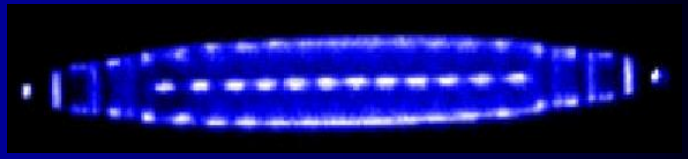

Plasma Parameters

Scio me nihil scire

Introduction to PLASMA PHYSICS

UFP 1A 2024

This presentation is only for students attending the lectures
INTRODUCTIO TO PLASMA PHYSICS at MFF UK,

Not for public use. Preliminary version without references.

Language – Czech, English, Slovak (česky, slovensky, anglicky) … in approximation … ?

Recommended literature :

Úvod do fyziky plazmatu
(Introduction to Plasma Physics) — E
Francis F. Chen
Academia Praha 1984 (Plenum press 1974)

Základy fyziky plazmy — Cz
Viktor Martišovič
Bratislava 2004
Učebný text pre 3. ročník magisterského štúdia

Fundamentals of plasma physics — E
J. A. Bittencourt
Springer,
Third Edition 2004

Physics of Ionized Gases — E
Boris M. Smirnov
John Wiley&Sons 2001

Základy klasické a kvantové fyziky plazmatu
„Velký Kracík“ — Cz
J.Kracík, B. Šesták a L. Aubrecht
Academia Praha 1974

Fyzika plazmatu
J.Kracík, J. Tobiáš — Cz
Academia, Praha 1966
„Malý Kracík“

ASTRONOMIE A FYZIKA NA PŘELOMU TISÍCILETÍ
Pod vedením Petra Kulhánka — Cz
Aldebaran Group for Astrophysics, 2004

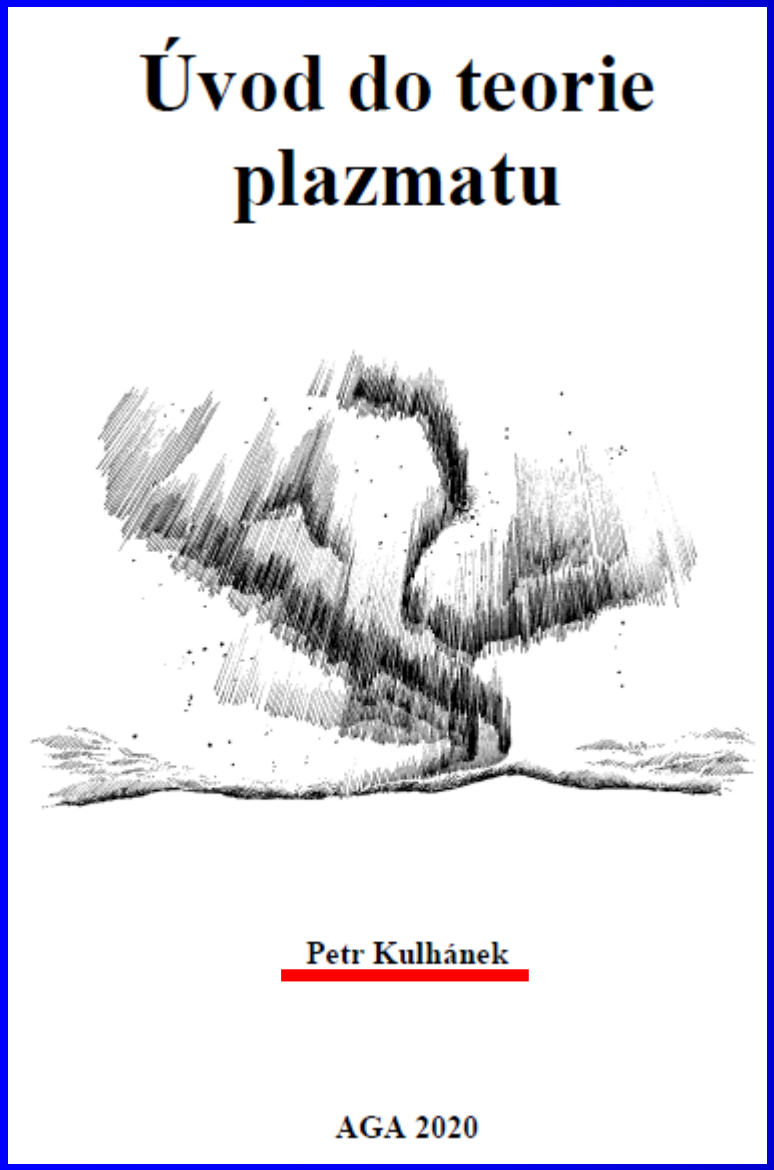

- V textu byly použity některé obrázky a text z knihy:

P. Kulhánek, Úvod do teorie plazmatu, AGA 2011, Praha.

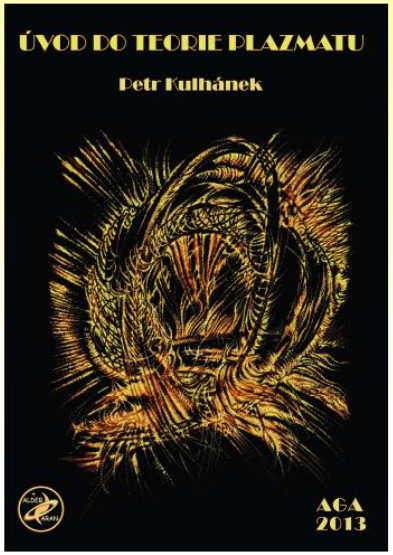

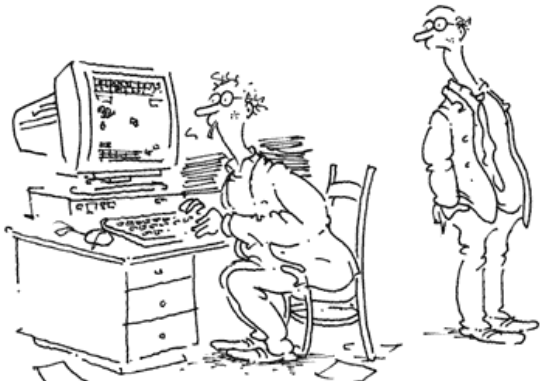

Information ….???

Scio me nihil scire

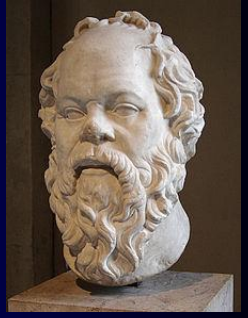

(I know that I know nothing)

1TB

THE EXPERTS SPEAK†

- "There is not the slightest indication that [nuclear] energy will ever be obtained" — *Albert Einstein, 1932*
- "Anyone who expects a source of power from the transformation of these atoms is talking moonshine." — *Ernest Rutherford, 1933*
- "A few decades hence, [when controlled fusion is achieved], energy will be free — just like the unmetered air." — *John von Neumann, 1956*
- "Radio has no future." — *Lord Kelvin, 1897*
- "I think there is a world market for about five computers." — *Thomas J. Watson, 1943*
- Where a calculator like ENIAC is equipped with 18,000 vacuum tubes and weighs 30 tons, computers in the future may have only 1,000 vacuum tubes and perhaps only weigh $1\frac{1}{2}$ tons." — *Popular Mechanics, March 1949*
- "640k ought to be enough for anybody." — *Bill Gates, 1981*

† C. Cerf and V. Navasky, Villard, New York, 1998

Socrates

Information ….

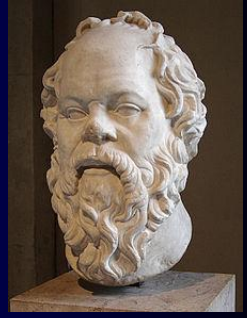

Scio me nihil scire

(„Vím, že nic nevím.“ I know that I know nothing)

THE EXPERTS SPEAK†

- “There is not the slightest indication that [nuclear] energy will ever be obtained” — *Albert Einstein, 1932*
- “Anyone who expects a source of power from the transformation of these atoms is talking moonshine.” — *Ernest Rutherford, 1933*
- “A few decades hence, [when controlled fusion is achieved], energy will be free — just like the unmetered air.” — *John von Neumann, 1956*
- “Radio has no future.” — *Lord Kelvin, 1897*
- “I think there is a world market for about five computers.” — *Thomas J. Watson, 1943*
- Where a calculator like ENIAC is equipped with 18,000 vacuum tubes and weighs 30 tons, computers in the future may have only 1,000 vacuum tubes and perhaps only weigh $1\frac{1}{2}$ tons.” — *Popular Mechanics, March 1949*
- “640k ought to be enough for anybody.” — *Bill Gates, 1981*

† C. Cerf and V. Navasky, Villard, New York, 1998

Plasma

History of the term "**plasma**" In the mid-19th century the Czech physiologist **Jan Evangelista Purkynje** introduced use of the Greek word plasma (meaning "formed or molded") to denote the clear fluid which remains after removal of all the corpuscular material in blood.

Half a century later, the American scientist **Irving Langmuir** proposed in **1922** that the electrons, ions and neutrals in an ionized gas could similarly be considered as corpuscular material entrained in some kind of fluid medium and called this entraining medium plasma. However it turned out that unlike blood where there really is a fluid medium carrying the corpuscular material, there actually is no "fluid medium" entraining the electrons, ions, and neutrals in an ionized gas. Ever since, plasma scientists have had to explain to friends and acquaintances that they were not studying blood!

Jan Evangelista Purkyně was a Czech anatomist and physiologist. In 1839, he coined the term protoplasm for the fluid substance of a cell. He was one of the best known scientists of his time. Wikipedia

Purkyně also introduced the scientific terms plasma (for the component of blood left when the suspended cells have been removed) and protoplasm (the substance found inside cells.)

Definition of a plasma

Although a plasma is loosely described as an electrically neutral medium of positive and negative particles, a more rigorous definition requires three criteria to be satisfied:

The plasma approximation:

Charged particles must be close enough together that each particle influences many nearby charged particles, rather than just the interacting with the closest particle (these collective effects are a distinguishing feature of a plasma). The plasma approximation is valid when the number of electrons within the sphere of influence (called the *Debye sphere* whose radius is the Debye (screening) length) of a particular particle is large. The average number of particles in the Debye sphere is given by the plasma parameter, Λ.

Bulk interactions:

The Debye screening length (defined above) is short compared to the physical size of the plasma. This criterion means that interactions in the bulk of the plasma are more important than those at its edges, where boundary effects may take place.

Plasma frequency:

The electron plasma frequency (measuring plasma oscillations of the electrons) is large compared to the electron-neutral collision frequency (measuring frequency of collisions between electrons and neutral particles). When this condition is valid, plasmas act to shield charges very rapidly (quasineutrality is another defining property of plasmas).

Charged Particle Trajectories Are Different In Plasmas

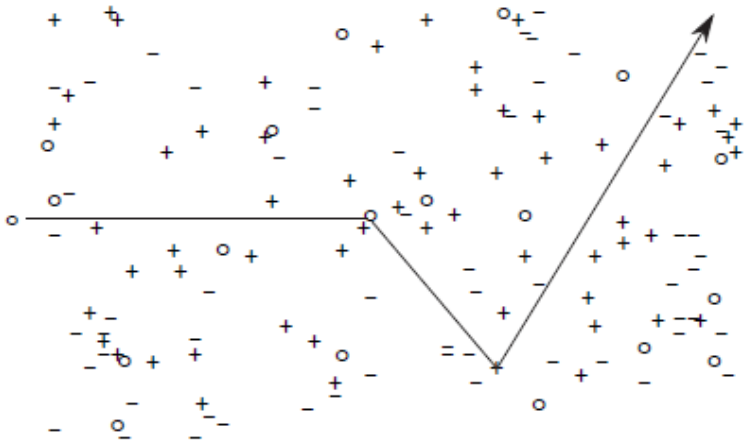

Figure 3: The trajectory of a neutral particle in a partially ionized gas exhibits "straight-line" motion between abrupt atomic collisions. The typical distance between neutral particle collisions is called the collision "mean free path." Symbols: neutrals (circles), electrons (minus signs) and ions (plus signs).

Plasma

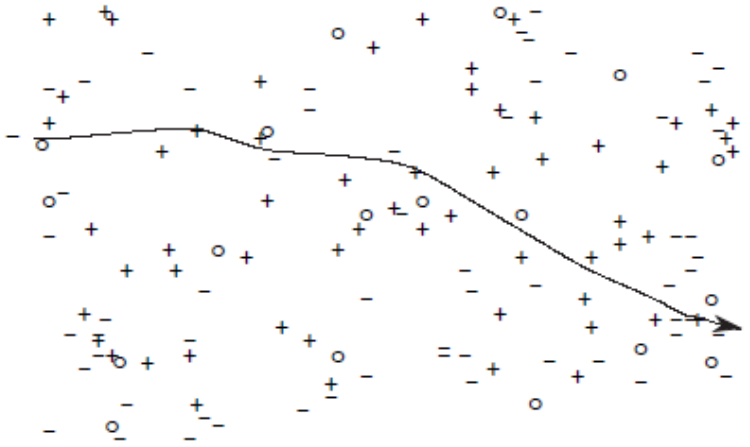

Figure 4: The trajectory of a "test" electron in a plasma exhibits continuous small-angle Coulomb collisional scatterings of its direction of motion. The "collision length" is the exponential decay length over which an average charged particle in a plasma loses its initially directed momentum.

Introduction to PLASMA PHYSICS

Prof. J. Glosík
KFPP MFF UK

????????

Burning Match Stick

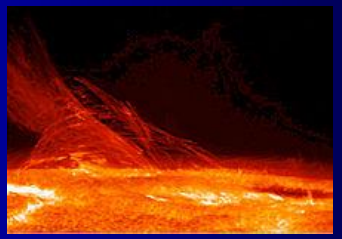
Sun

Andromeda composite

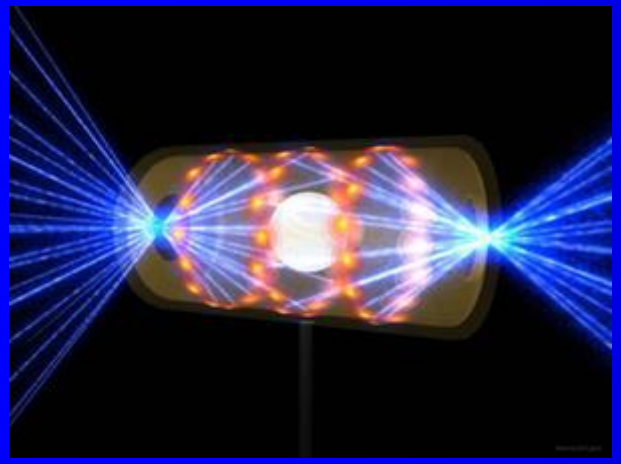

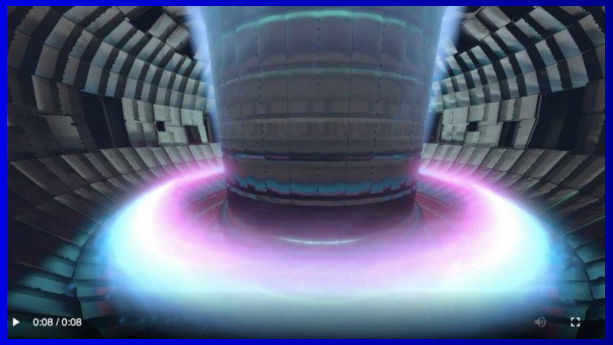

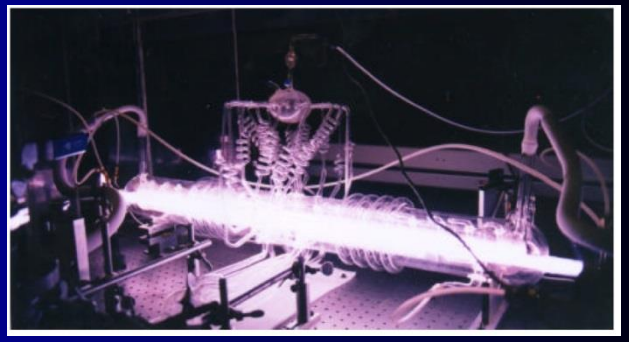

Fusion in a flash. At the National Ignition Facility (NIF) at Lawrence Livermore National Lab, 192 powerful lasers blast a BB-sized fuel pellet inside a metallic cylinder to generate nuclear fusion.


Aurora

Ultra cold Plasma
Experiment: $T \sim 6$ mK

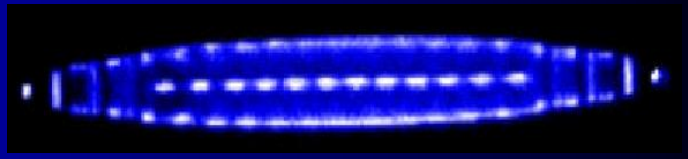

Plasma Parameters

Scio me nihil scire

Temperature of the Sun ???

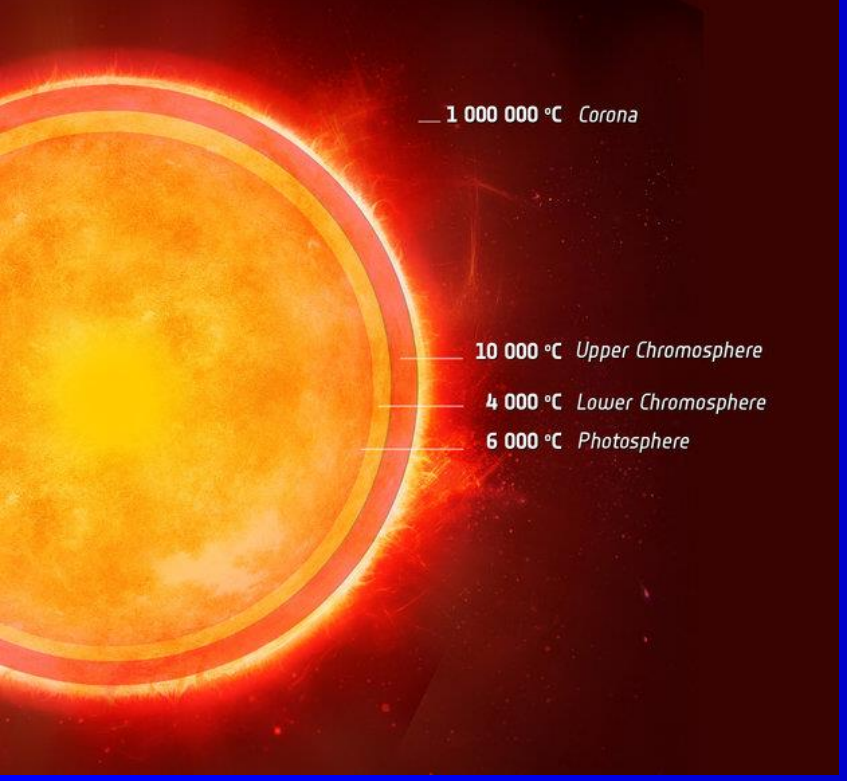

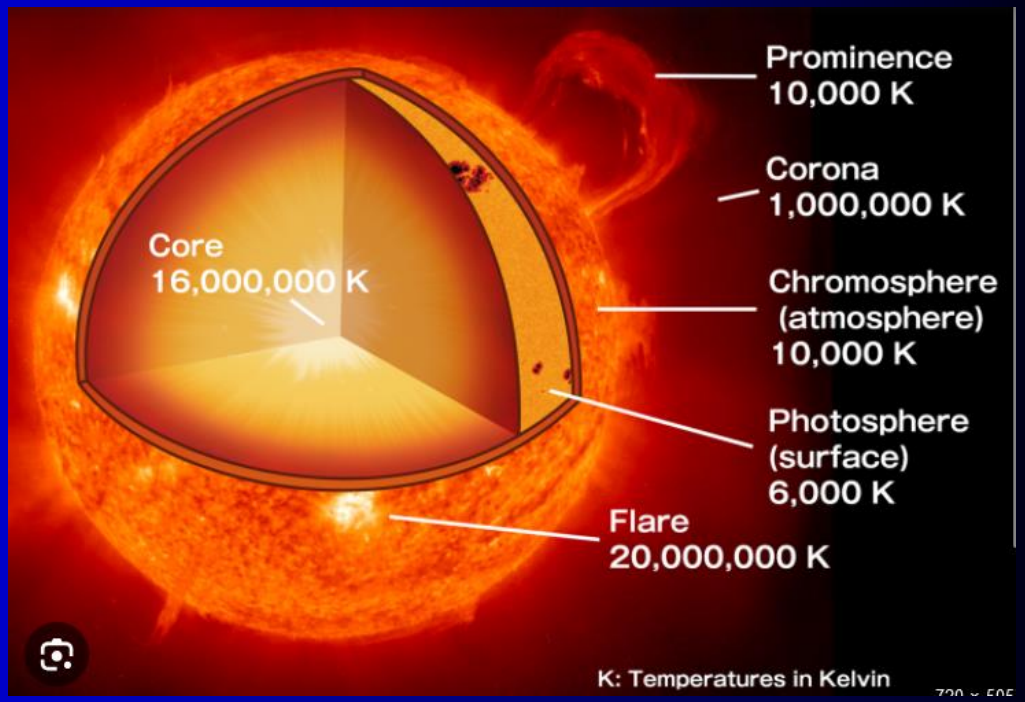

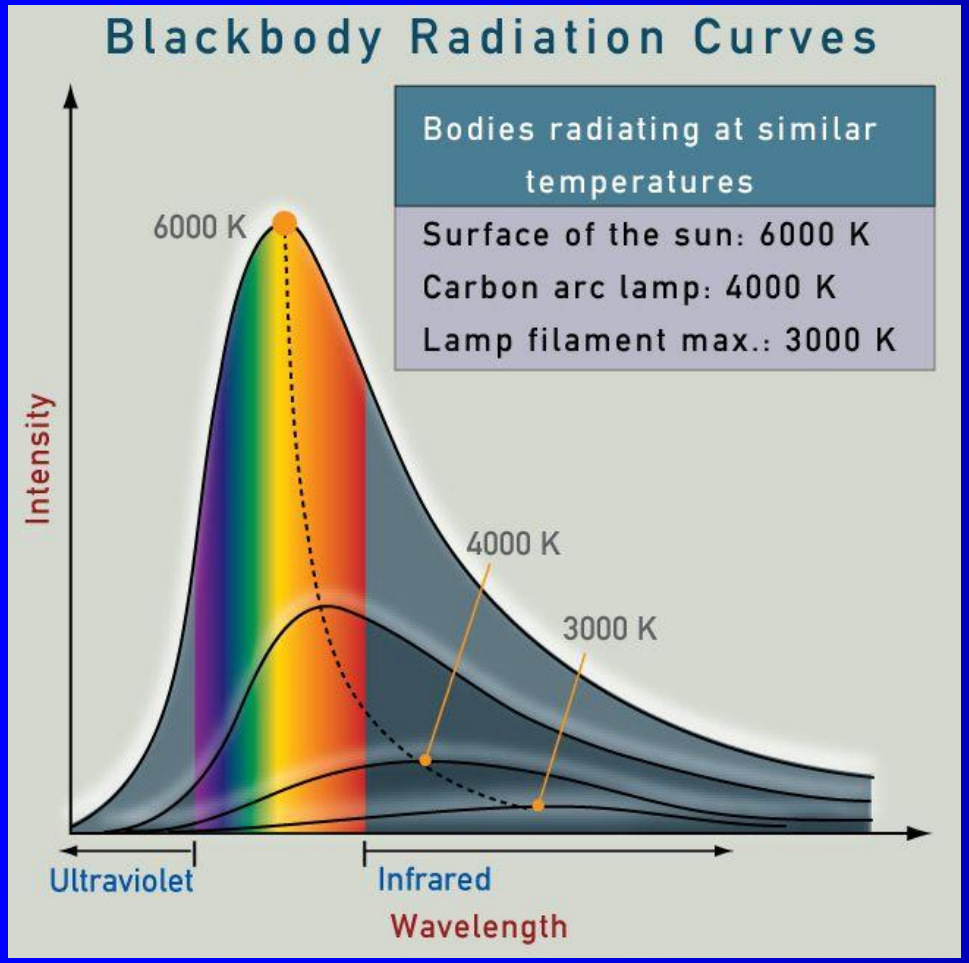

SURFACE TEMPERATURE OF THE SUN & EARTH

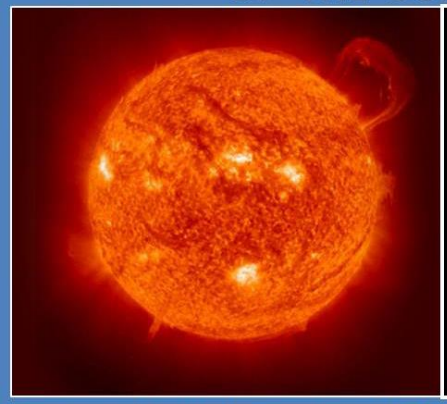

6,000K (5,727˚C or 10,340˚F)

288K (15˚C or 59˚F)

Temperatures and energies

$E \leftrightarrow kT$

1eV ~ 11 604.505 K

1K ~ 9×10^{-5}eV

$\log T_e$ (K)

PLASMA AS A STATE OF MATTER

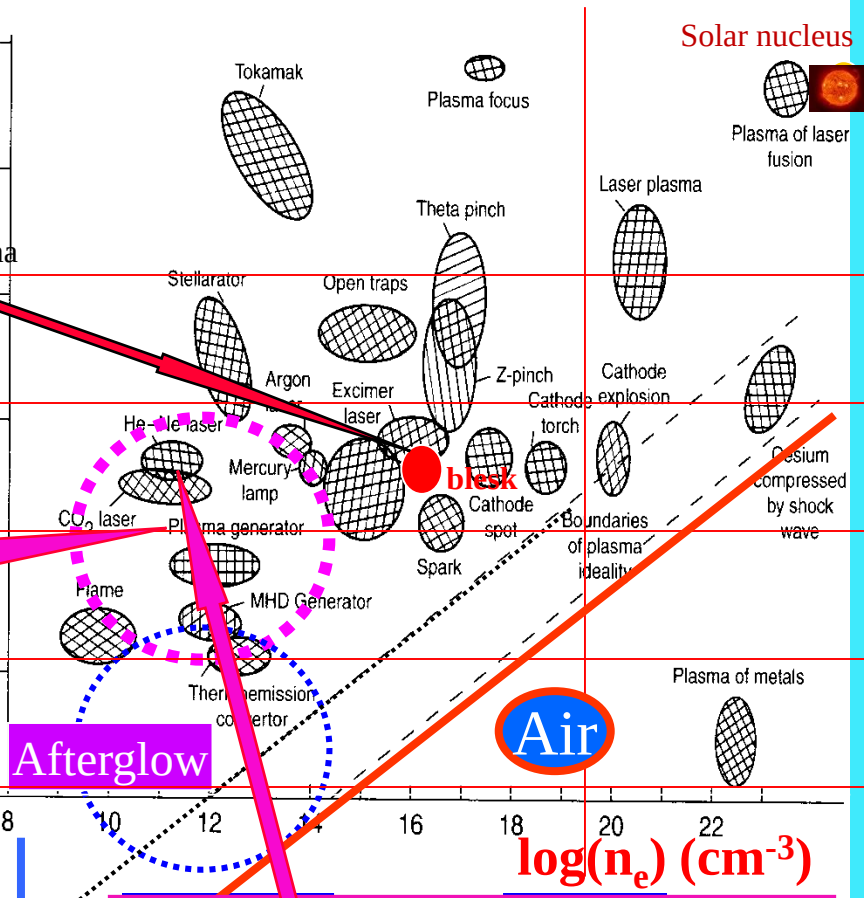

Plasma in earth's magnetosphere

Solar corona

100eV 10^6 K

10eV 10^5 K

Solar wind near the Earth

1eV 10^4 K

Ionosféra

0.1eV 1000 K F_2 F_1

D E

0.01eV 100 K

Afterglow

Air

ISM

1meV 10 K

ATHENA

4 K

ATRAP

4 K

0.1meV 1 K

e^+, p

$\log(n_e)$ (cm^{-3})

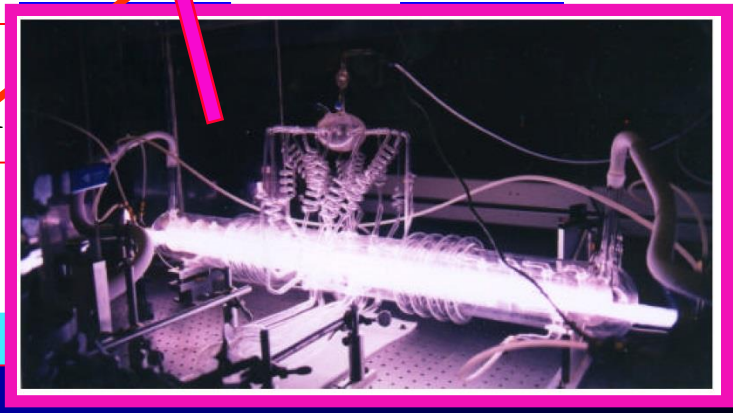

Not actualized, approximation

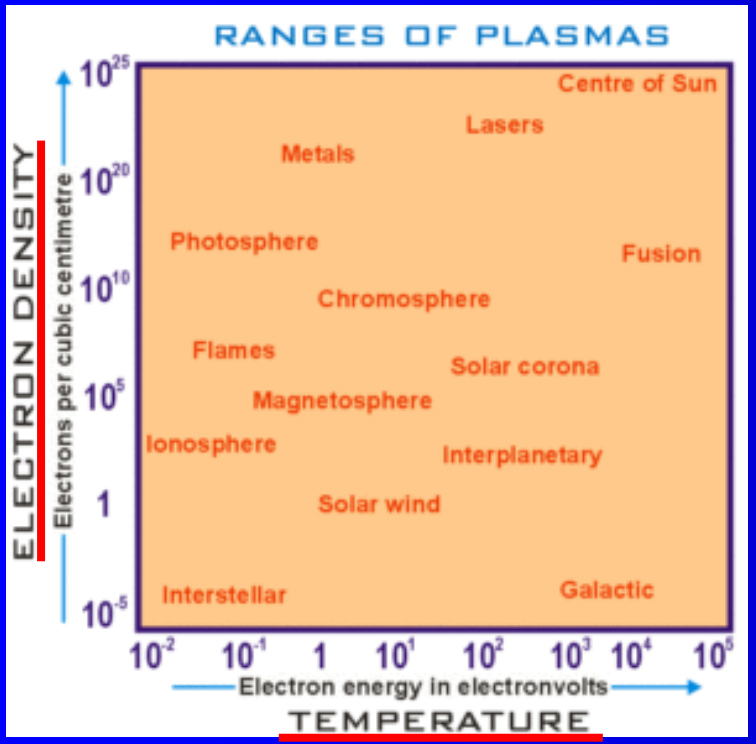

Ranges of plasma parameters

Density increases upwards, temperature increases towards the right. The free electrons in a metal may be considered an electron plasma. Plasma parameters can take on values varying by many orders of magnitude, but the properties of plasmas with apparently disparate parameters may be very similar (see plasma scaling). The following chart considers only conventional atomic plasmas and not exotic phenomena like quark gluon plasmas:

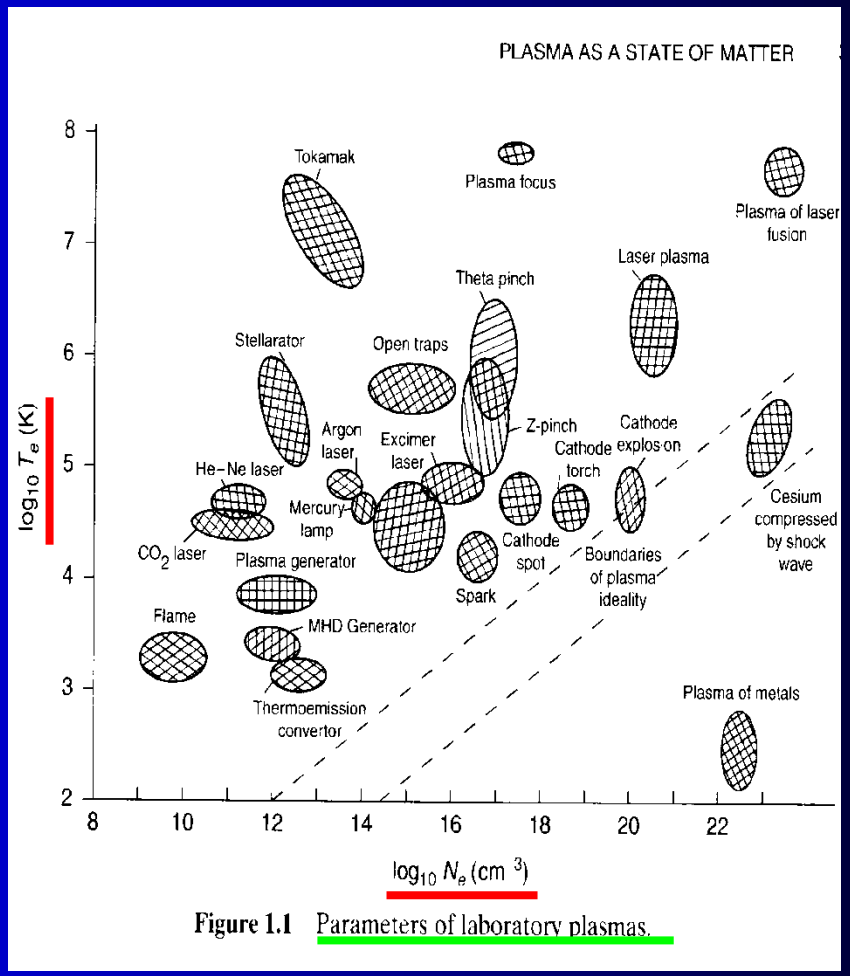

Figure 1.1 Parameters of laboratory plasmas.

Approximation ….

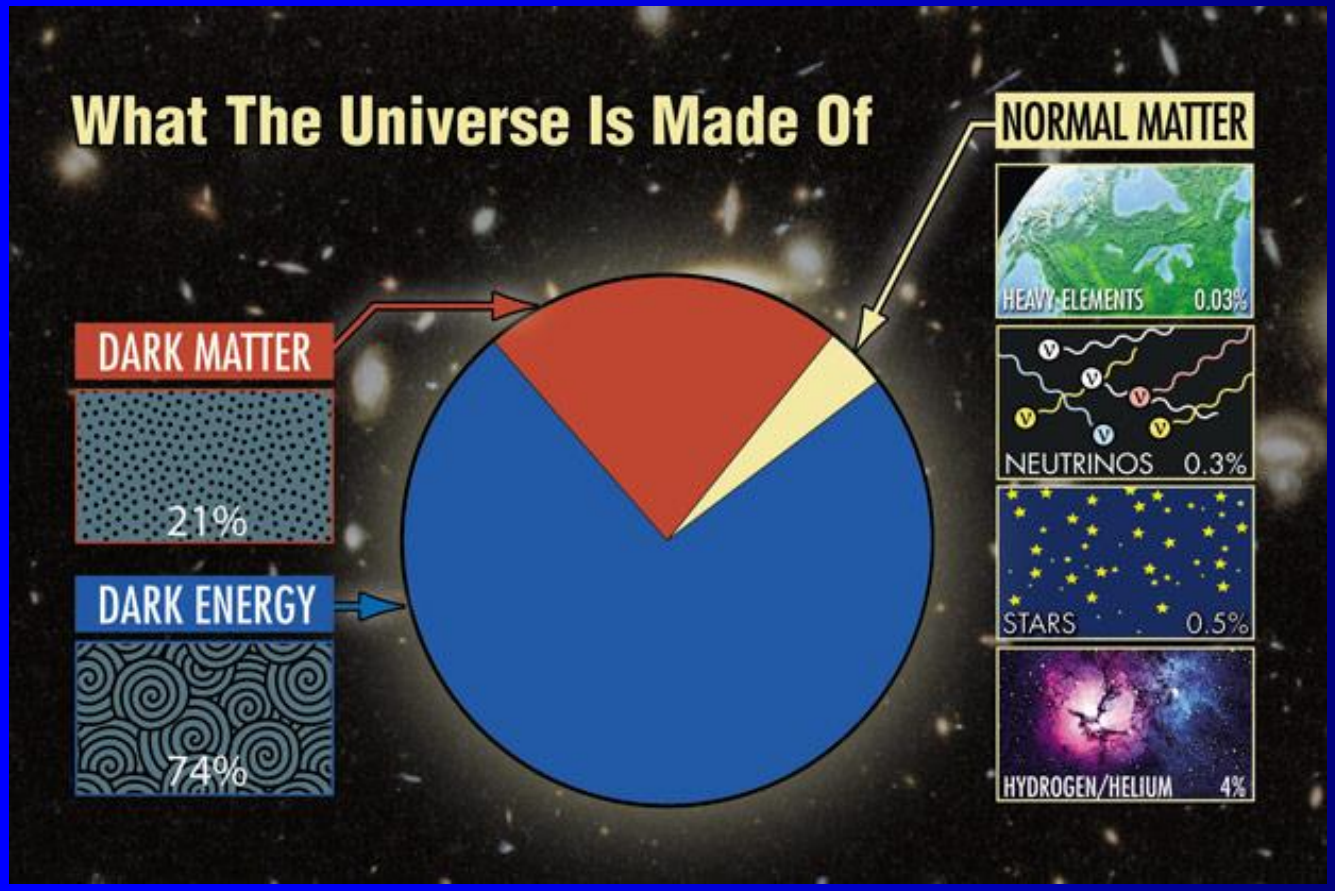

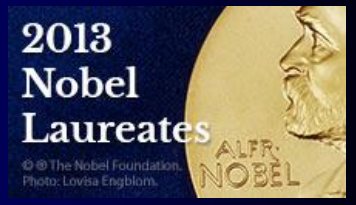

Peter W. Higgs

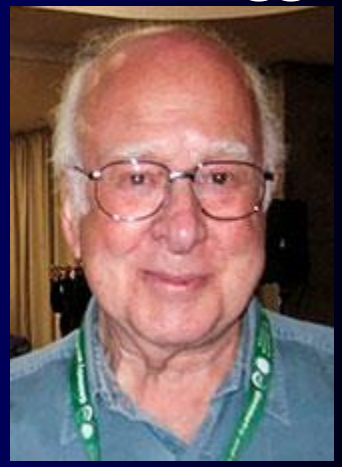

François Englert

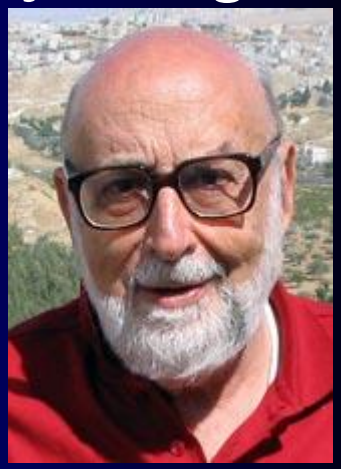

The Nobel Prize in Physics 2013
François Englert and Peter W. Higgs "for the theoretical discovery of a mechanism that contributes to our understanding of the origin of mass of subatomic particles, and which recently was confirmed through the discovery of the predicted fundamental particle, by the ATLAS and CMS experiments at CERN's Large Hadron Collider"

Normal matter ….4.83%

… and now it is clear ….

Scio me nihil scire

Motivation:

$e^-, H^+, H, H^-, H_2^+, H_2, \ldots . H_3^+$

Just for pleasure.

$$\psi(x) \propto \sum_n A_n e^{ip_n x/\hbar},$$

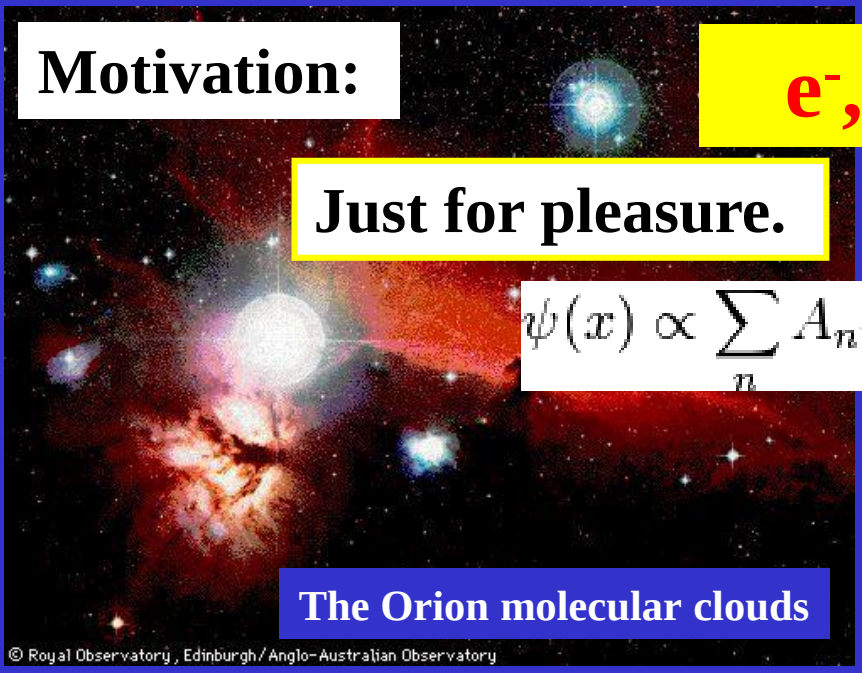

The Orion molecular clouds

92.1% of nucleons in the universe are protons
7.8% are helium nuclei !

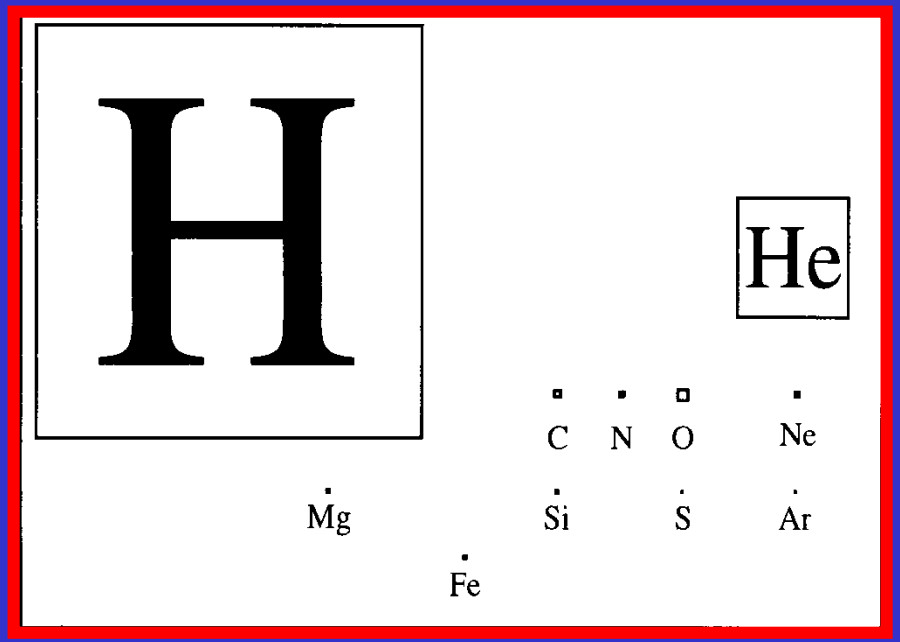

Cosmic Abundance of some elements

Element	Abundance
hydrogen (H)	1.000.000
helium	80.147
oxygen	739
carbon	445
neon	138
nitrogen	91
magnesium	40
Silcon	37
Sulfur	19

The Privilege of Being a Physicist

Victor F. Weisskopf

There are certain obvious privileges that a physicist enjoys in our society. He is reasonably paid; he is given instruments, laboratories, complicated and expensive machines, and he is asked not to make money with these tools, like most other people, but to spend money. Furthermore, he is supposed to do what he himself finds most interesting, and he accounts for what he spends to the money givers in the form of progress reports and scientific papers that are much too specialized to be understood or evaluated by those who give the money—the federal authorities and, in the last analysis, the taxpayer. Still, we believe that the pursuit of science by the
ported by the p
have to look dee
ence to society
physics only; we
ral sciences, bu
ences, that is,
formed without

"Intelligent play with simple, natural phenomena, the joys of discovery of unexpected experiences, are much better ways of learning to think than any teaching by rote."

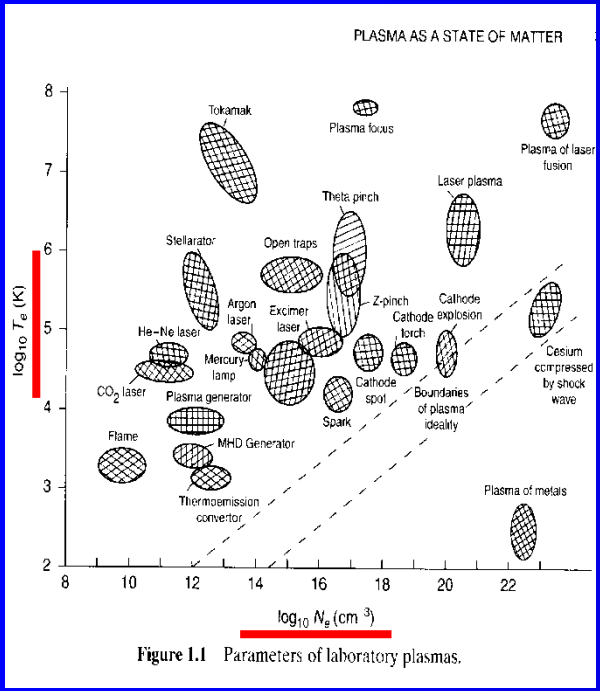

Figure 1.1 Parameters of laboratory plasmas.

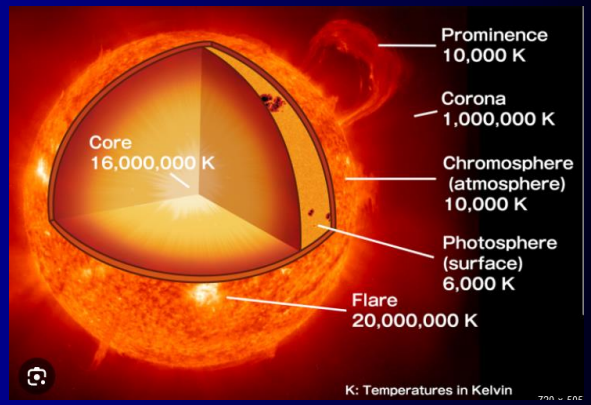

Typical ranges of plasma parameters

Characteristic	Terrestrial plasmas	Cosmic plasmas
Size in metres	10^{-6} m (lab plasmas) to 10^{2} m (lightning)	10^{-6} m (spacecraft sheath) to 10^{25} m (intergalactic nebula)
Lifetime in seconds	10^{-12} s (laser-produced plasma) to 10^{7} s (fluorescent lights)	10^{1} s (solar flares) to 10^{17} s (intergalactic plasma)
Density in particles per cubic metre	10^{7} m^{-3} to 10^{32} m^{-3} (inertial confinement plasma)	10^{0} (i.e., 1) m^{-3} (intergalactic medium) to 10^{30} m^{-3} (stellar core)
Temperature in kelvins	~0 K (crystalline non-neutral plasma) to 10^{8} K (magnetic fusion plasma)	10^{2} K (aurora) to 10^{7} K (solar core)
Magnetic fields in teslas	10^{-4} T (lab plasma) to 10^{3} T (pulsed-power plasma)	10^{-12} T (intergalactic medium) to 10^{11} T (near neutron stars)

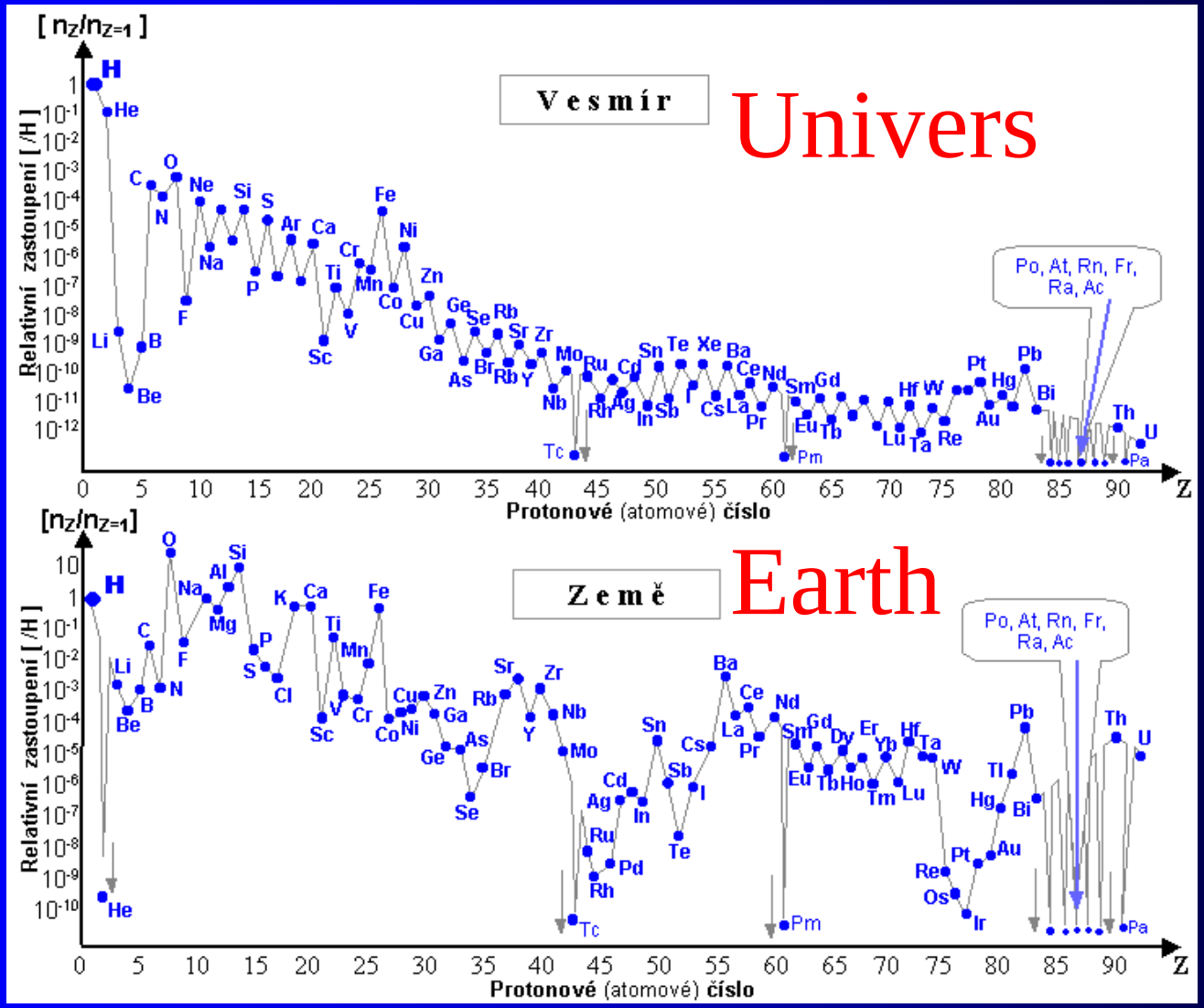

Relativní zastoupení prvků v přírodě v závislosti na jejich protonovém (atomovém) čísle Z, vztažené k vodíku Z=1.
Nahoře: Nynější průměrné zastoupení prvků ve vesmíru. **Dole:** Výskyt prvků na Zemi (v zemské kůře) a terestrických planetách.
Vzhledem k velkému rozpětí hodnot je relativní zastoupení prvků (vztažené k vodíku Z=1) na svislé ose vyneseno v logaritmickém měřítku; to ale může zvláště na horním grafu opticky zkreslit velký rozdíl v zastoupení vodíku a hélia oproti těžším prvkům..

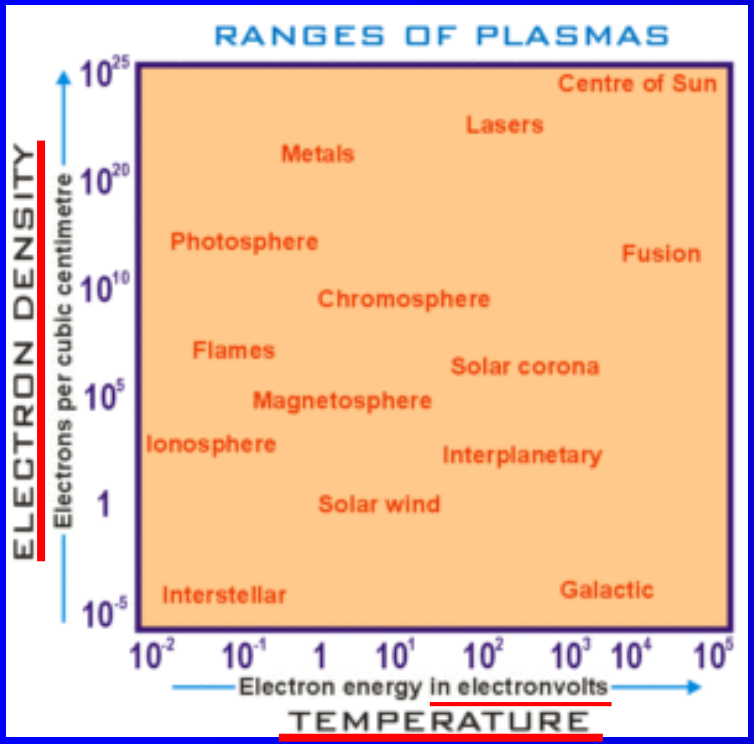

Ranges of plasma parameters

Density increases upwards, temperature increases towards the right. The free electrons in a metal may be considered an electron plasma [11]Plasma parameters can take on values varying by many orders of magnitude, but the properties of plasmas with apparently disparate parameters may be very similar (see plasma scaling). The following chart considers only conventional atomic plasmas and not exotic phenomena like quark gluon plasmas:

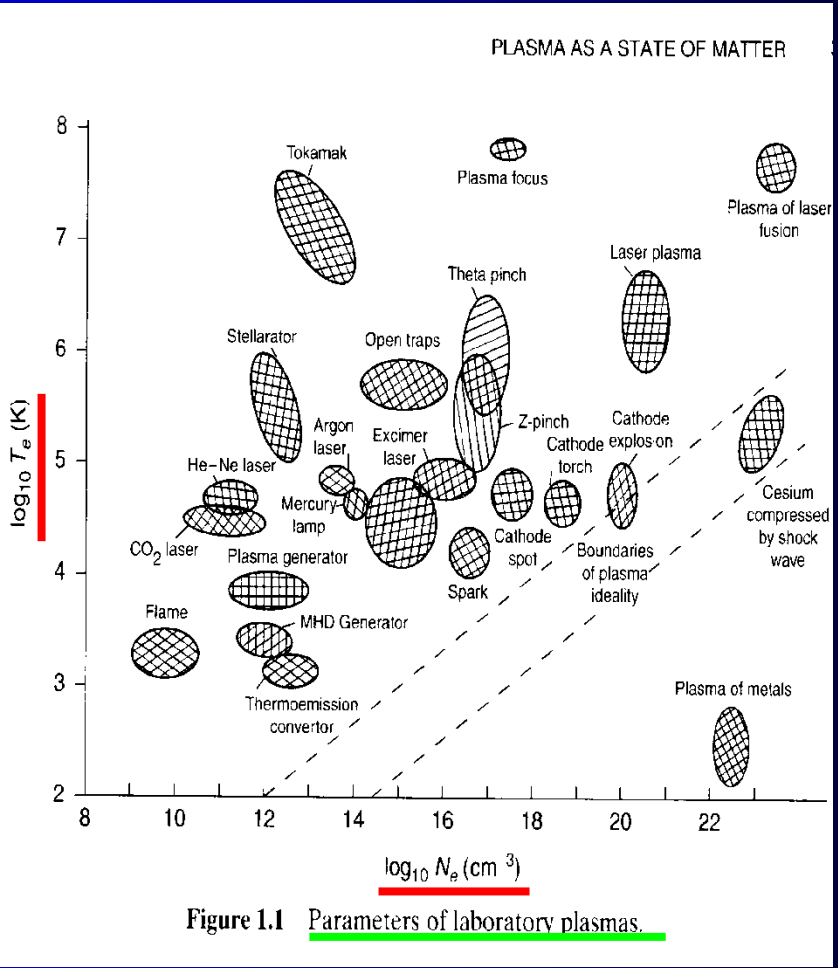

Figure 1.1 Parameters of laboratory plasmas.

05. 10. 2021

04. 10. 2022

26. 10. 2023

Energie

	220	054	686	Energie spotřebovaná dnes (MWh), z toho: energy consumed today
	187	322	974	- z neobnovitelných zdrojů non-renewable resources
	33	138	316	- z obnovitelných zdrojů renewable resources
1 378	873	597	221	Solární energie dopadající na Zemi dnes (MWh)

Information

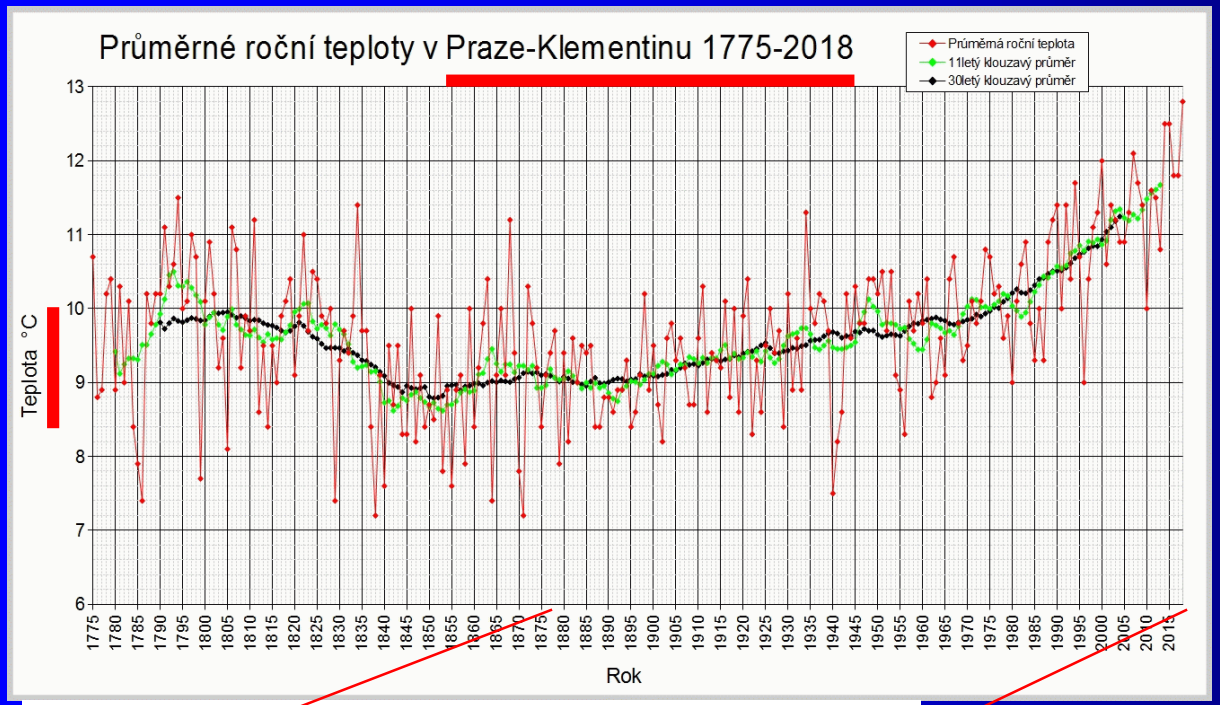

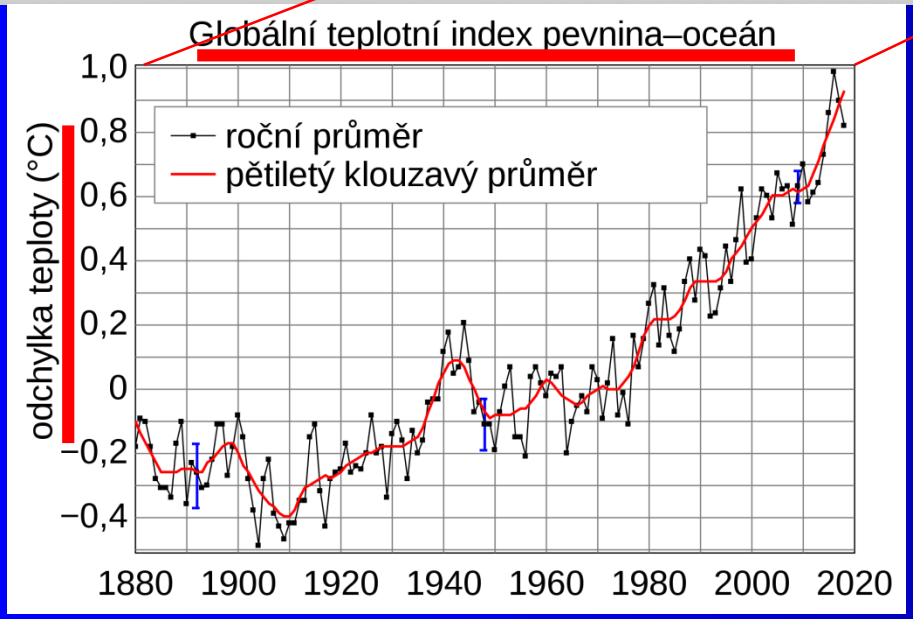

"Kdo z vás je bez hříchu, první hoď na ni kamenem"

(see ref.: **Nový zákon,** … Ježíš … hora Olivetska …)

Jesus
He that is *without sin* among *you,* let him be the *first* to *cast a stone at her*.

https://cs.wikipedia.org/wiki/

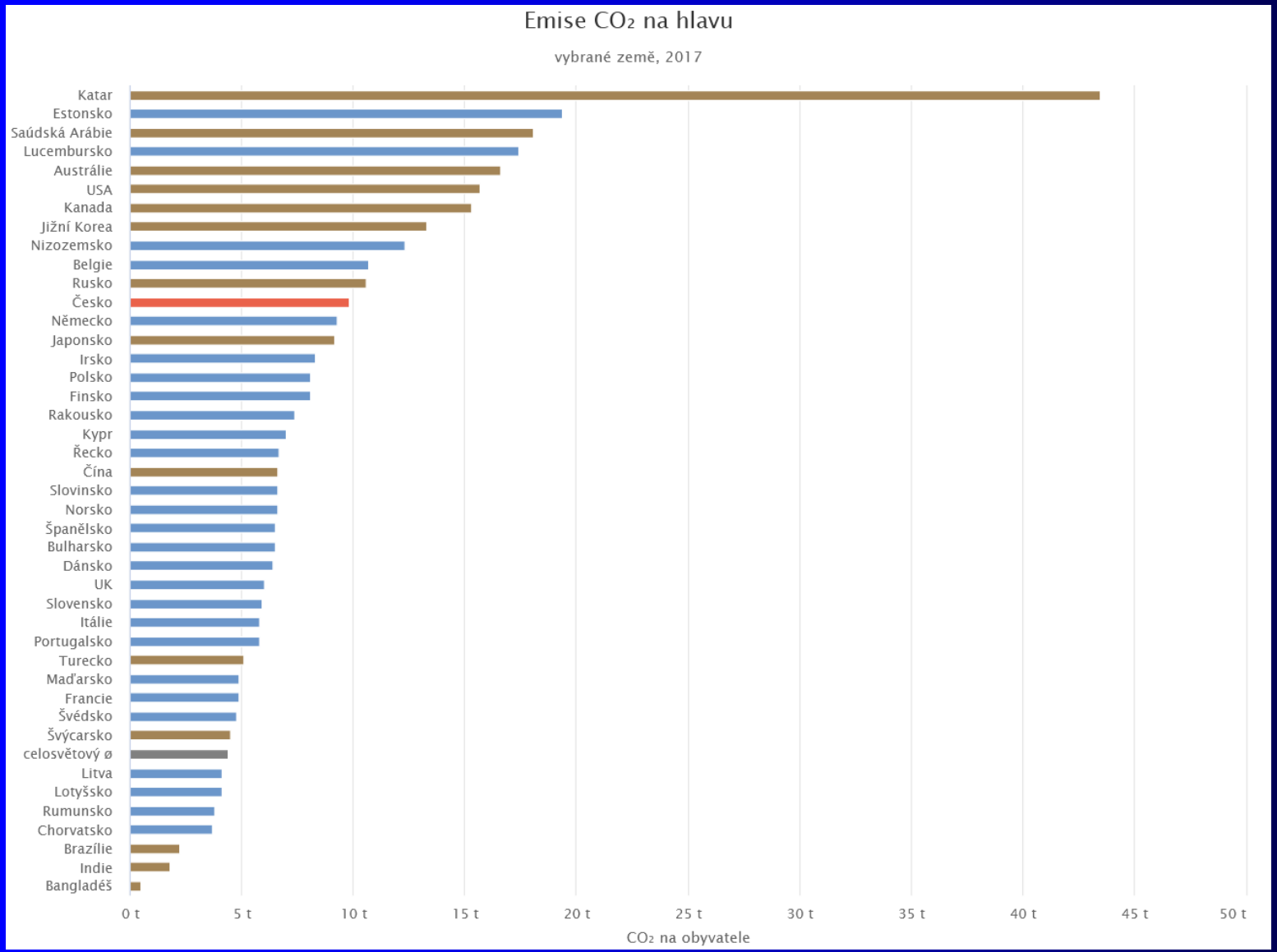

"Kdo z vás je bez hříchu, první hoď na ni kamenem"

(see ref.: **Nový zákon,** Jan 8 … hora Olivetska …)

Jesus
He that is *without sin* among *you*, let him be the *first* to *cast a stone at her*.

Průměrná roční teplota

1775–2021, Praha-Klementinum

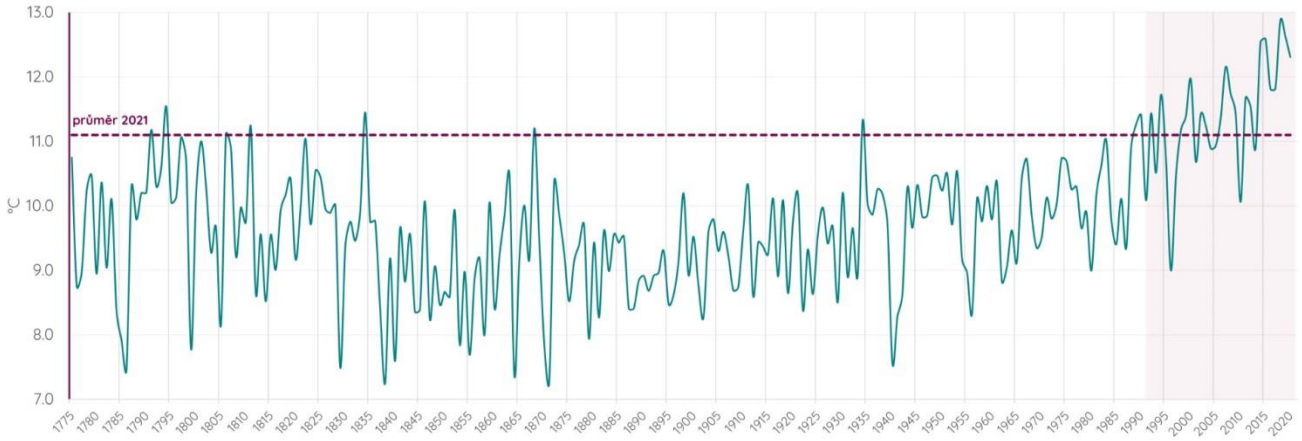

Graf výše ukazuje průměrné roční teploty na stanici Praha-Klementinum za období 1775 až 2020. V grafu je vyznačena přerušovanou čarou hladina průměrné roční teploty za rok 2021 a vyšrafováno je období 1991 až 2020.

Jak ukazuje výše uvedená infografika, v kontextu posledních 30 let (období 1991 až 2020) a zejména pak poslední dekády (2011 až 2020) opravdu byl rok 2021 chladnější. Při hodnocení klimatu však nejsou podstatné krátkodobé výkyvy, ale dlouhodobý trend. Z grafu výše je jasně patrné, že v dlouhodobém hledisku byl i rok 2021 velmi teplý a do roku 1990 bychom za více než 200 let našly jen 9 roků, které byly v průměru teplejší. Oproti předchozímu třicetiletí 1961-1990 to byl rovněž rok silně nadnormální (+1,1 °C). Trend je zcela zřejmý, a to dlouhodobé zvyšování teploty, které se v posledních letech velmi akcelerovalo. To však neznamená, že se nemůže vyskytnout chladnější rok (a stejně tak globální oteplování neznamená, že se v zimě nemohou vyskytnout velmi chladné dny, dlouhodobě jich ale ubývá). Ještě lepším příkladem než rok 2021 je v tomto směru rok 1996 a 2010. Ani tyto dva roky ale nelze považovat za velmi chladné z dlouhodobého hlediska. Při pohledu na celkový průběh je patrné, že rok 1996 byl blízko průměru 1775-1990 a rok 2010 byl z dlouhodobého pohledu teplotně nadprůměrný.

Zdroj: Český hydrometeorologický ústav

Carbon dioxide heats the atmosphere

Increased levels of carbon dioxide lead to higher temperatures in the lower atmosphere, while the upper atmosphere gets colder. Manabe thus confirmed that the variation in temperature is due to increased levels of carbon dioxide; if it was caused by increased solar radiation, the entire atmosphere should have warmed up.

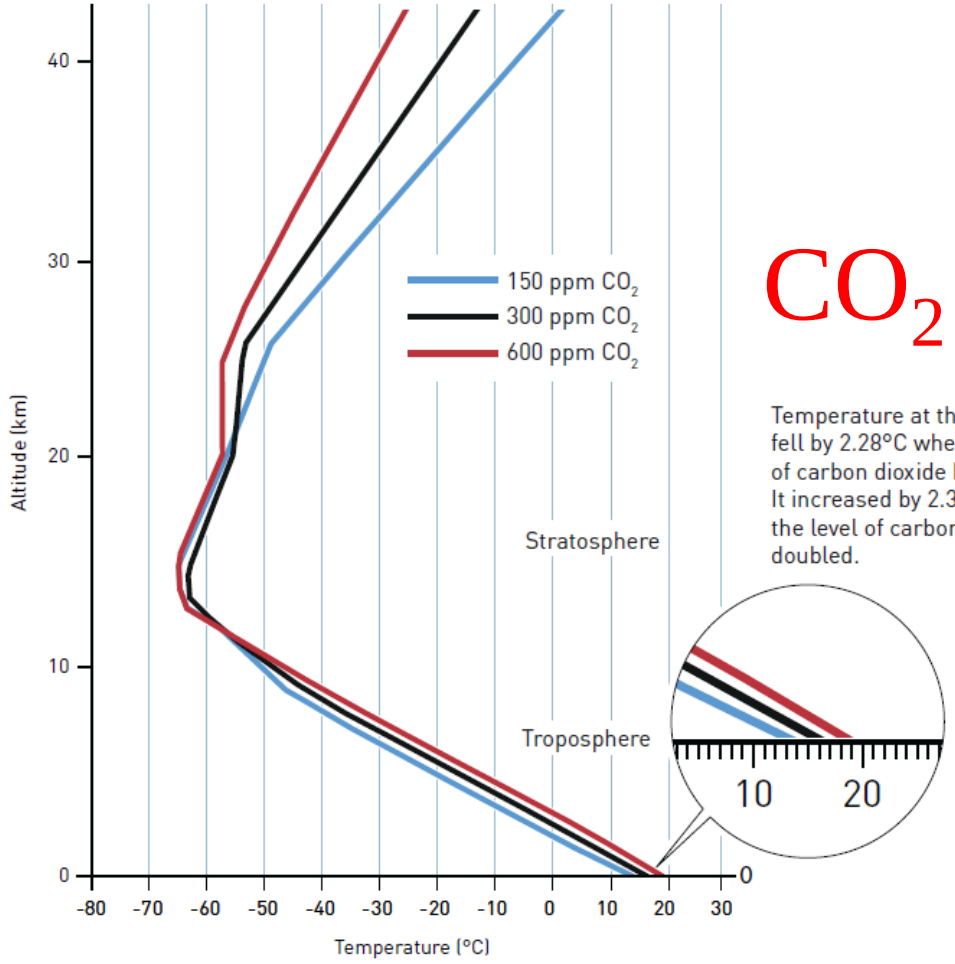

CO_2

Temperature at the surface fell by 2.28°C when the level of carbon dioxide halved. It increased by 2.36°C when the level of carbon dioxide doubled.

Source: Manabe and Wetherald (1967) Thermal equilibrium of the atmosphere with a given distribution of relative humidity, *Journal of the atmospheric sciences*, Vol. 24, Nr 3, May.

Emissions of CO_2 per person

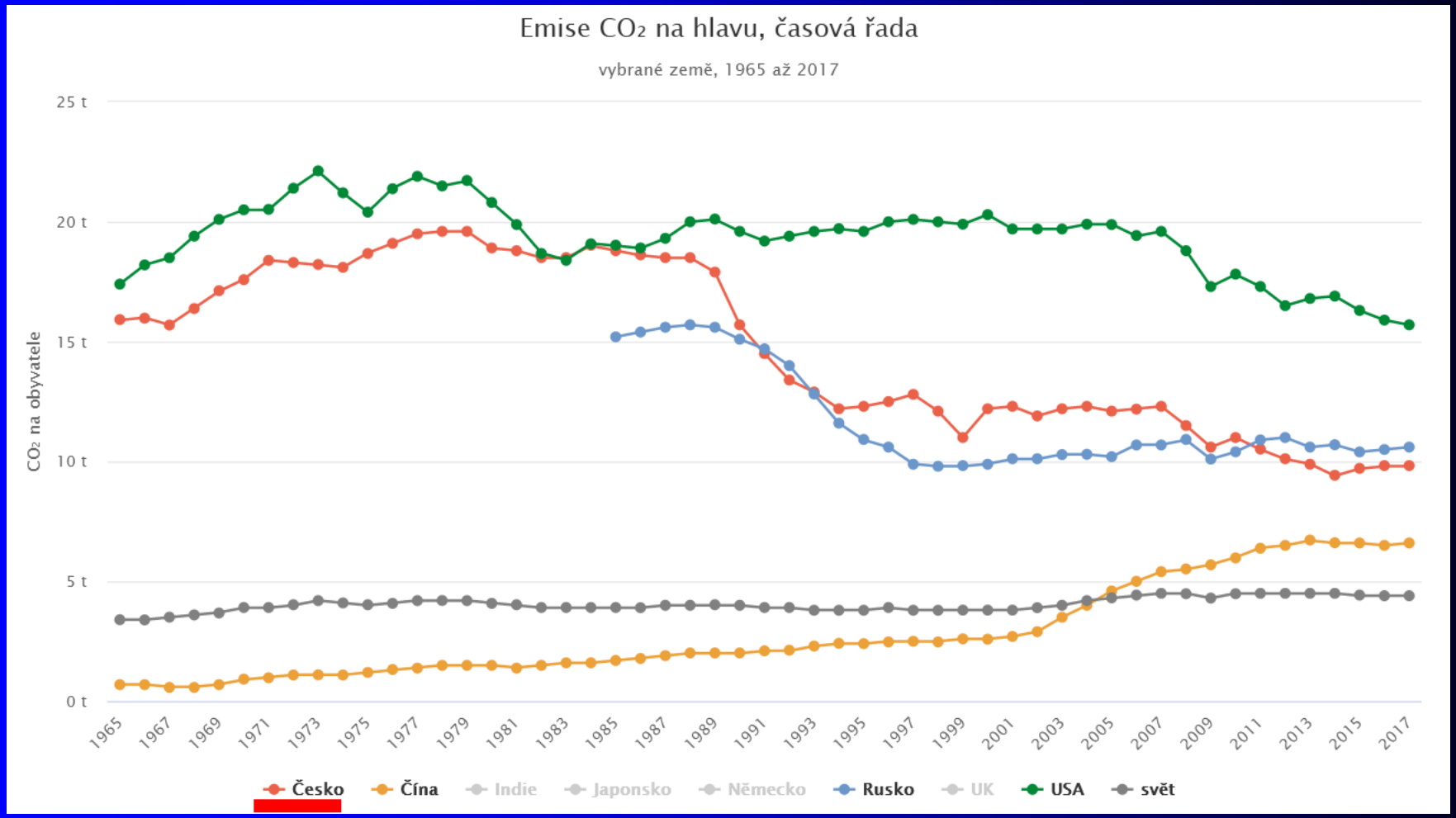

Not actualized, approximation

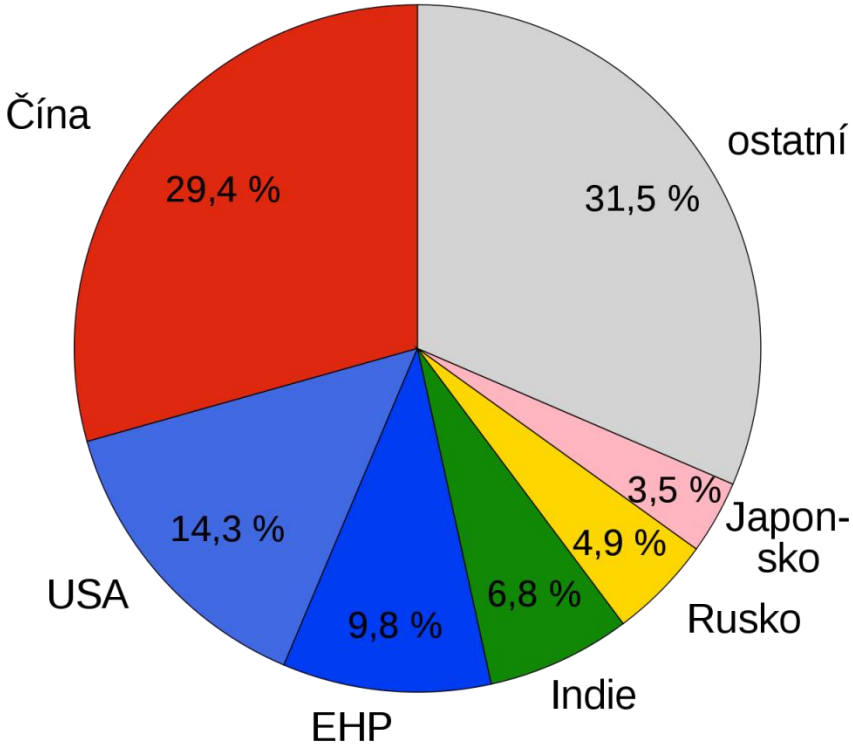

Největší producenti CO2 na světě

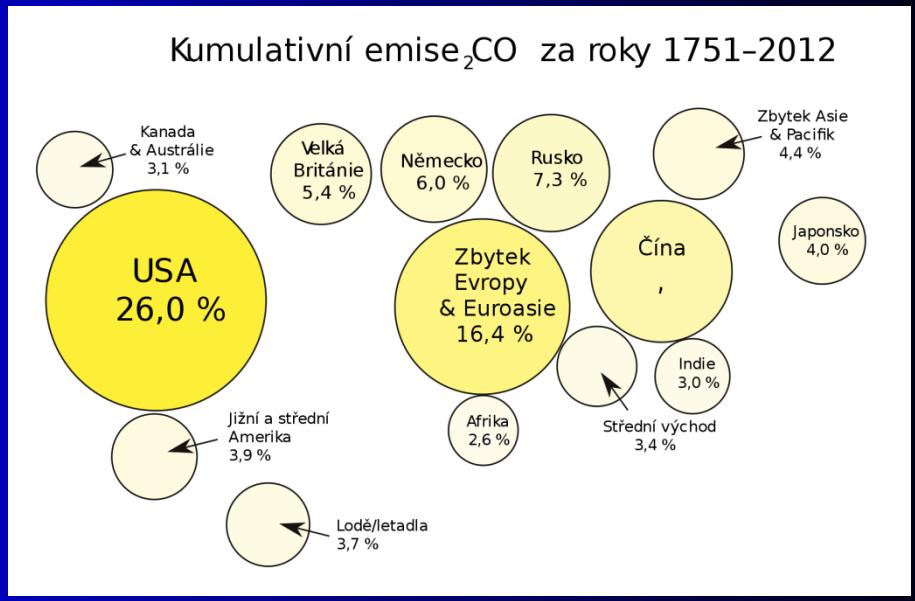

Podíl na globálních emisích CO_2 mezi roky 1751–2012 podle různých regionů

Kdo z vás je bez hříchu, první hoď na ni kamenem

Jesus

***He that* is *without sin* among *you*, let him be the *first* to *cast a stone at her*.**

https://cs.wikipedia.org/wiki/

Not actualized, approximation

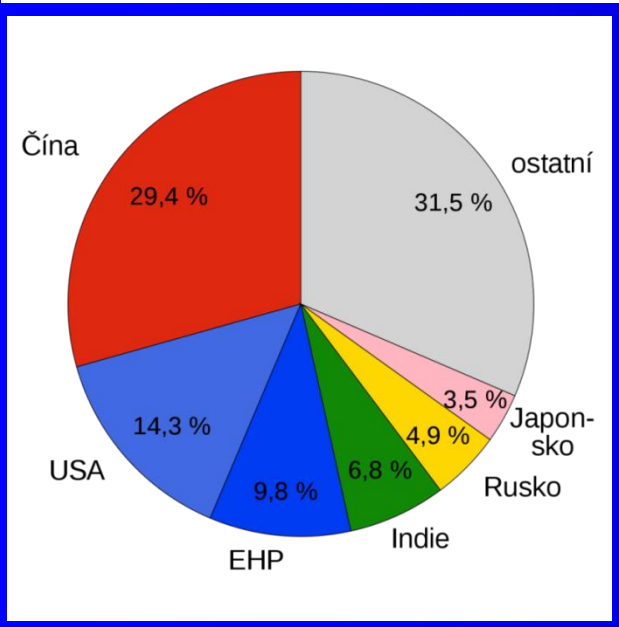

Největší producenti CO2 na světě

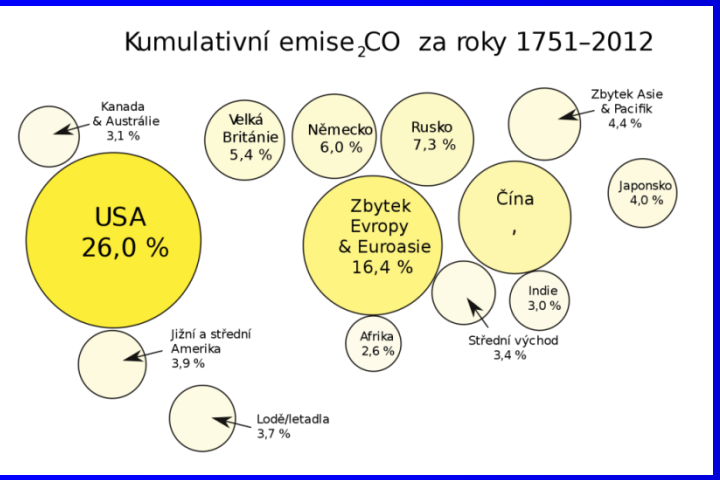

Podíl na globálních emisích CO_2 mezi roky 1751–2012 podle různých regionů

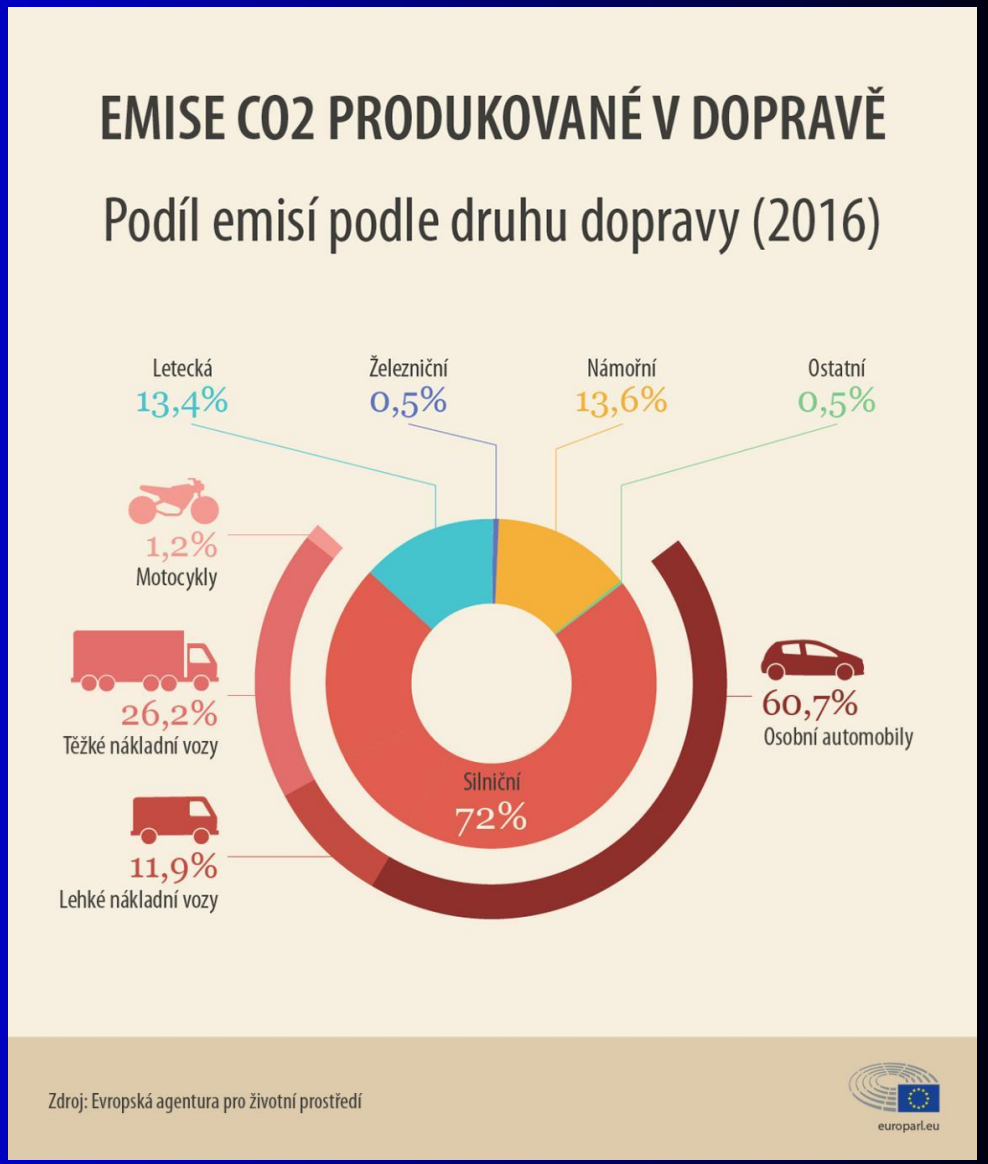

https://cs.wikipedia.org/wiki/

Jesus
***He that* is *without sin* among *you*, let him be the *first* to *cast a stone at her*.**

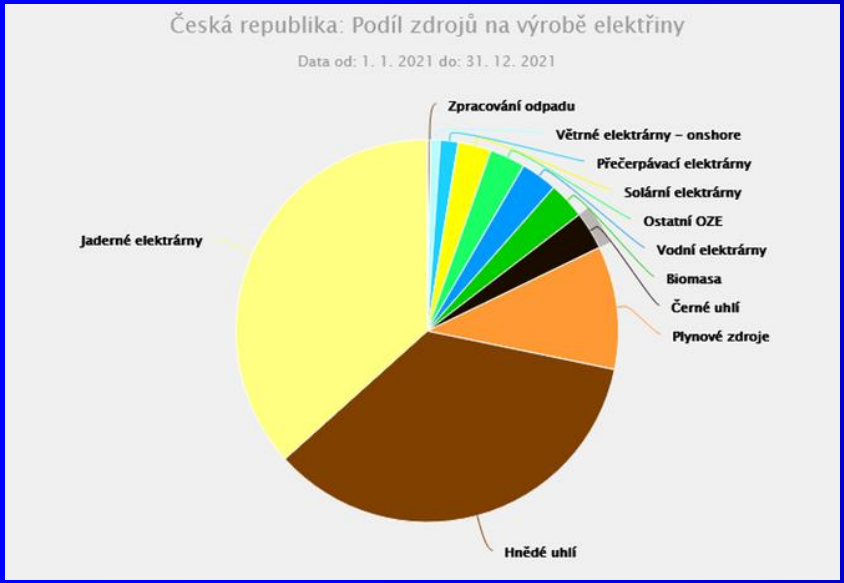

Podíl zdrojů na výrobě elektřiny v roce 2021
(v %)

	Česko	Slovensko	Maďarsko	Rakousko	Německo	Polsko	Francie
Jaderné elektrárny	36.6	54.3	51.2	0	13	0	70.4
Hnědé uhlí	35.1	3.5	10.3	0	19.5	26.1	0
Plynové zdroje	10.4	13.7	29.2	16.1	10.4	8	6.4
Černé uhlí	3.2	1.3	0	0	10.3	50.4	0.8
Biomasa	3.1	3.1	3.8	2.6	7.8	1.2	0.6
Vodní elektrárny	4.7	15.5	0.6	65.2	4.7	1.8	11.9
Fotovoltaické elektrárny	2.9	2.1	0	1.6	9.4	2.9	2.7
Větrné elektrárny	0.9	0	2.1	12.6	22.8	9.6	6.9
Ostatní obnovitelné zdroje	3	1.8	0.8	1.6	1.5	0	0.3
Ostatní	0.1	4.7	2	0.3	0.6	0	0
Celkem OZE	**14.6**	**22.5**	**7.3**	**83.6**	**46.2**	**15.5**	**22.4**

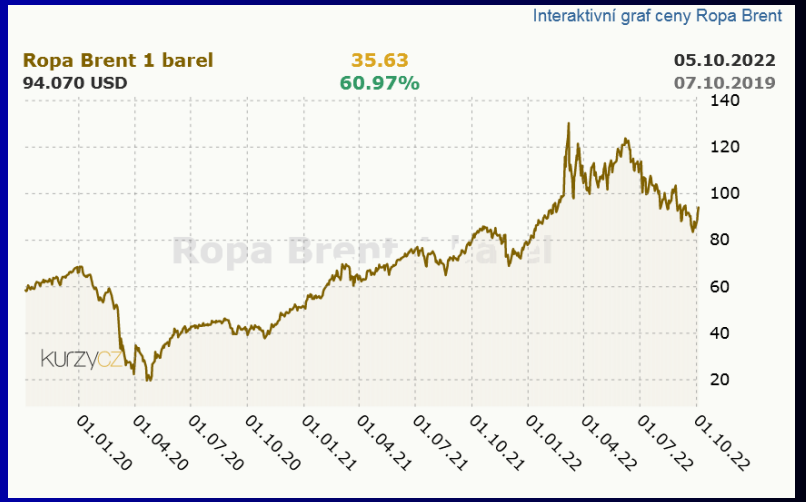

Cui bono?

Qui Bonum

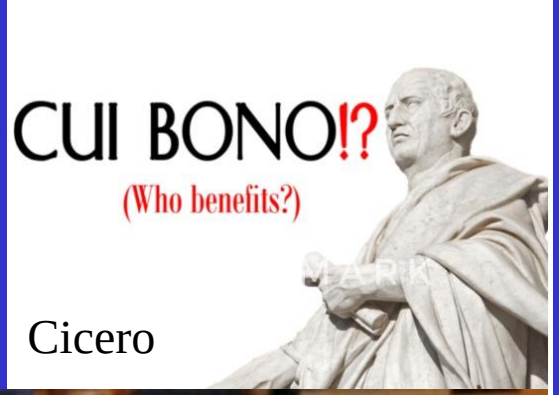
CUI BONO!?
(Who benefits?)
Cicero


H_3^+

Manabe's work in the 1960s demonstrated how increased levels of carbon dioxide in the atmosphere caused the Earth's temperature to rise. In doing so, he "laid the foundation for the development of current climate models," the Royal Swedish Academy of Sciences said in a statement.

A decade later, Hasselmann "created a model that links together weather and climate."

Parisi's discoveries, meanwhile, "make it possible to understand and describe many different and apparently entirely random complex materials and phenomena." This is not only true for physics but also for other areas, such as mathematics, biology, neuroscience and machine learning, the academy added.

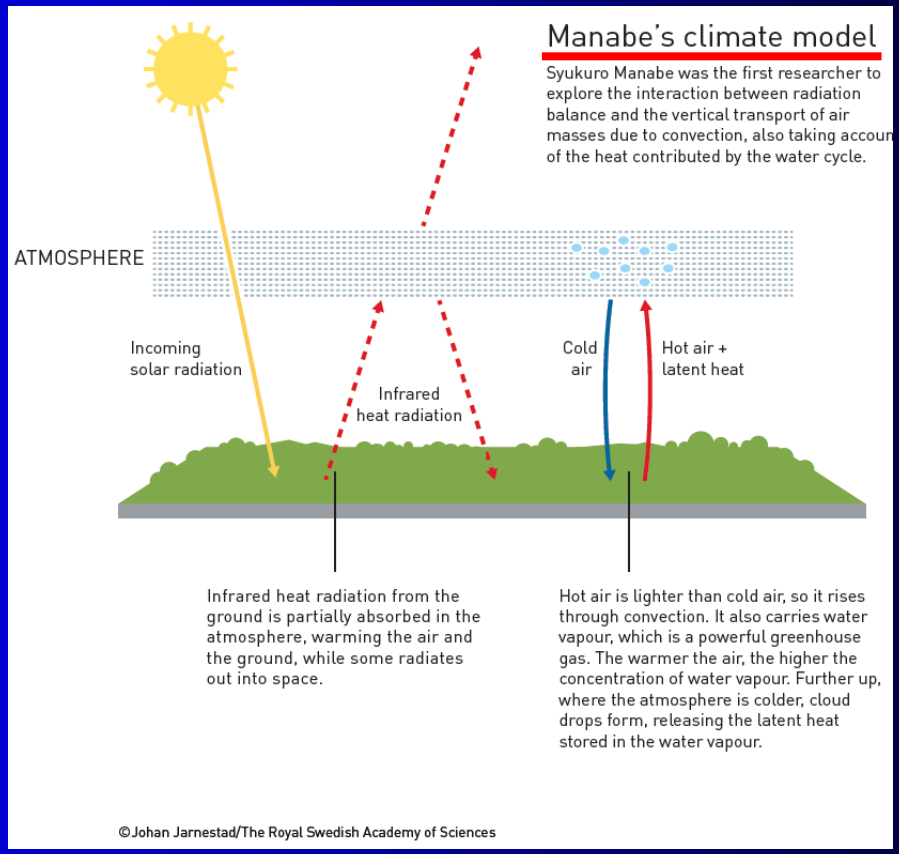

05. 10. 2021

The committee's decision to recognize pioneering work on climate change comes weeks before the world's leaders meet at COP26, a crucial summit in the United Kingdom.

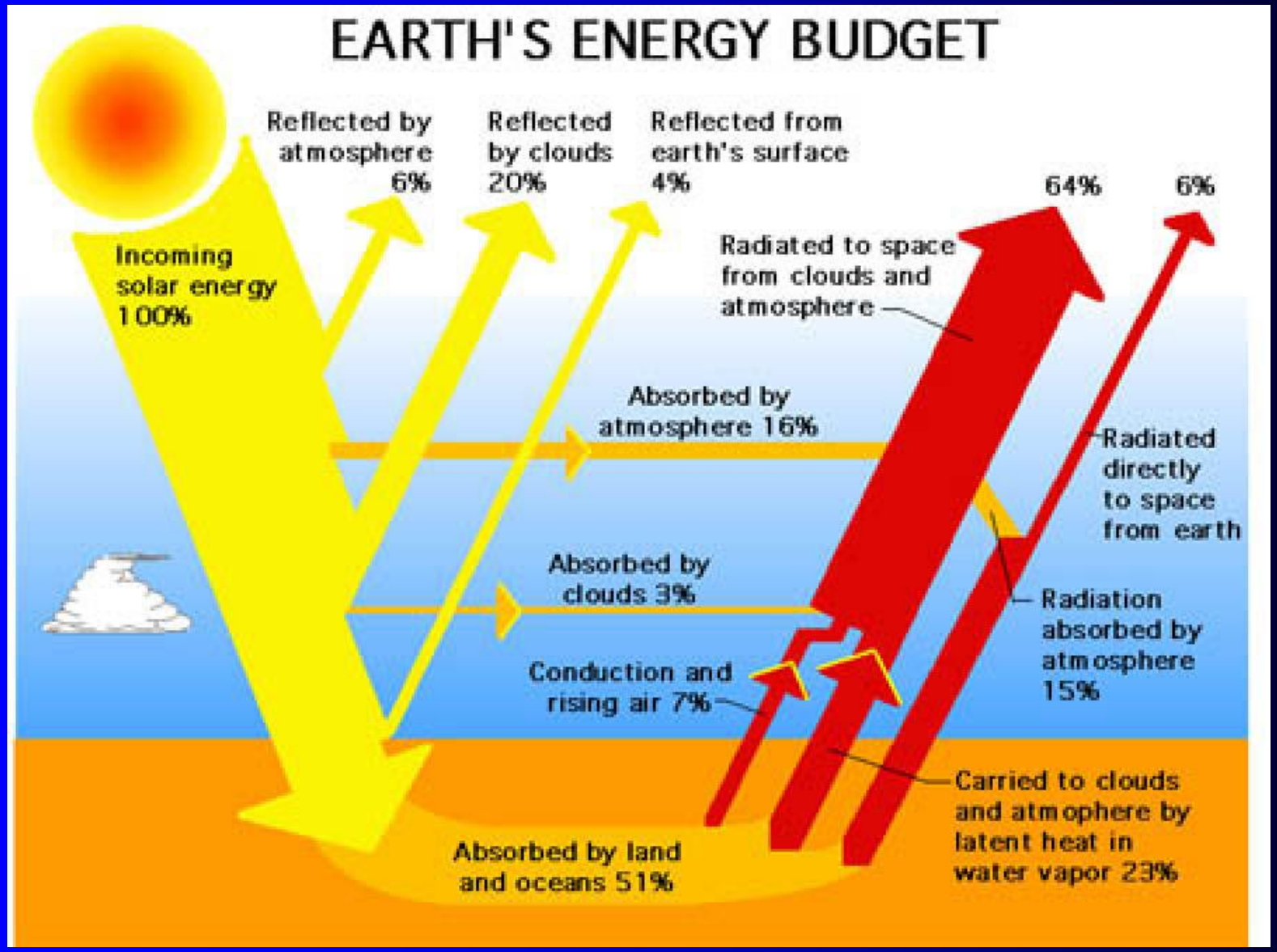
EARTH'S ENERGY BUDGET
Reflected by atmosphere 6%
Reflected by clouds 20%
Reflected from earth's surface 4%
64%
6%
Incoming solar energy 100%
Radiated to space from clouds and atmosphere
Absorbed by atmosphere 16%
Radiated directly to space from earth
Absorbed by clouds 3%
Radiation absorbed by atmosphere 15%
Conduction and rising air 7%
Carried to clouds and atmophere by latent heat in water vapor 23%
Absorbed by land and oceans 51%

Not actualized, approximation

wikipedia.org/wiki/Terestriální_záření

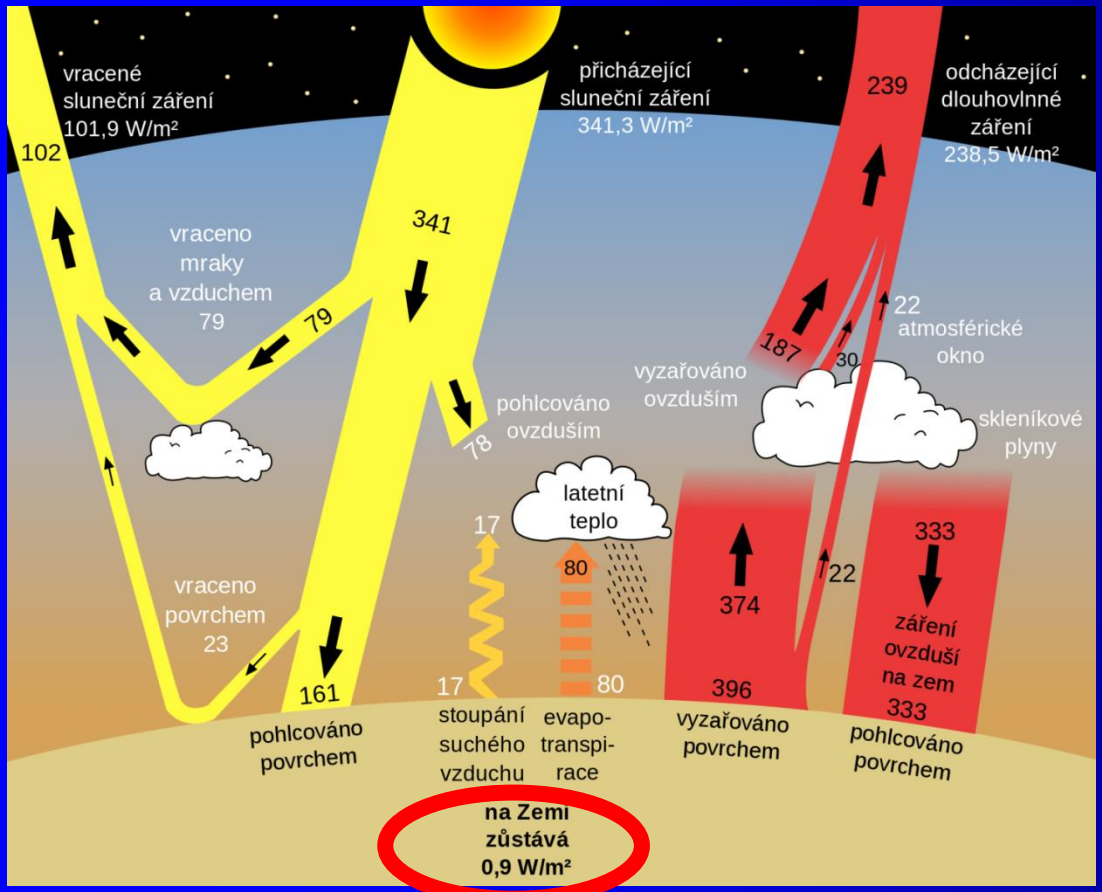

units W/m^2

difference $(E_{in} - E_{out}) = 0.9\ W/m^2$

Krátkovlnné záření ze Slunce dopadající na zemský povrch a atmosféru. Dlouhovlnná část záření je emitována z povrchu a téměř zcela absorbována do atmosféry.

V tepelné rovnováze je absorbovaná energie z atmosféry ~ stejná jako ta vydávaná do vesmíru.

Čísla ukazují výkon záření ve wattech na metr čtvereční **v období let 2000–2004**

Průměrná hustota toku energie ze zemského povrchu vzhůru činí asi 400 W/m^2, což odpovídá teplotě 16 °C; hustota toku, který Země vyzařuje do vesmíru, činí ale jen asi 240 W/m^2 a odpovídá to teplotě zhruba 255 K. Terestriální (též terestrické, pozemské) záření je v naprosté většině dlouhovlnné infračervené záření.

https://cs.wikipedia.org/wiki/

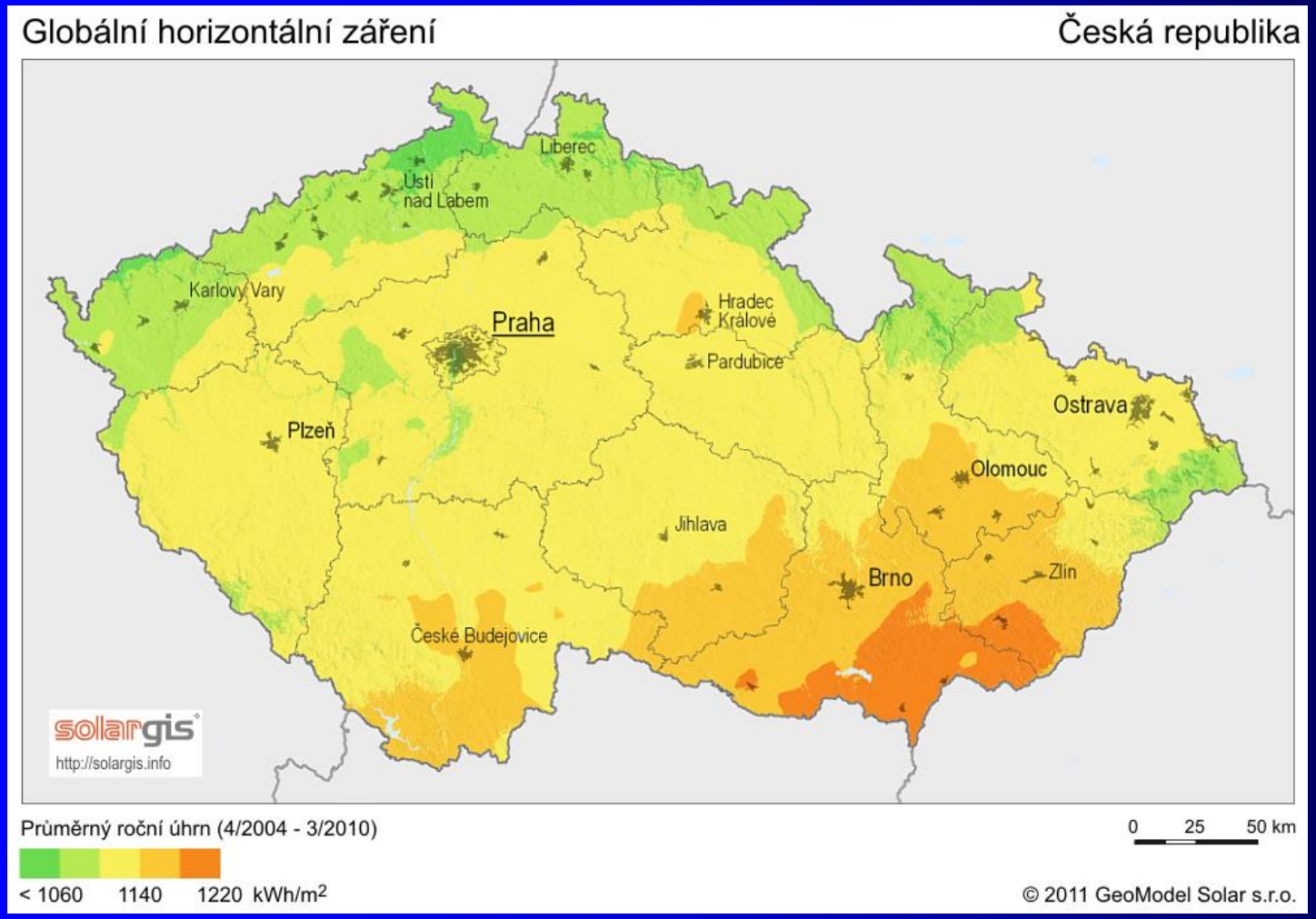

…. elektřiny stanoven na **6 Kč/kWh s DPH**

…. plynu na 3 Kč/kWh s DPH.

Temperature (???) in the ionosphere

Temperatures in the ionosphere

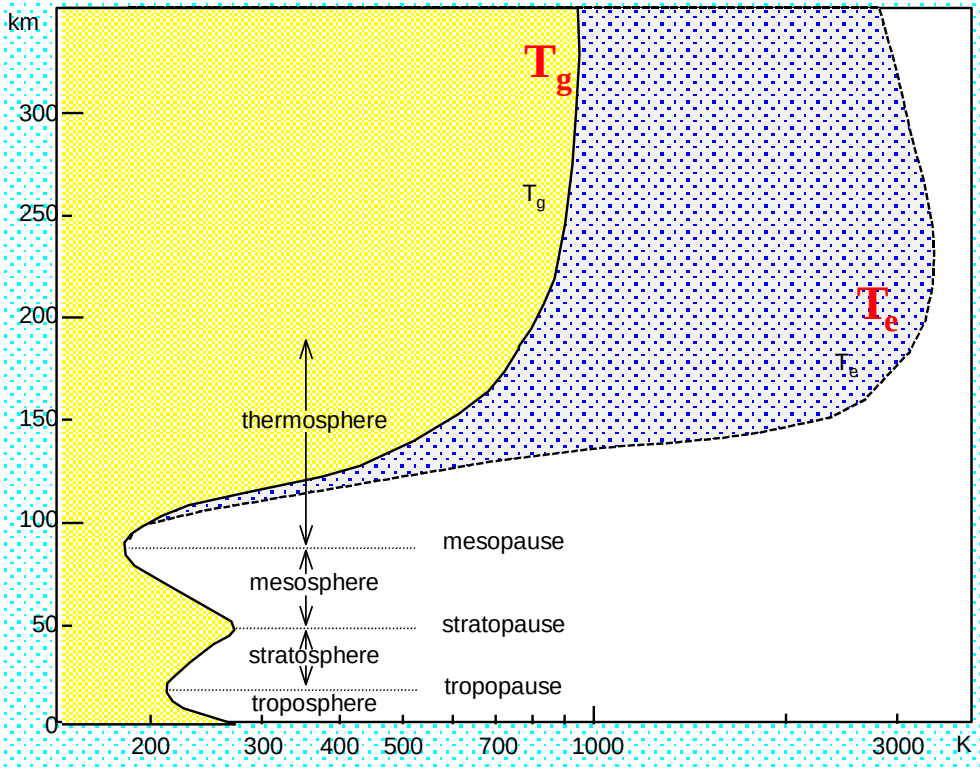

Ions chemistry

n_0 = 2,686 781 1(15)×10^{19} cm^{-3}.

Ions in the terrestrial atmosphere

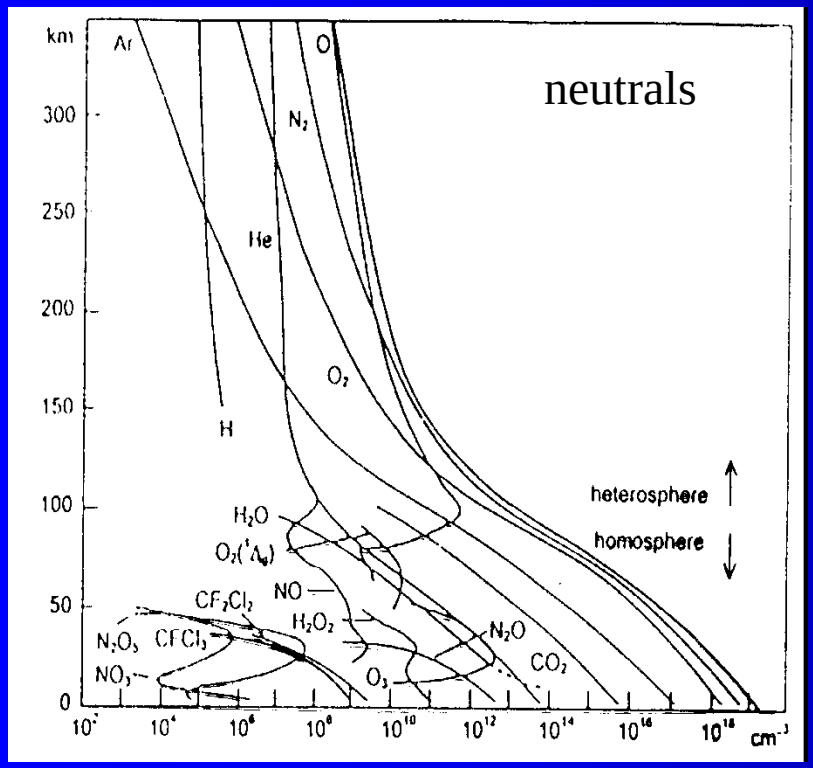

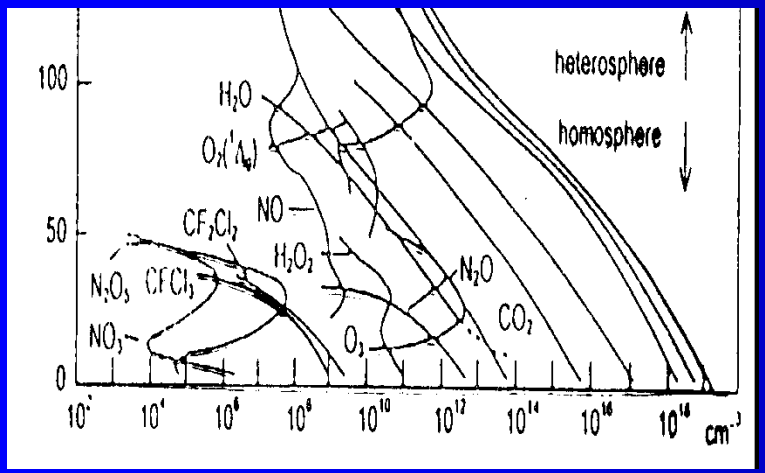

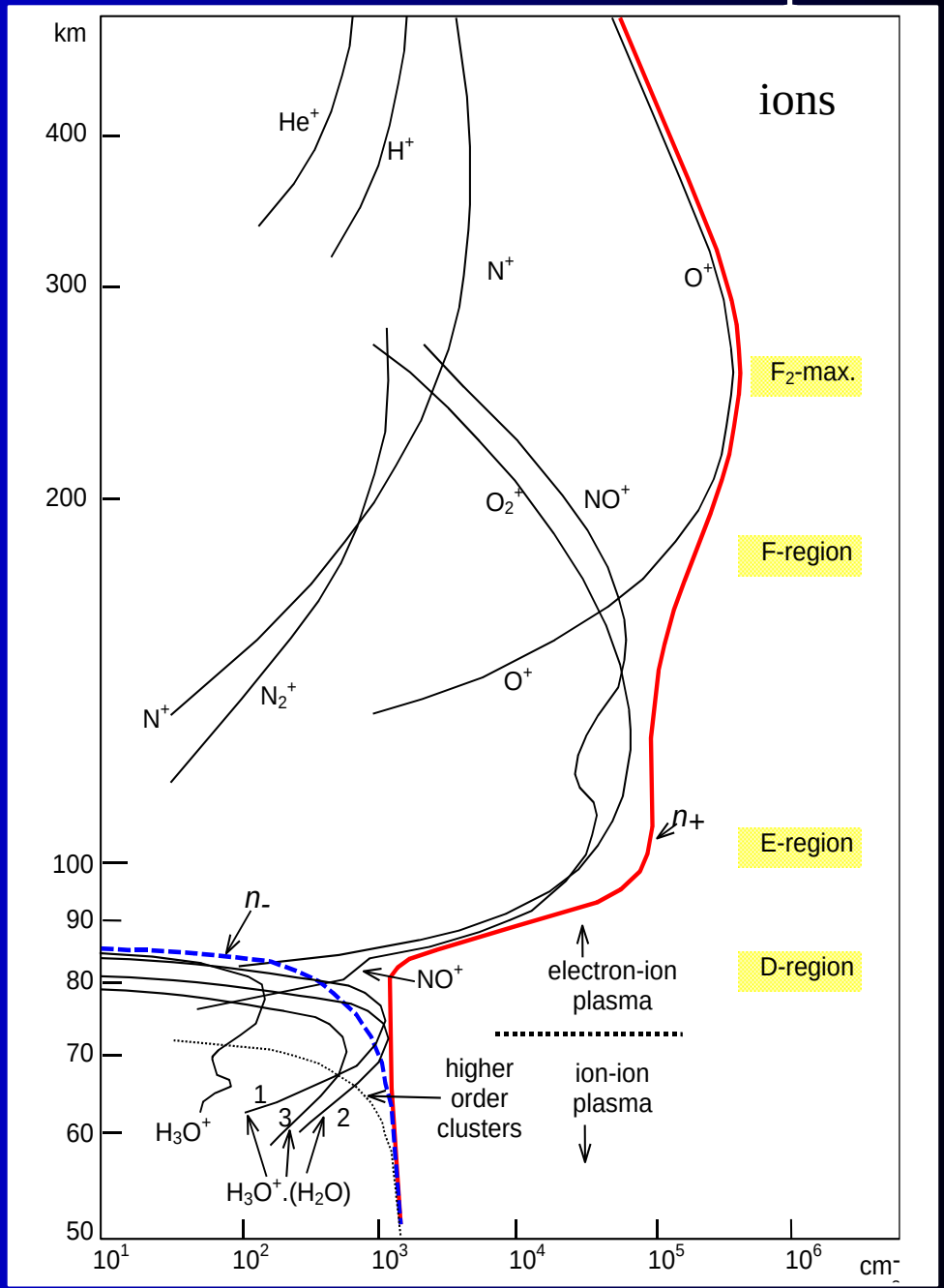

Ions in the terrestrial atmosphere

Temperatures in the ionosphere

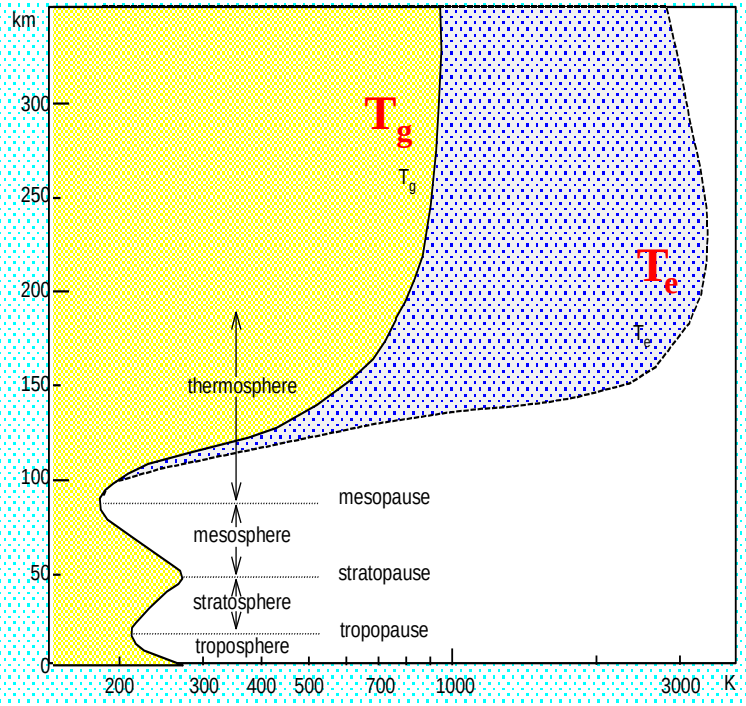

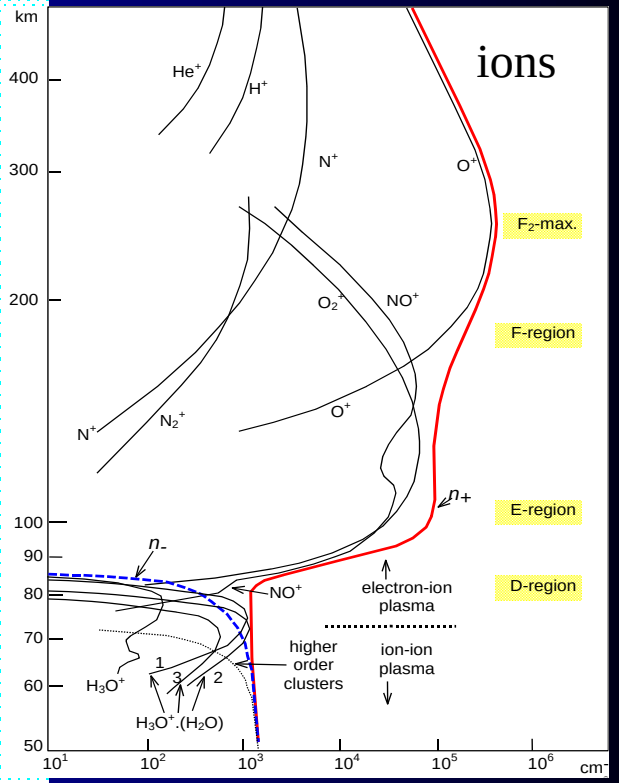

Recombination?? $\alpha(T)$

Spektrum elektromagnetického záření

Information

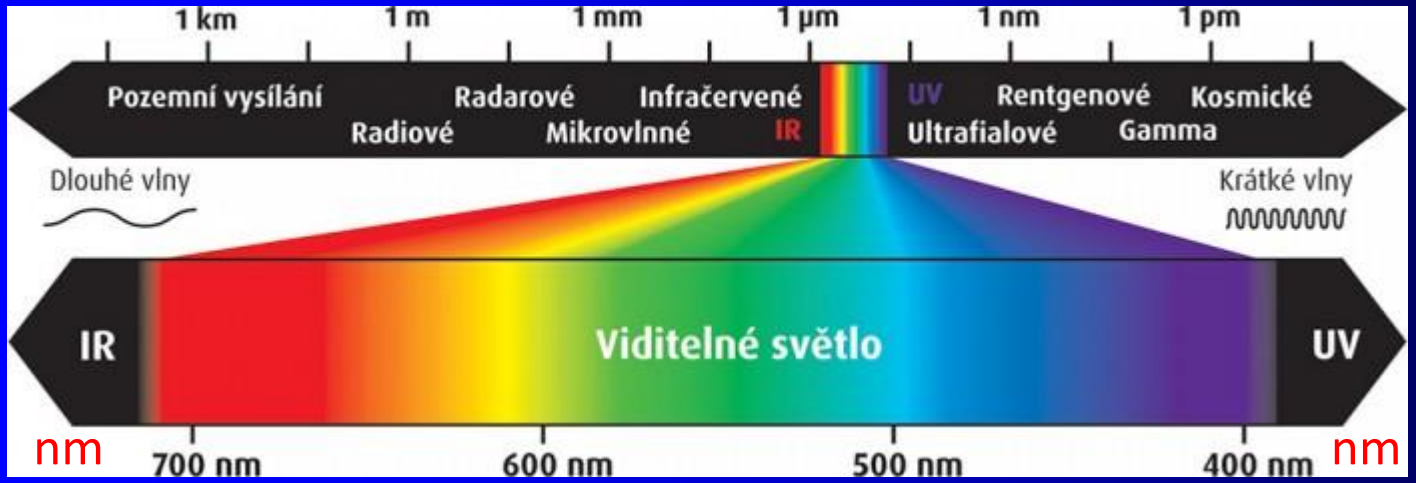

Viditelné světlo - elektromagnetické záření v rozmezí vlnových délek **380–760 nm.**

Visible light

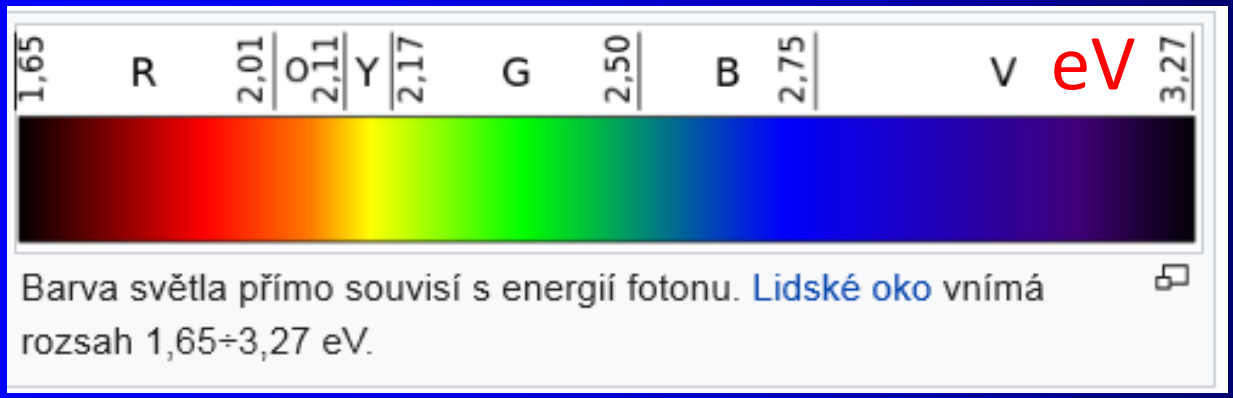

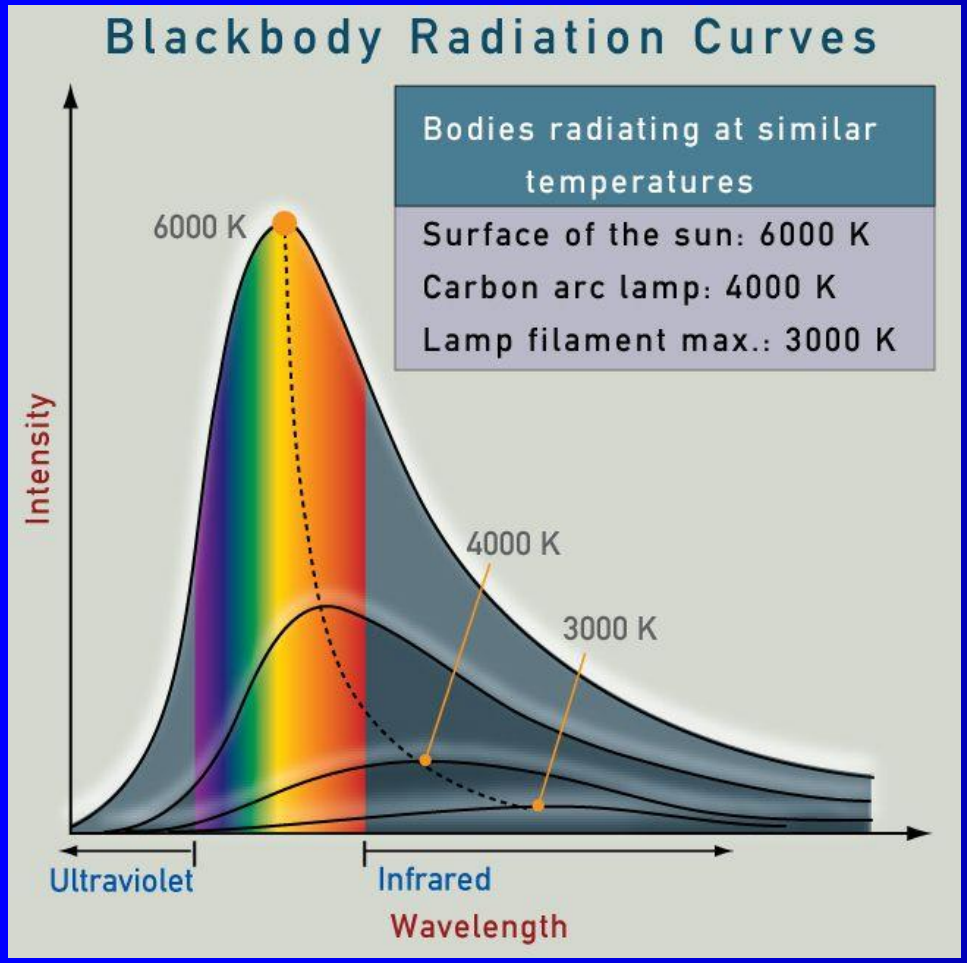

SURFACE TEMPERATURE OF THE SUN & EARTH

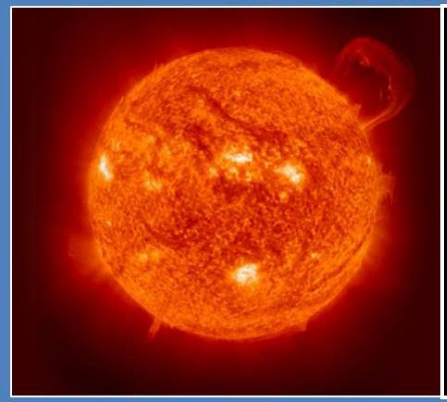

6,000K (5,727˚C or 10,340˚F)

288K (15˚C or 59˚F)

Black body radiation at ~ 5 800 K

Temperature on Sun ~ 5 800 K

Záření černého tělesa

Max Planck (1858 – 1947)

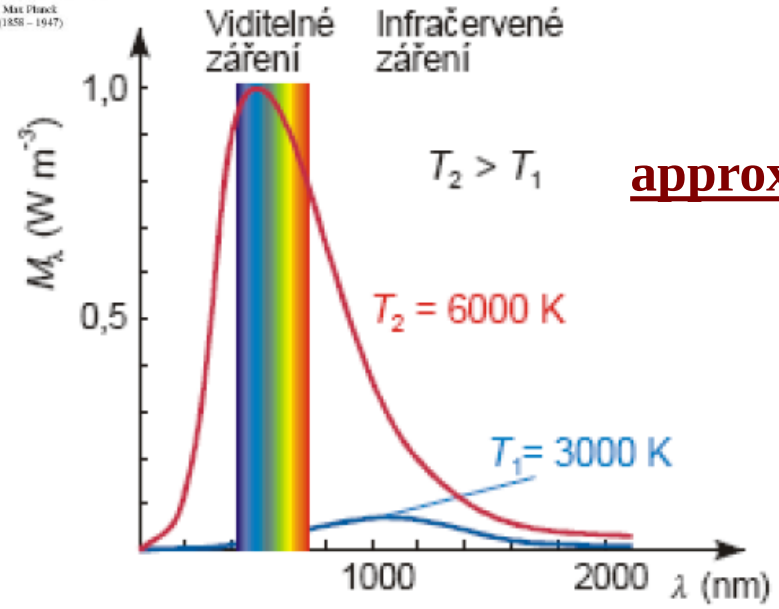

approximately

approximately

Průběh spektrální intenzity vyzařování v závislosti na vlnové délce a teplotě.
S rostoucí termodynamickou teplotou tělesa se zvyšuje maximum spektrální intenzity vyzařování a posouvá se směrem k nižší vlnové délce

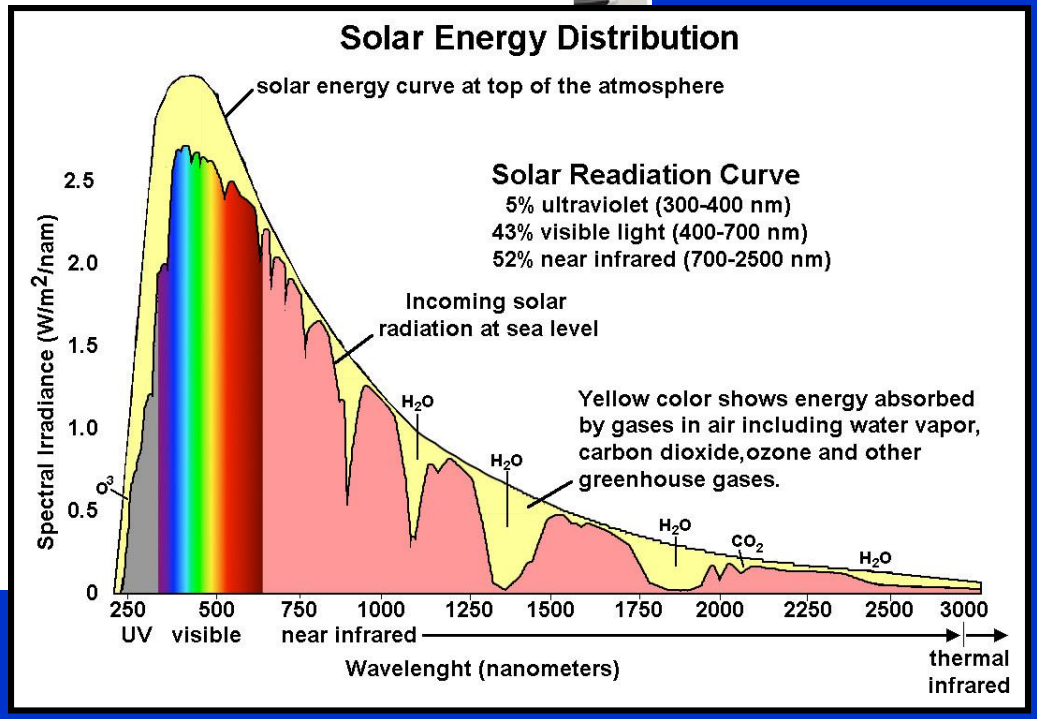

Spectrum of solar radiation modified by atmospheric absorption

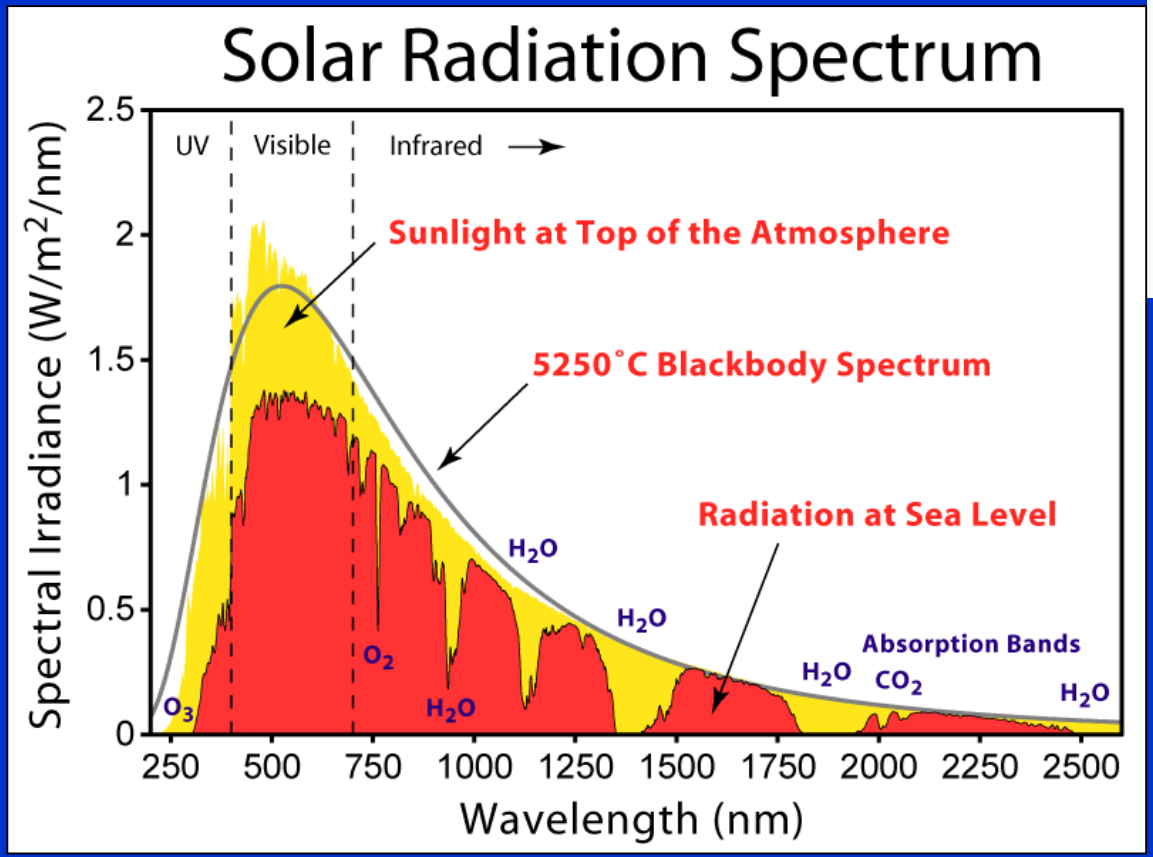

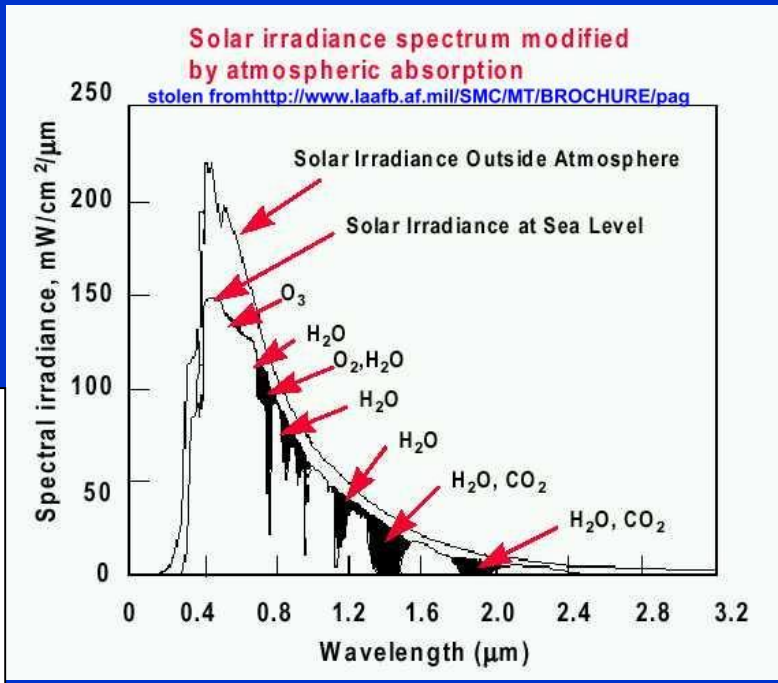

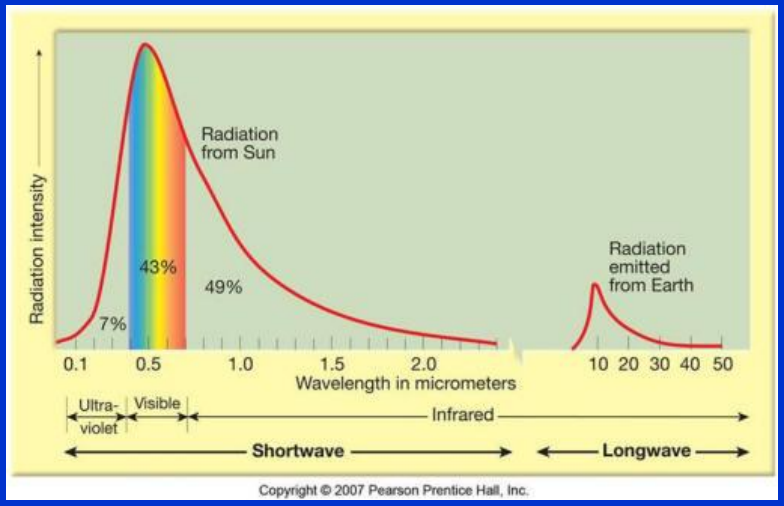

Detail 0.1-100 μm

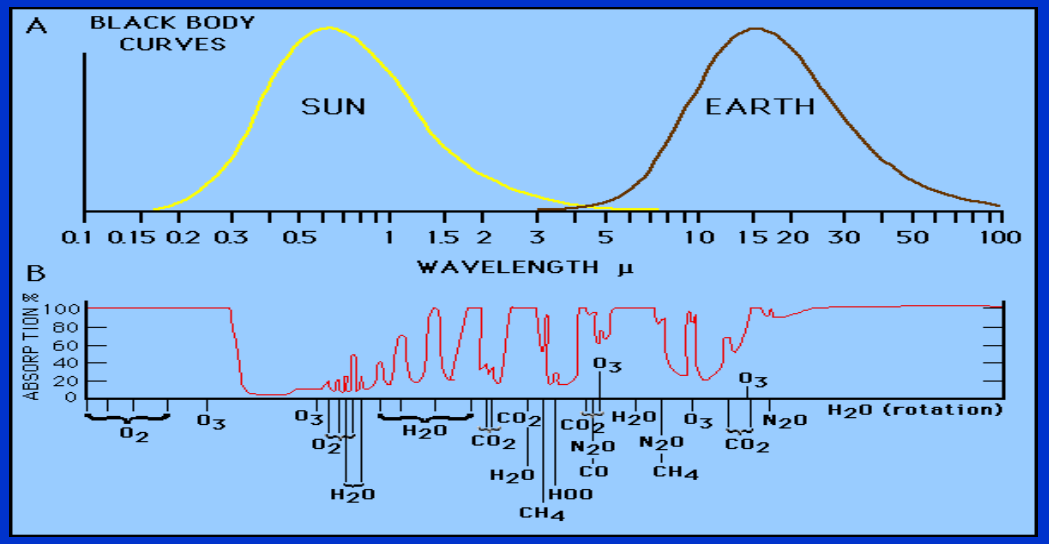

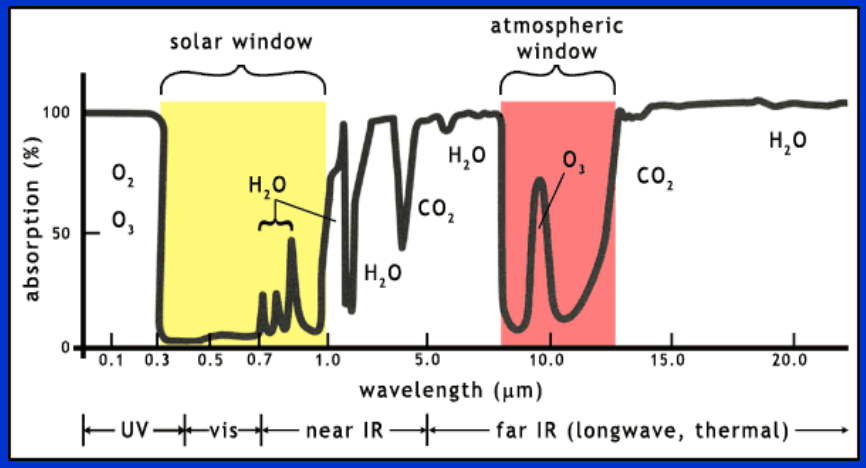

Figure 3. ***The wavelengths of incoming solar radiation and emitted radiation absorbed by the Earth's atmosphere, showing the solar window and atmospheric (thermal) window. The graph shows the regions of the electromagnetic spectrum (light) that are absorbed by specific molecules. Key: CO_2, carbon dioxide; H_2O, water; IR, infrared light; O_2, oxygen; O_3, ozone; UV, ultraviolet light; vis, visible light (adapted from a figure in Turco 2002, p334)***

Absorption

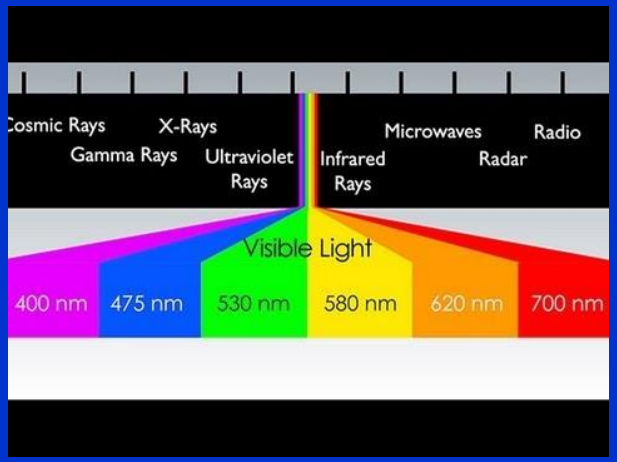

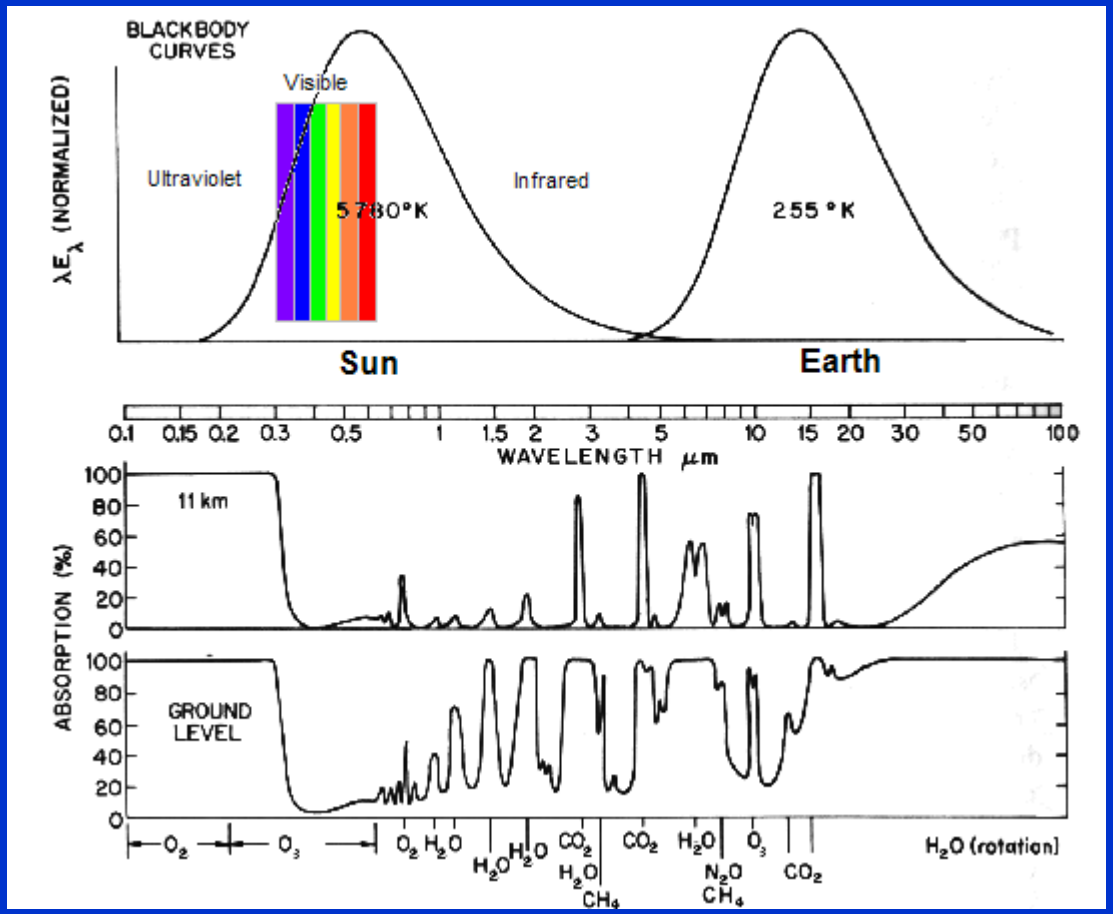

11 km

Ground level

approximation

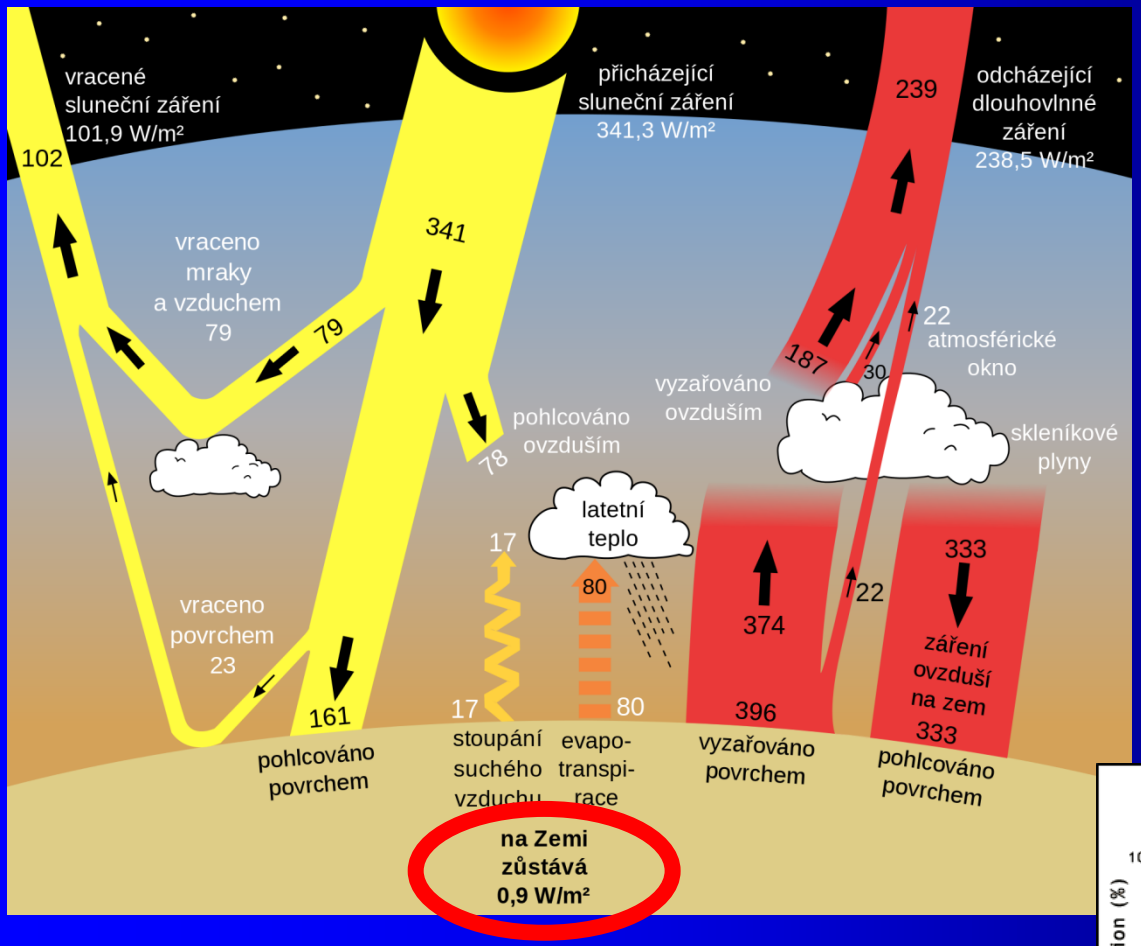

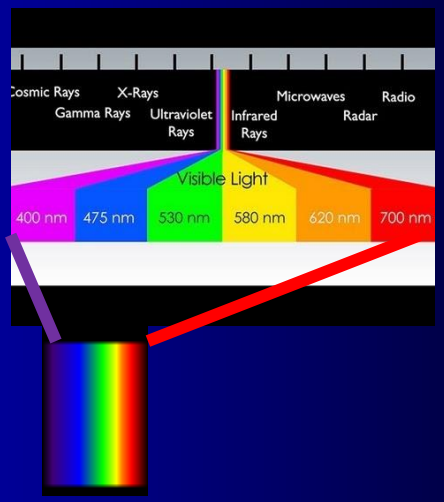

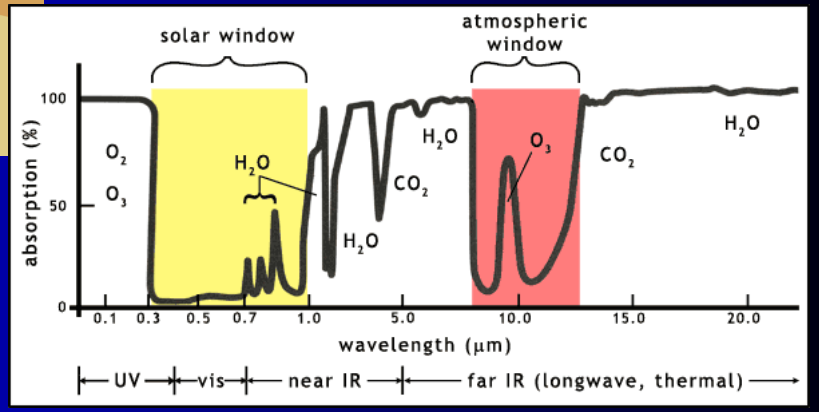

Krátkovlnné záření ze Slunce dopadající na zemský povrch a atmosféru. Dlouhovlnná část záření je emitována z povrchu a téměř zcela absorbována do atmosféry. V tepelné rovnováze je absorbovaná energie z atmosféry stejná jako ta vydávaná do vesmíru. Čísla ukazují výkon záření ve wattech na metr čtvereční v období let 2000–2004

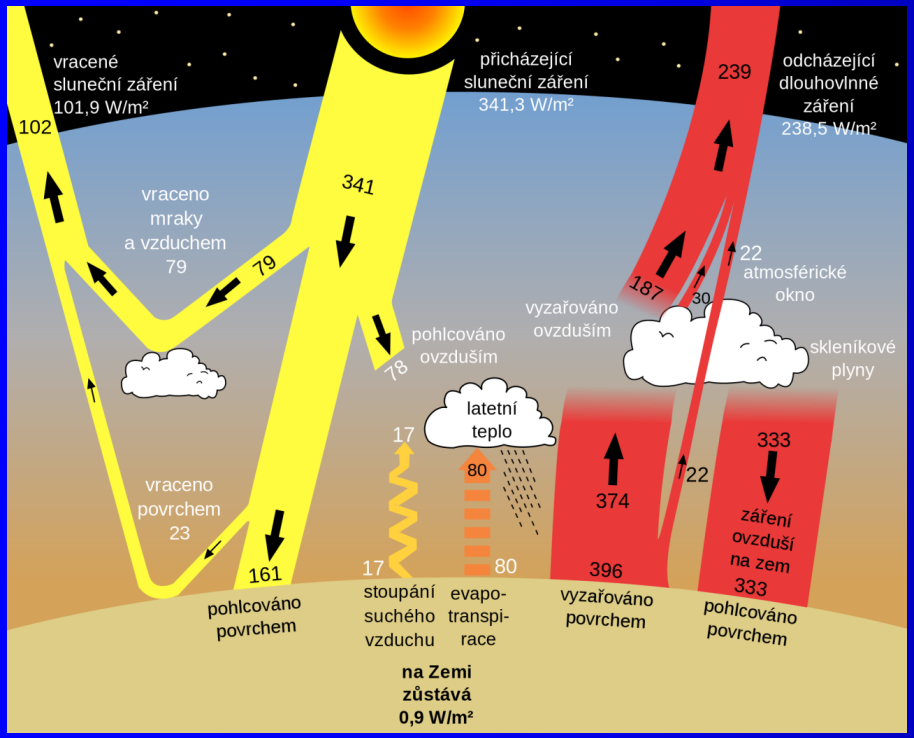

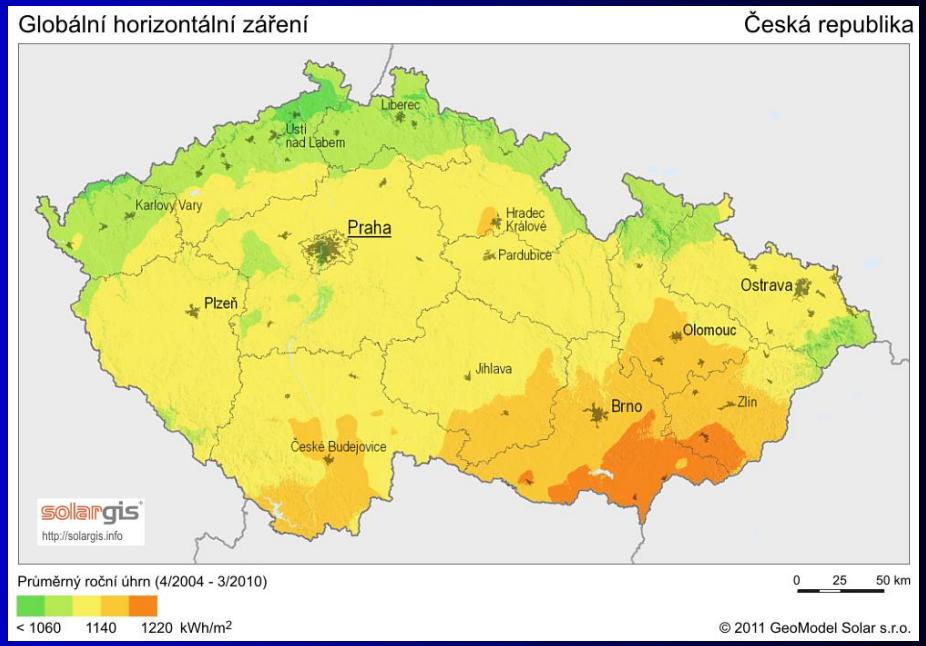

…. elektřiny stanoven na **6 Kč/kWh s DPH**

…. plynu na 3 Kč/kWh s DPH.

Back to PLASMA PHYSICS

Kinetic energy of single particle
Temperature of the gas….
Temperature of plasma ….Electrons ….. Ions….. Neutrals

$E \leftrightarrow kT$

1eV ~ 11 604.5 K

1K ~ 9×10^{-5}eV

$E \leftrightarrow 3/2 * kT$

……

Niels Bohr

Energy levels of H atom

Spektrum atomu vodíku

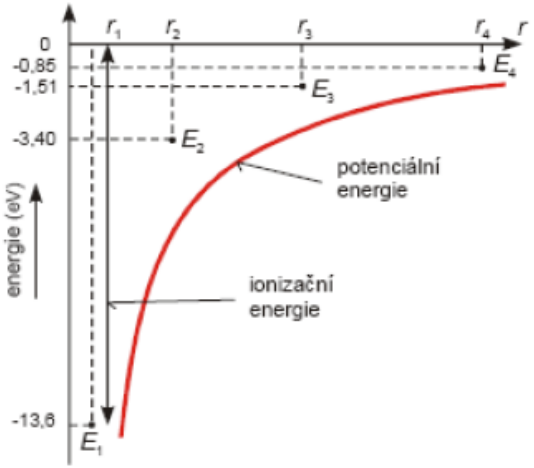

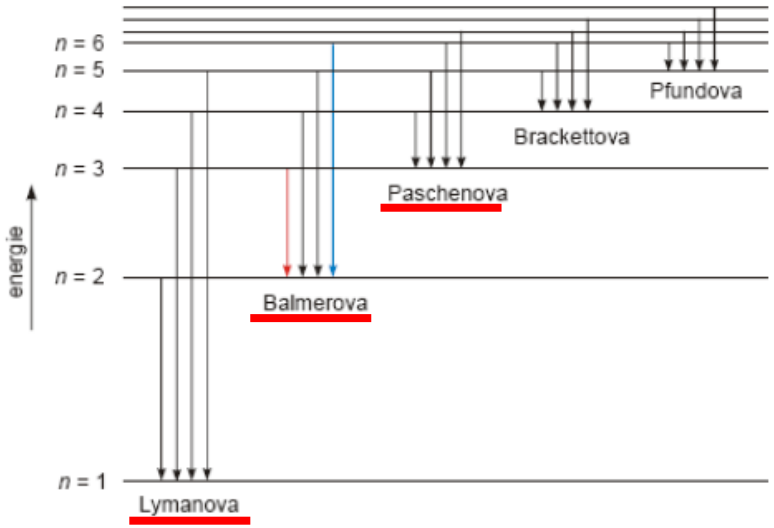

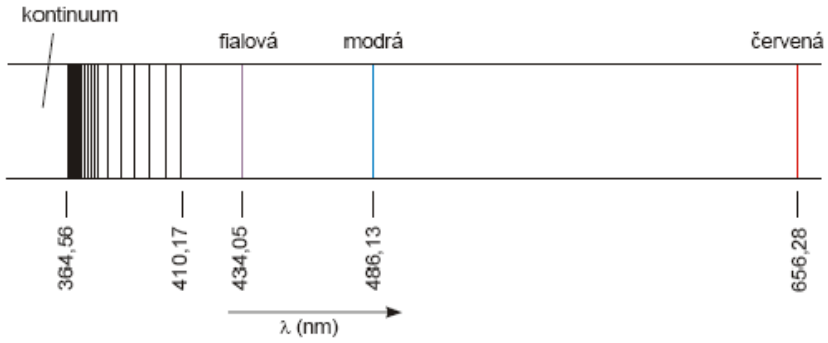

$$h\nu = 13.6\left(\frac{1}{n_f^2} - \frac{1}{n_i^2}\right)[eV]$$

Energy levels of H atom

Selection rule $\Delta l = \pm 1; \quad \Delta m_l = 0, \pm 1$

Angular momentum of photon is s=1

Grotrian diagram H

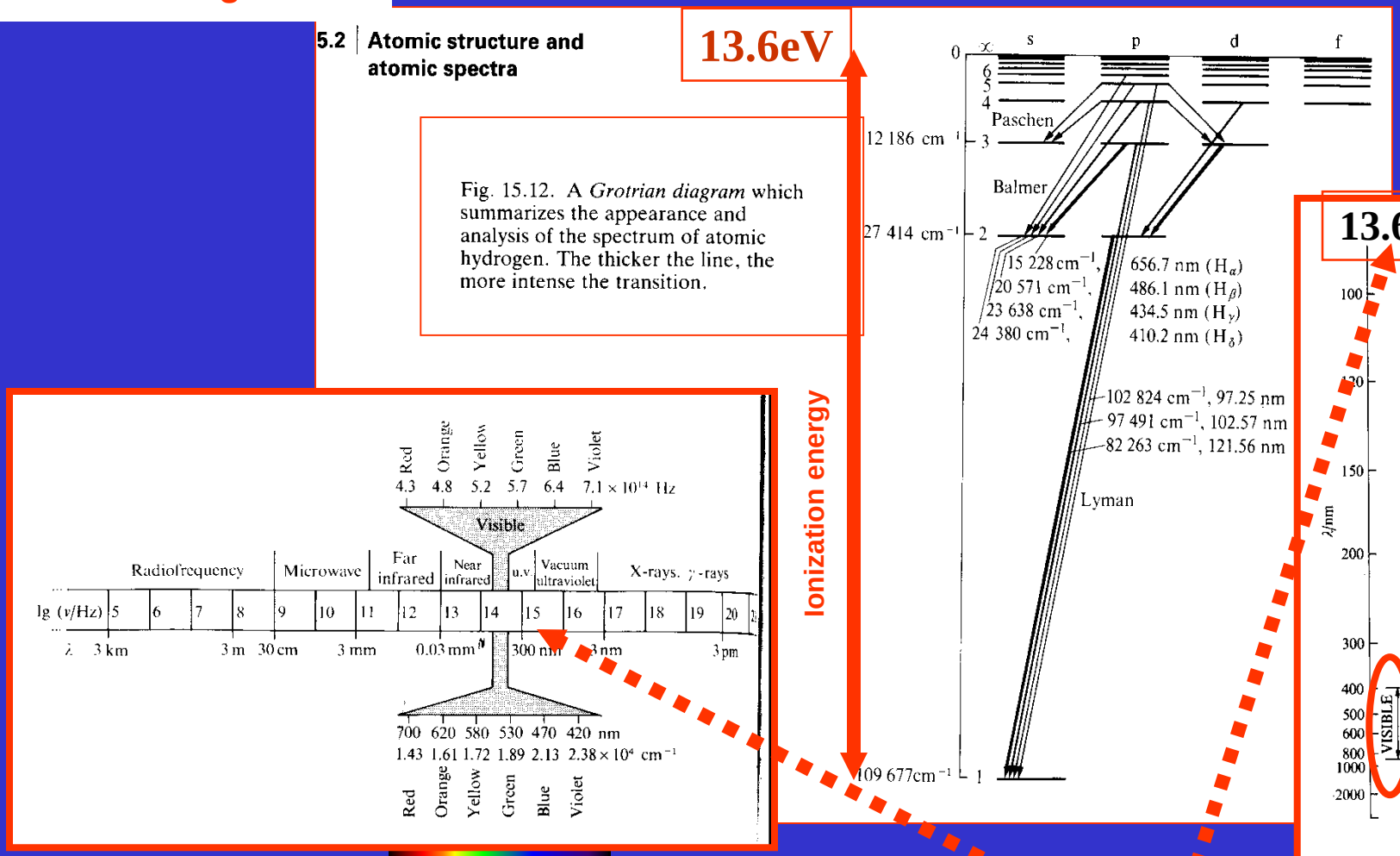

5.2 | Atomic structure and atomic spectra

Fig. 15.12. A *Grotrian diagram* which summarizes the appearance and analysis of the spectrum of atomic hydrogen. The thicker the line, the more intense the transition.

Fig. 15.1. The spectrum of atomic hydrogen. The spectrum is shown on the left, and is analysed into its overlapping series on the right. Note that the Balmer series lies in the visible region.

$$E_n = -\frac{Z^2 \mu e^4}{32\pi^2 \varepsilon_0^2 \hbar^2} x \frac{1}{n^2}$$

$$h\nu = 13.6\left(\frac{1}{n_f^2} - \frac{1}{n_i^2}\right)[eV]$$

13.6eV x 8065,5 cm^{-1}→ 109000 cm^{-1}→ 91nm

He energies

Energy levels of He

Grotrian diagram He
Ionization energy He

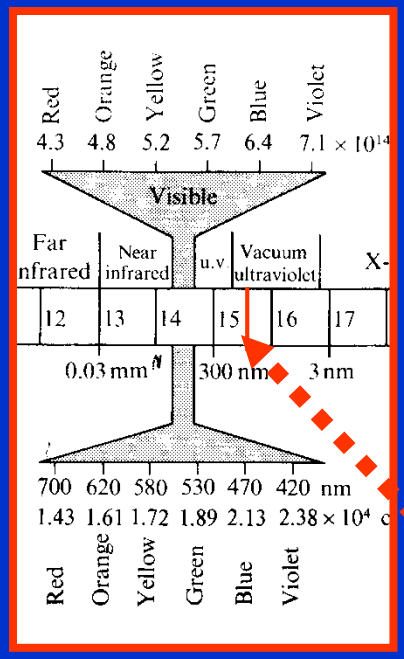

24.46eV

He ionization energy

24.46eV → ~198400 cm^{-1} → ~50nm
vacuum ultraviolet

PARA

ORTHO

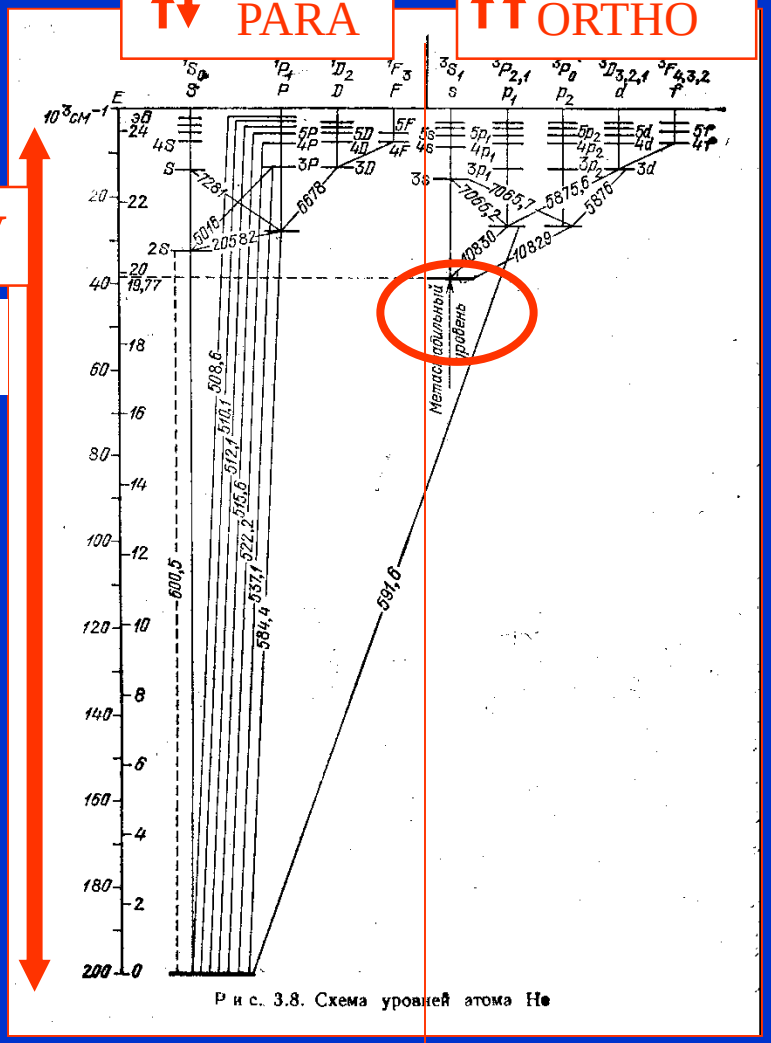

Singlet

Triplet

Spin of electrons

He^{+} ionization energy

$$E_n = -\frac{Z^2 \mu e^4}{32\pi^2 \varepsilon_0^2 \hbar^2} x \frac{1}{n^2} = -4x \frac{\mu e^4}{32\pi^2 \varepsilon_0^2 \hbar^2} x \frac{1}{n^2}$$

$$h\nu = 4x13.6\left(\frac{1}{n_i^2} - \frac{1}{n_f^2}\right)[eV]$$

He^{+} ionization energy (to form He^{++}) = 54.4 eV

Rydberg atom

$$\langle r \rangle_{n,l} = n^2 \left\{ 1 + \frac{1}{2}\left(1 - \frac{l(l+1)}{n^2} \right) \right\} x \frac{a_0}{Z}$$

$$\langle r \rangle_{n,l=0} = n^2 \left\{ \frac{3}{2} \right\} x \frac{a_0}{Z}$$

Scientific American 1981

Highly Excited Atoms

They are floppy, fragile and huge. Some of them have been found to have a diameter of almost a hundredth of a millimeter, which is 100,000 times the diameter of an atom in its lowest energy state

by Daniel Kleppner, Michael G. Littman and Myron L. Zimmerman

Bohr radius ~ 0.5 A (**angstrom**)
1A = 10^{-8} cm^{-1}

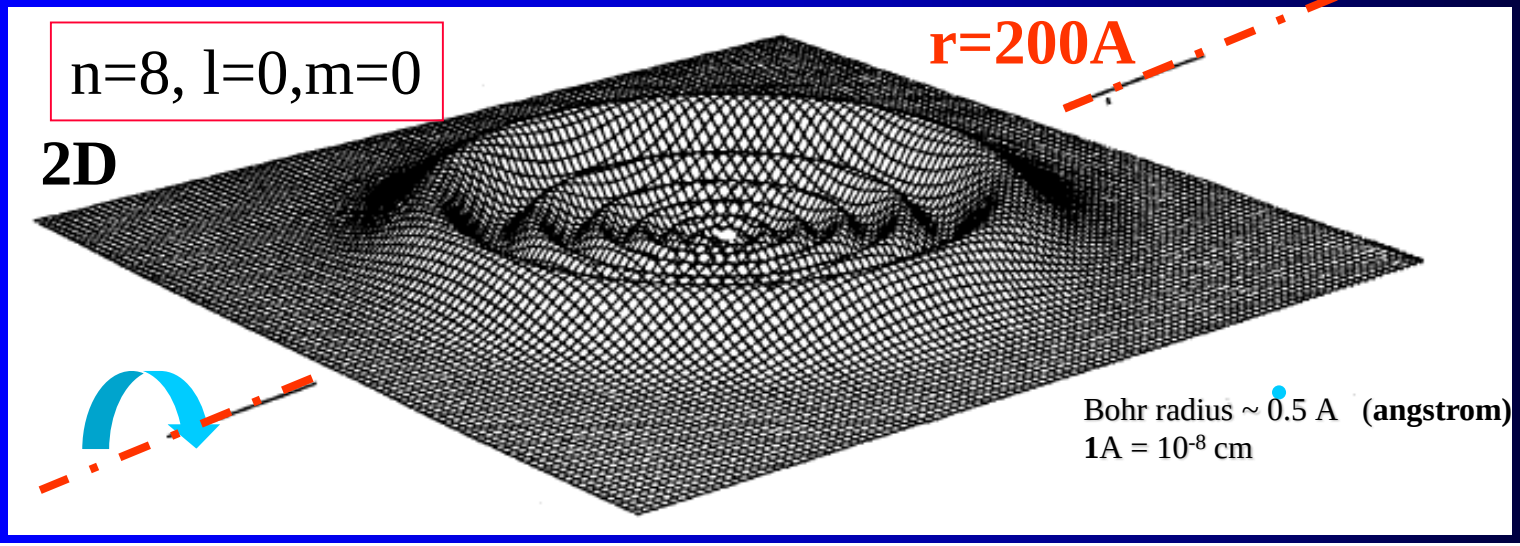

ELECTRON-CHARGE DENSITY OF HYDROGEN is graphed on a plane passing through the single proton that forms the nucleus of the atom (*colored dot*). The states of hydrogen are described by the three quantum numbers n, l and m; n is a positive integer that designates the energy level of the electron, l is an integer between 0 and $n-1$ that corresponds to the magnitude of the eccentricity (or angular momentum) of the electron's orbit and m is an integer between $-l$ and $+l$ that describes the orbit's orientation. In the state where $n=8$, $l=0$ and $m=0$ (*upper graph*) charge density is a series of concentric wavelike peaks. In three dimensions the charge density can be visualized as a series of spherical shells formed by rotating the graph about an axis passing through the nucleus. The distance from the nucleus to the edge of the plane corresponds to 2×10^{-6} centimeter, which is 380 times the Bohr radius (the radius of a hydrogen atom in the lowest energy state). In a weak electric field (*lower graph*) the electron in an $n=8$ state of hydrogen "stands" far to one side of the proton, forming an electric dipole. (In this state $m=0$ and the angular momentum is a mixture of all possible values of l from zero to 7.) A dipole consists of two equal and opposite charges separated by a fixed distance. Many atoms act as dipoles, but most of them are not true dipoles: there is no separation of charges but only a slight distortion of the charge cloud. In the diagrammed state the separation is real. An atom whose outermost electron has been excited to a high energy level is often called a Rydberg atom. All Rydberg atoms are true dipoles.

Rydberg atom in electric field

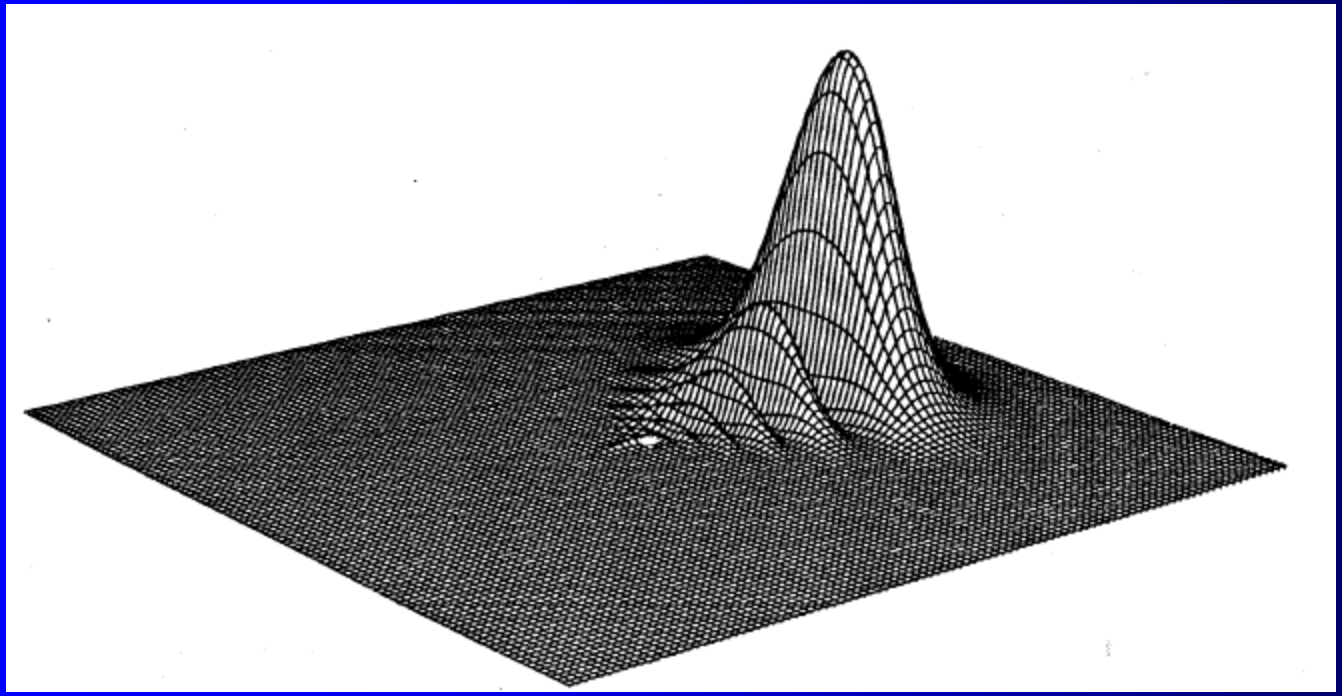

n=8, l=0,m=0

All Rydberg atoms are true dipoles.

Properties of Rydberg atoms

Table 1. Properties of Rydberg atoms.

Property	n dependence	Numerical values $n=1$	$n=10$	$n=100$	$n=1000$
Bohr radius	$n^2 a_0$	5.3×10^{-9} cm	5.3×10^{-7} cm	5.3×10^{-5} cm	5.3×10^{-3} cm
Binding energy	R/n^2	13.6 eV	136 meV	1.36 meV	13.6 μeV
RMS velocity of Rydberg electron	v_0/n	2.2×10^{8} cm s^{-1}	2.2×10^{7} cm s^{-1}	2.2×10^{6} cm s^{-1}	2.2×10^{5} cm s^{-1}
Orbital period	$n^3\tau$	1.5×10^{-16} s	1.5×10^{-13} s	1.5×10^{-10} s	1.5×10^{-7} s
Classical field ionization threshold	$\frac{1}{16}n^4$	3.2×10^{8} V cm^{-1}	3.2×10^{4} V cm^{-1}	3.2 V cm^{-1}	3.2×10^{-4} V cm^{-1}

Bohr radius ~ 0.5 Å (**angstrom**)

1Å = 10^{-8} cm^{-1}

Small differences in zero point energies ….
not sufficient to describe IMR @ low T
nuclear spin selection rules

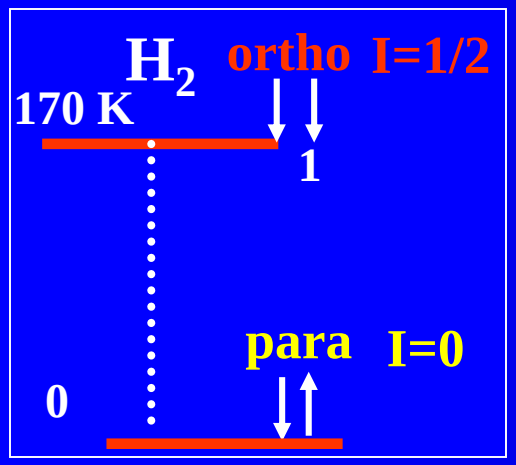

H_2

Energy levels
Rotational states

***E*←→kT**
1eV ~ 11 604.5 K
1K ~ 9×10^{-5}eV

Energies of H_2 and D_2

1eV corresponds to ~ 11604K

H_2	B_e=60.80
D_2	B_e=30.429
HD	B_e=45.655

	j	E/meV	E/in K	300K	250K	80K	35K	low
H_2	0	0	0	0.128	0.150	0.248	0.25	1/4
	1	14.7	170.6	0.657	0.694	0.75	0.75	3/4
	2	44	510.6	0.117	0.098	0.002	0	
	3	87	1009.5	0.092	0.055	0	0	
	4	145	1682.6	0.004	0.0016	0	0	
	5	215	2494.9	0.001	0.0002	0	0	
D_2	0	0	0	0.179	0.213	0.552	0.664	2/3
	1	7.3	84.71	0.202	0.227	0.329	0.333	1/3
	2	22	255.29	0.383	0.384	0.114	0.002	
	3	44	510.6	0.115	0.098	0.004	0	
	4	72	835.5	0.098	0.066	0.0001	0	
	5	108	1253.2	0.015	0.008	0	0	
HD	0	0	0					1
	1	11.04	128.1					
	2	33.05	383.4					

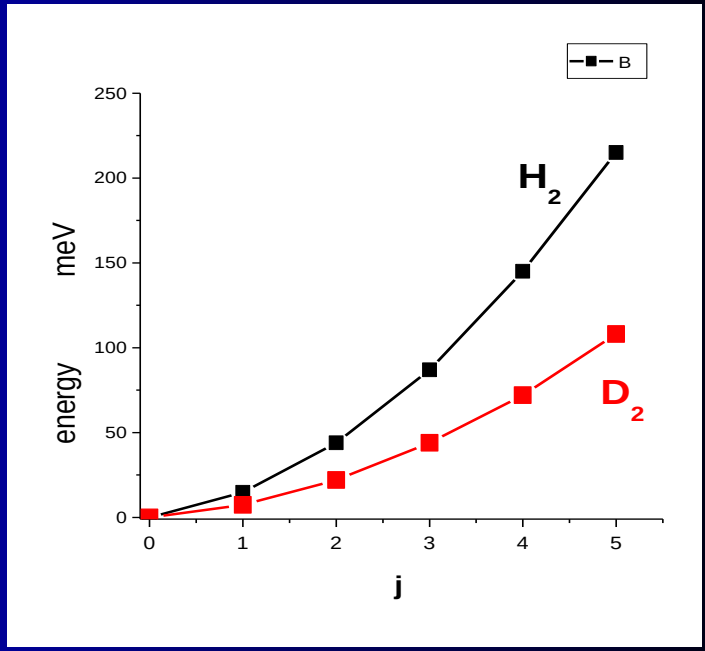

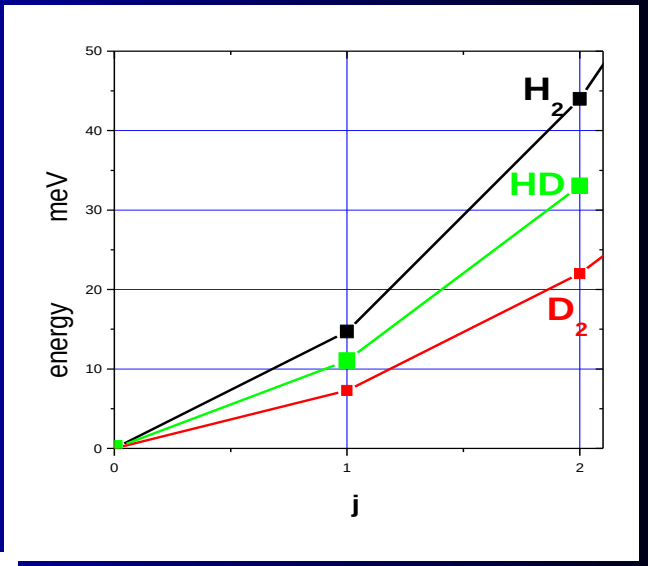

H_2 and D_2 are taken from O. Wick dissertation
HD is calculated using B_e from Herzberg and comparison with H_2 from table

Energy levels
Rotational states

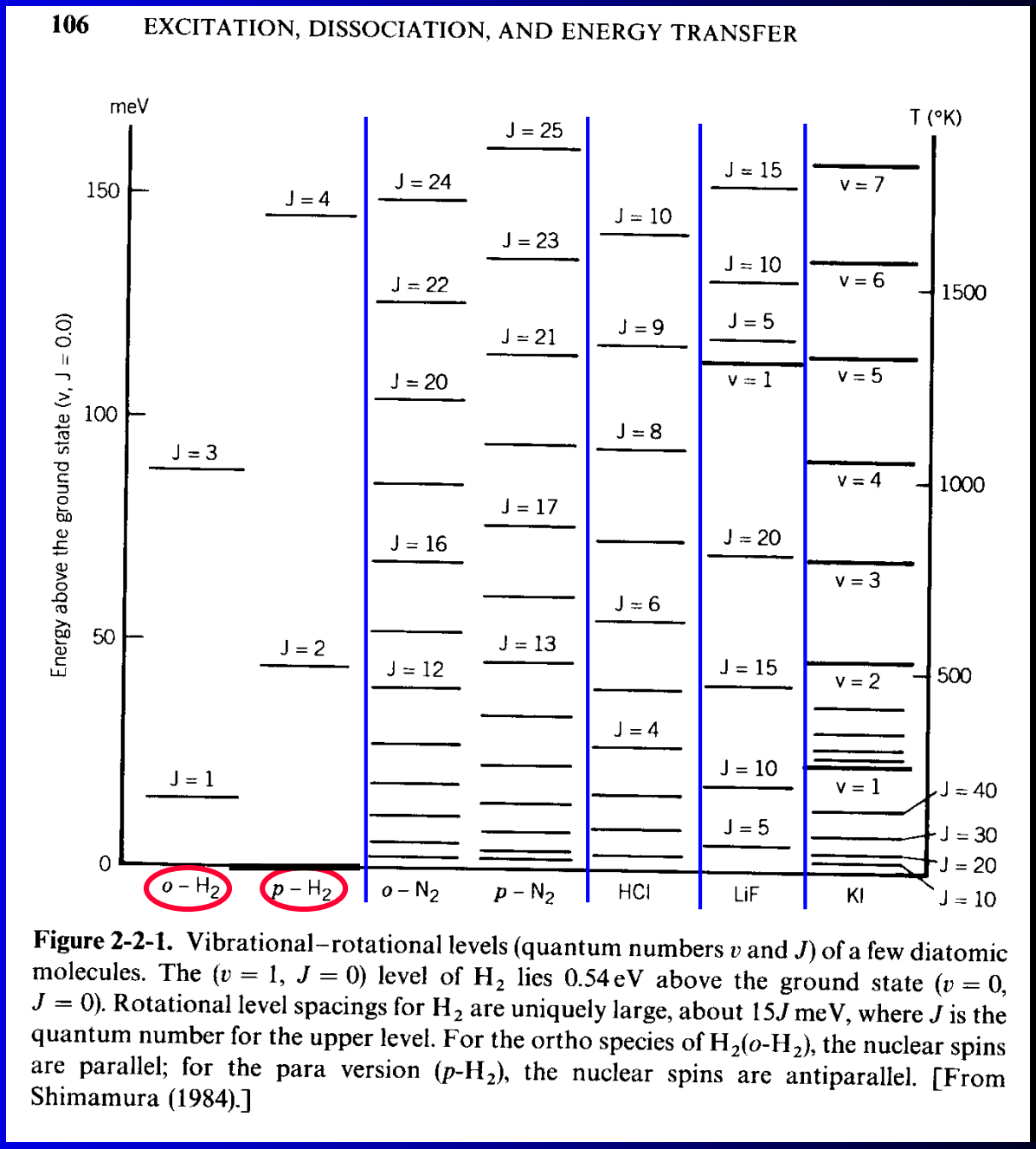

Figure 2-2-1. Vibrational–rotational levels (quantum numbers v and J) of a few diatomic molecules. The ($v = 1$, $J = 0$) level of H_2 lies 0.54 eV above the ground state ($v = 0$, $J = 0$). Rotational level spacings for H_2 are uniquely large, about $15J$ meV, where J is the quantum number for the upper level. For the ortho species of H_2(o-H_2), the nuclear spins are parallel; for the para version (p-H_2), the nuclear spins are antiparallel. [From Shimamura (1984).]

$E \leftrightarrow kT$
1eV ~ 11 604.5 K
1K ~ 9×10^{-5}eV

Potential curves N_2 , N_2^+

Vibrational states
Electronic states
Ionisation

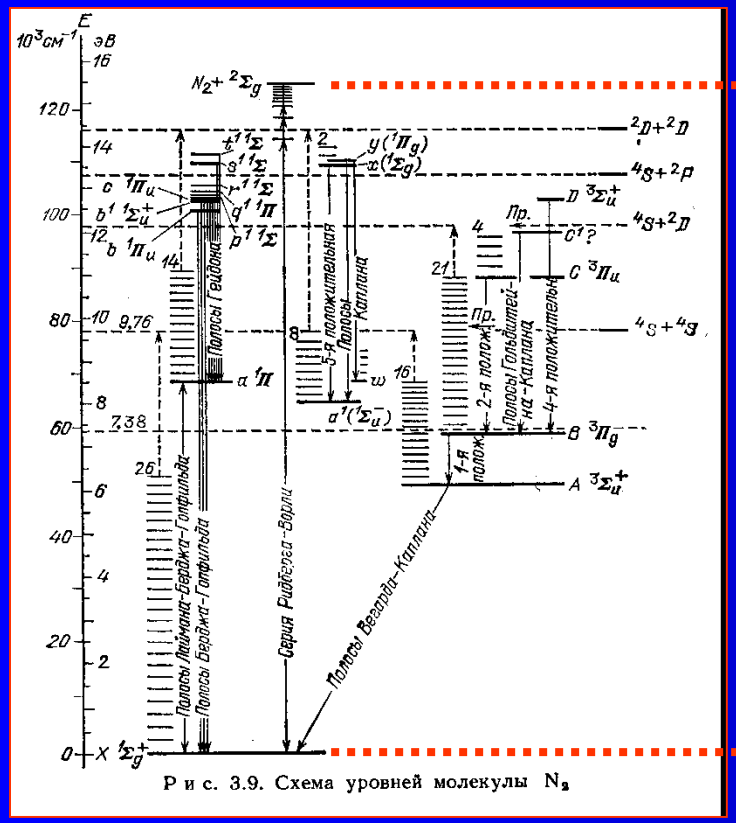

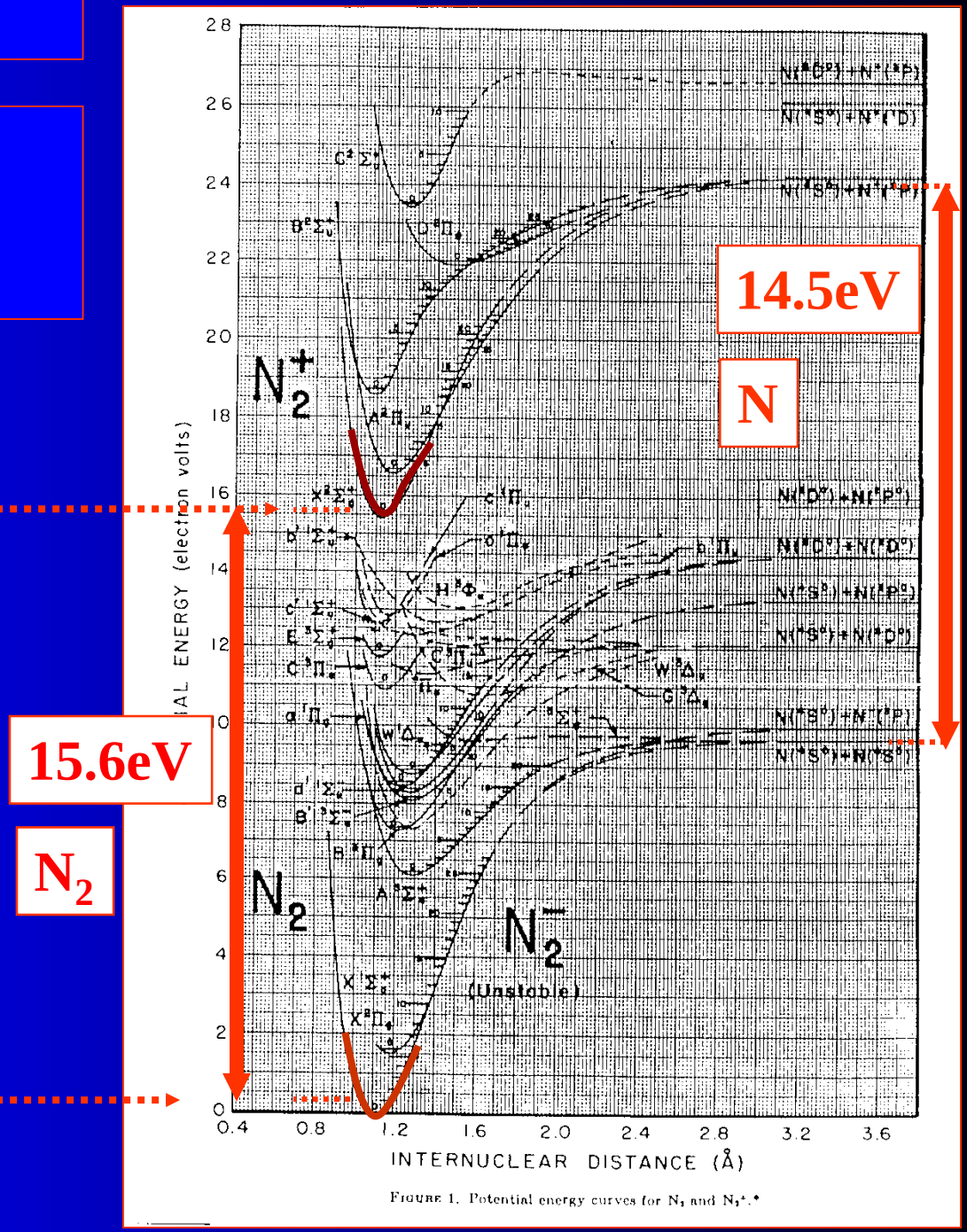

Information

Classical or quantum approach?

Electron:

1eV → $v=5.9\times10^{7}$cm s^{-1}

$\tau\sim a_0/v \sim 10^{-8}/ 5.9\times10^{7}=2\times10^{-16}$s

$\lambda\sim 2A = 2\times10^{-8}$cm de Broglie

za 1μs…….. 1μs x 5.9×10^{7}cm s^{-1}=59cm

Ar+:

1eV → $v=2\times10^{5}$cm s^{-1}

$\tau\sim a_0/v \sim 10^{-8}/ 2\times10^{5}\sim6\times10^{-14}$s

$\lambda\sim 9\times10^{-11}$cm de Broglie

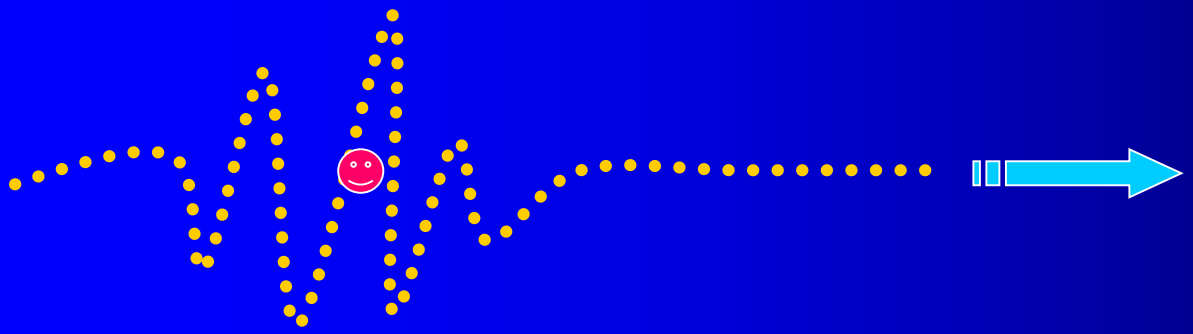

De Broglie wave length

$$\lambda = \frac{h}{p} = \frac{h}{mv}\sqrt{1 - \frac{v^2}{c^2}}$$

$$\lambda_e(4K) \sim 540\,A \sim 54x10^{-9}\,m$$

$$\lambda_e(1eV) \sim 11.6\,A \sim 1.16x10^{-9}\,m$$

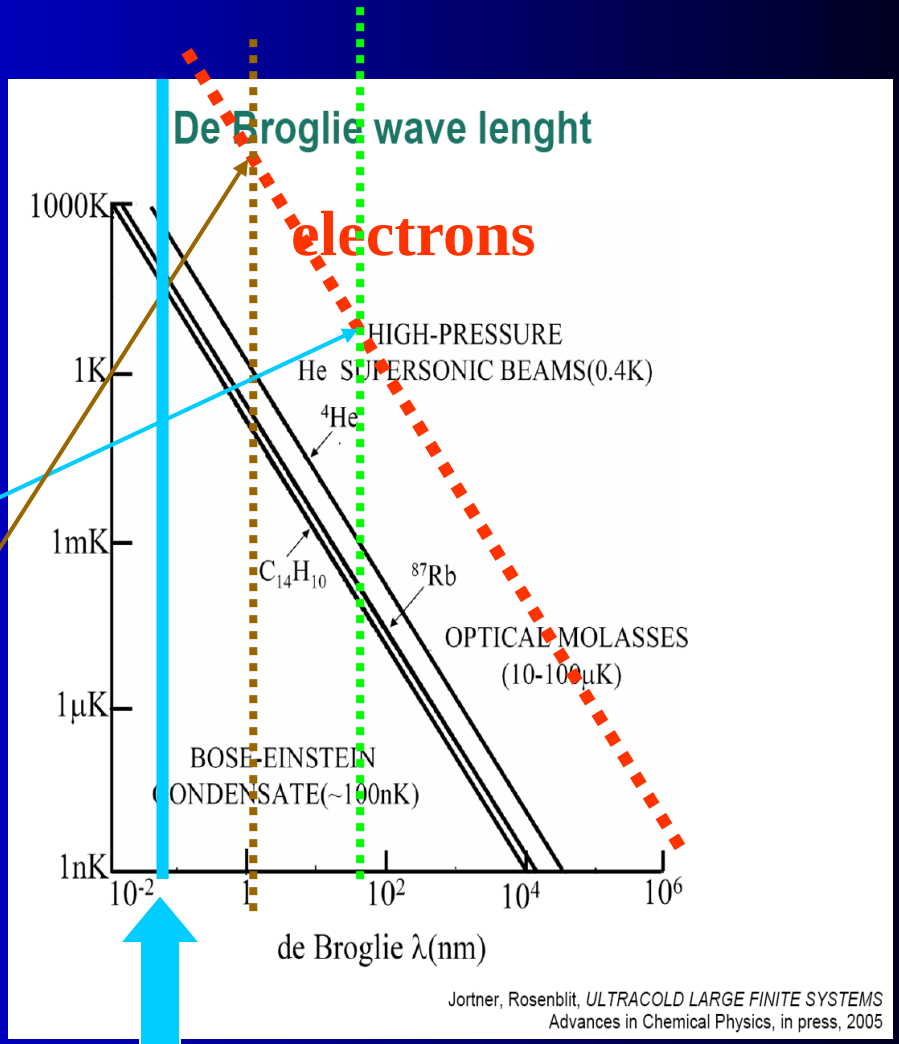

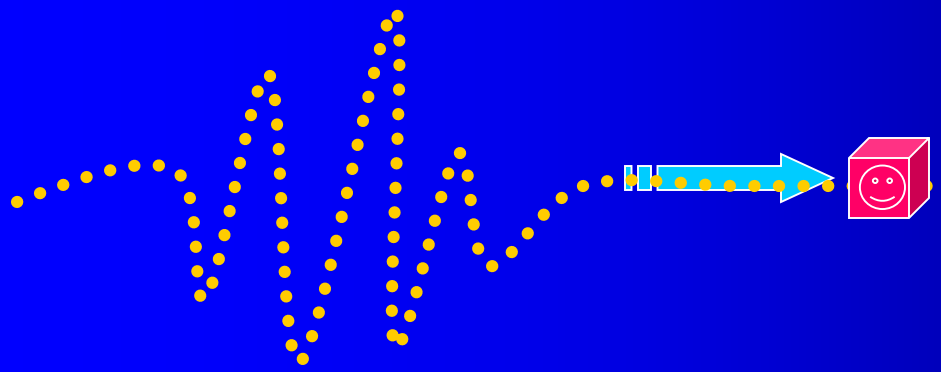

a_0

Electronvolt

$E \leftrightarrow kT$
1eV ~ 11 604.5 K
1K ~ 9×10^{-5}eV

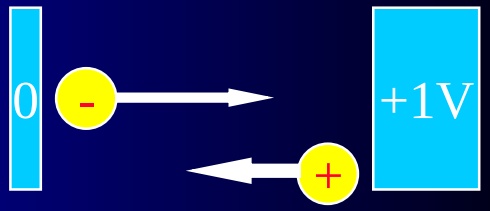

By definition, it is equal to the amount of kinetic energy gained by
a single unbound electron when it accelerates through an electric potential difference of one volt

Conversion factors:
1 eV = 1.6021765(40)×10^{-19}J (the conversion factor is numerically equal to the elementary charge expressed in coulombs).
1 eV (per atom) is 96.485 kJ/mol.

1.65 to 3.27 eV: the photon energy of visible light.

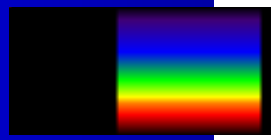

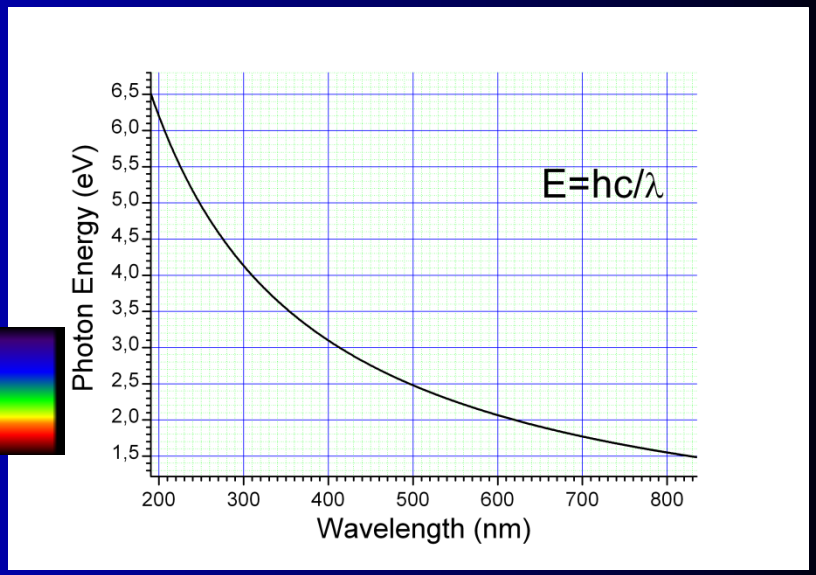

13.6 eV: The energy required to ionize atomic hydrogen.
Molecular bond energies are on the order of one eV per molecule

1 TeV: A trillion electronvolts, or 1.602×10^{-7} J, about the kinetic energy of a flying mosquito

14 TeV: the design proton collision energy at the Large Hadron Collider (which has operated at half of the energy since March 30, 2010). ….

Mol (značka mol) je základní fyzikální jednotka látkového množství.
Jeden mol libovolné látky obsahuje stejný počet částic, jaký je obsažen atomů v 12 g nuklidu uhlíku.
Tento počet udává Avogadrova konstanta, jejíž hodnota je přibližně 6,022×10^{23} mol^{-1}.

Conversion factors

$$1\,\mathrm{eV}/k = \frac{1\,\mathrm{eV}}{8{,}617\,333\,262 \times 10^{-5}\,\mathrm{eV/K}} = 11\,604{,}518\,12\ldots\,\mathrm{K}$$

E←→kT
1eV ~ 11 604.5 K
1K ~ 9x10^{-5}eV

Atkins
Physical chemistry

$RT = 2.4789\,\mathrm{kJ\,mol^{-1}}$

$RT/F = 25.693\,\mathrm{mV}$

$2.3026RT/F = 59.159\,\mathrm{mV}$

$kT/hc = 207.223\,\mathrm{cm^{-1}}$

$V_m^{\ominus} = RT/p^{\ominus} = 2.4465 \times 10^{-2}\,\mathrm{m^3\,mol^{-1}} = 24.465\,\mathrm{dm^3\,mol^{-1}}$

T/K	100.00	298.15	500.00	1000.0	1500.0	2000.0
(kT/kc)/cm^{-1}	69.50	207.22	347.51	659.03	1042.5	1390.1

$p^{\ominus} = 100\,\mathrm{kPa} = 1 \times 10^5\,\mathrm{N\,m^{-2}}$

$1\,\mathrm{atm} = 101.325\,\mathrm{kPa} = 1.013\,25 \times 10^5\,\mathrm{N\,m^{-2}} = 1.013\,25 \times 10^5\,\mathrm{J\,m^{-3}}$

$1\,\mathrm{atm} = 760\,\mathrm{Torr}$ (exactly)

$1\,\mathrm{Torr} = 133.322\,\mathrm{Pa}$ (exactly)

$1\,\mathrm{mmHg} = 133.3224\,\mathrm{Pa}$

$1\,\mathrm{eV} = 1.602\,19 \times 10^{-19}\,\mathrm{J} \triangleq 96.485\,\mathrm{kJ\,mol^{-1}} \triangleq 8065.5\,\mathrm{cm^{-1}}$

$1\,\mathrm{cm^{-1}} \triangleq 1.986 \times 10^{-23}\,\mathrm{J} \triangleq 11.96\,\mathrm{J\,mol^{-1}} \triangleq 0.1240\,\mathrm{meV}$

$hc = 1.986\,48 \times 10^{-23}\,\mathrm{J\,cm}$

$hc/k = 1.438\,79\,\mathrm{cm\,K}$

$g/\mathrm{m\,s^{-2}} = 9.8064 - 0.0259\cos\{2(\mathrm{latitude})\} = 9.811$ at 50°

$1\,\mathrm{cal} = 4.184\,\mathrm{J}$

$1\,\mathrm{D}$ (debye) $= 3.335\,64 \times 10^{-30}\,\mathrm{C\,m}$

$1\,\mathrm{N} = 1\,\mathrm{J\,m^{-1}} = 10^5$ dyne	$1\,\mathrm{W} = 1\,\mathrm{J\,s^{-1}}$	$1\,\mathrm{T} = 1\,\mathrm{J\,C^{-1}\,s\,m^{-2}}$
$1\,\mathrm{J} = 10^7$ erg	$1\,\mathrm{A} = 1\,\mathrm{C\,s^{-1}}$	$1\,\mathrm{J} = 1\,\mathrm{A\,V\,s}$

Detail 0.1nm-1 km

Opacity is the measure of impenetrability to electromagnetic or other kinds of radiation, especially visible light.

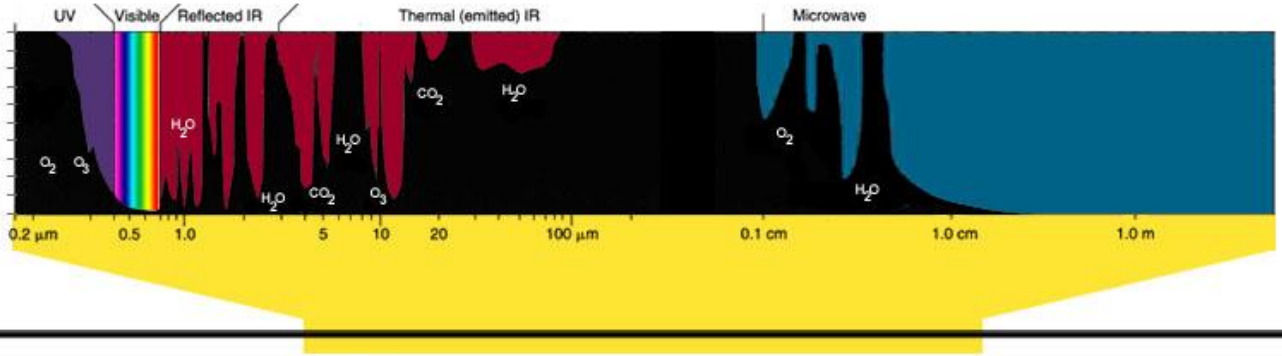

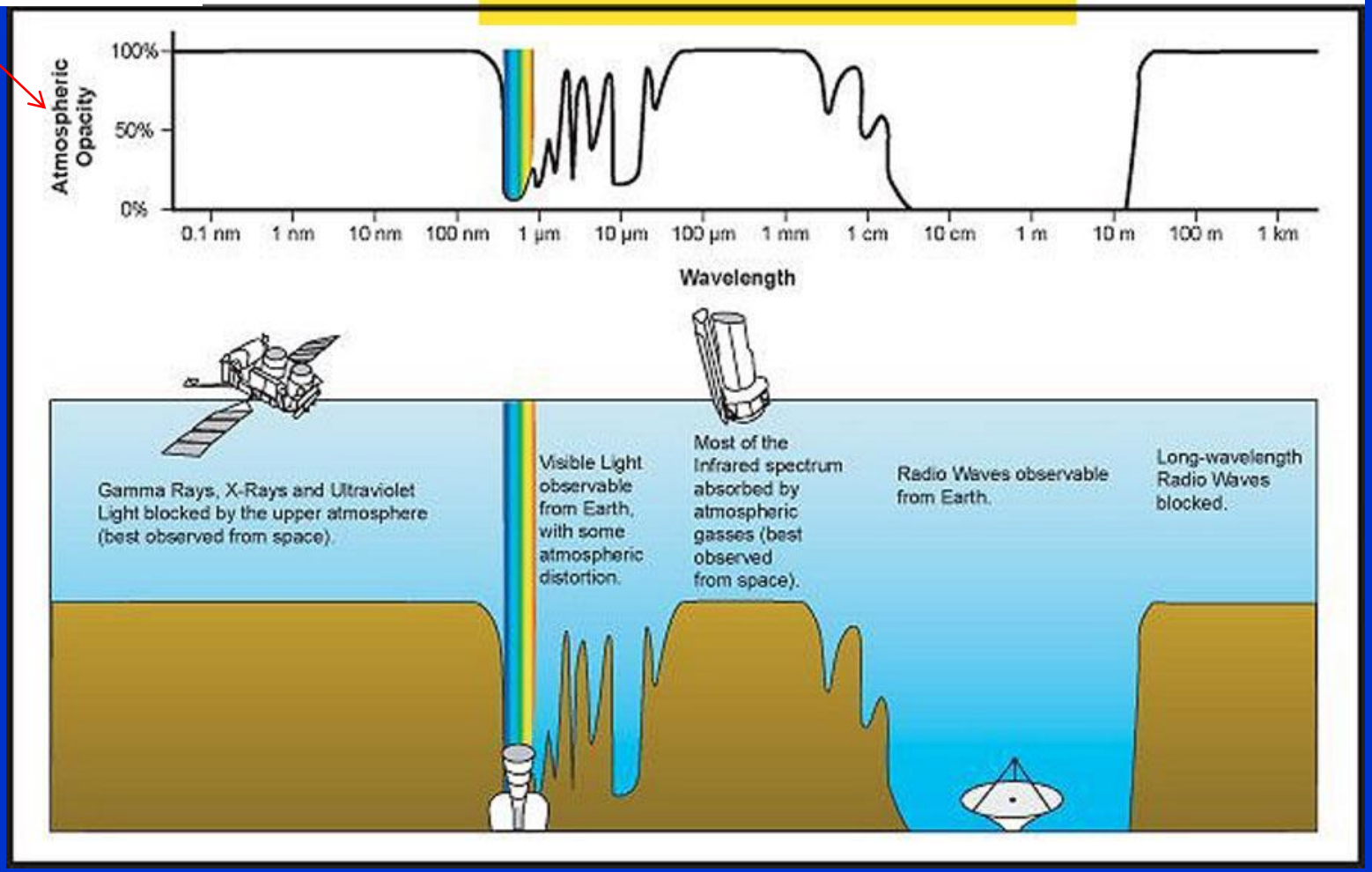

Before

Johannes Kepler

The Supernova of 1604

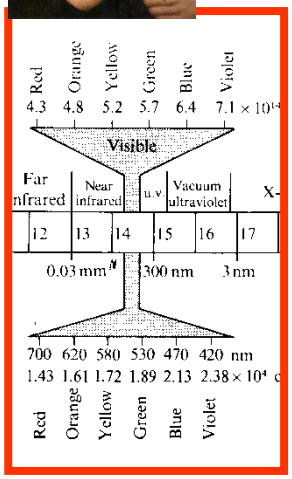

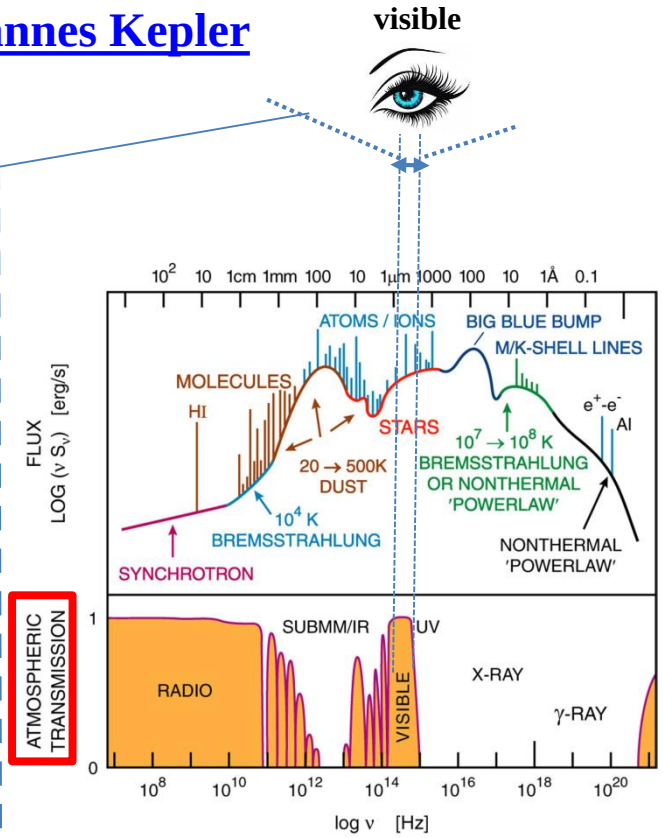

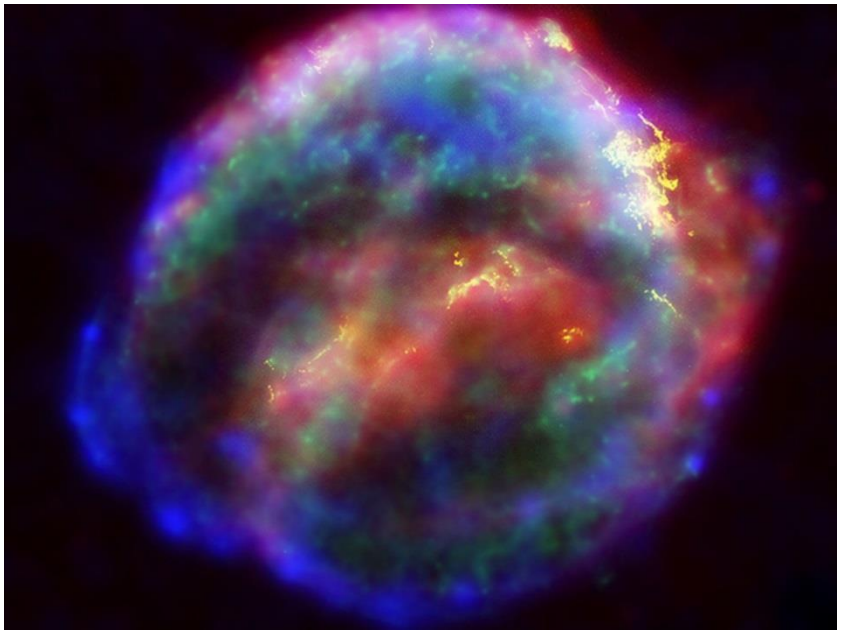

The first recorded observation was in northern Italy on October 9, 1604.[2] Johannes Kepler began observing the luminous display while working at the imperial court in Prague for Emperor Rudolf II on October 17.[3] It was subsequently named after him because his observations tracked the object for an entire year and because of his book on the subject, entitled *De Stella nova in pede Serpentarii* ("On the new star in Ophiuchus's foot", Prague 1606).

It was the second supernova to be observed in a generation (after SN 1572 seen by Tycho Brahe in Cassiopeia). No further supernovae have since been observed with certainty in the Milky Way, though many others outside our galaxy have been seen since S Andromedae and SN 1987A in the Large Magellanic Cloud was visible to the naked eye.

Golden Age of Astro-plasma and Astro-chemistry

Klementinum and astronomy.

Astronomická věž

Věž byla dokončena v roce 1722. Na vrcholu věže stojí socha Atlanta (olověná socha s železnou vnitřní konstrukcí, váha asi 600 kg, výška 2,4 m). Atlas nese nebeskou sféru (průměr asi 1,6 m, váha asi 150 kg) s korouhví.

(Pravděpodobně

Matyáš Braun)

Golden Age of Astrochemistry

4. Oktober 1957 19:28 UTC

Byla zkonstruována koncem 50. let 20. století Sergejem Koroljovem v Sovětském svazu. Byla vynesena 4. října 1957 19:28 UTC upravenou dvoustupňovou nosnou raketou R-7, která byla z vojenské verze pro kosmonautiku upravena a přejmenována na raketu Sputnik. Odstartovala z kosmodromu Bajkonur na území Kazašské SSR. Vypuštěna byla v rámci Mezinárodního geofyzikálního roku.[2] Patří do kategorie vědeckých družic.

Družice měla sférický tvar o průměru 58 cm a hmotnost 83,6 kg.

3. November 1957

Sputnik 2

Lajka

Hmotnost 508 kg

3. listopadu 1957 z kosmodromu Bajkonur.

2021

~ 64 rokov

Golden Age of Astrochemistry

United Kingdom Infrared Telescope
Mauna Kea, Hawaii

Five-hundred-meter Aperture Spherical radio Telescope (China: **Tianyan, 2016**)

The **Arecibo Observatory**
RT in Puerto Rico (~1960)

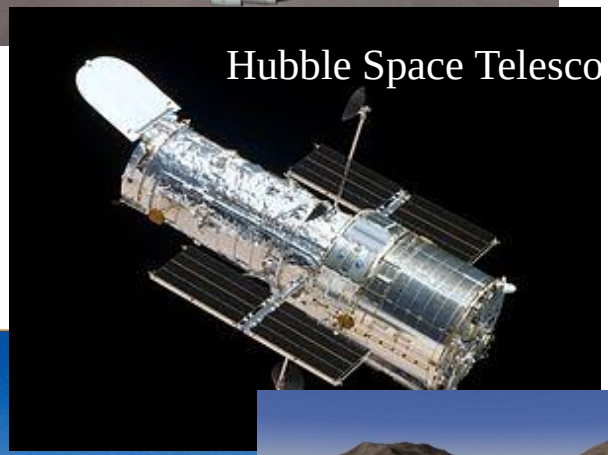

RATAN-600 Radio Telescope (Russia, 1974)

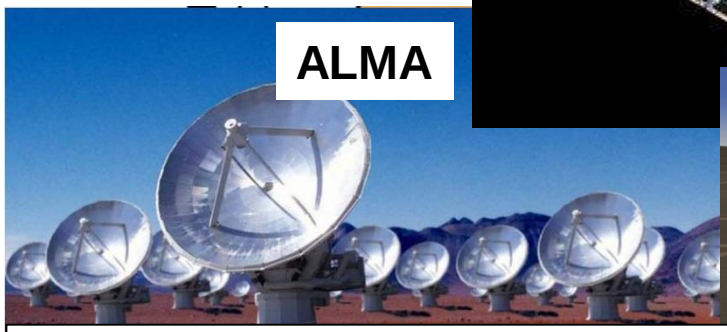

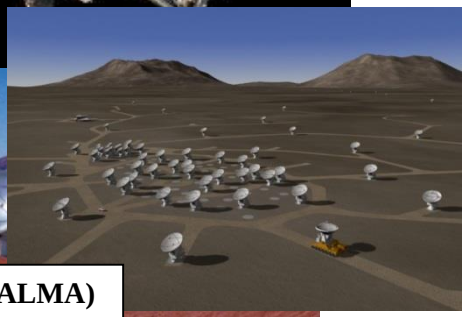

The Atacama Large Millimeter/sub-millimeter Array (ALMA)
astronomical interferometer of radio telescopes
Atacama desert of northern Chile

Golden Age of Astrochemistry

United Kingdom Infrared Telescope
Mauna Kea, Hawaii

Five-hundred-meter Aperture Spherical radio Telescope (China: **Tianyan, 2016**)

The **Arecibo Observatory**
RT in Puerto Rico (~1960)

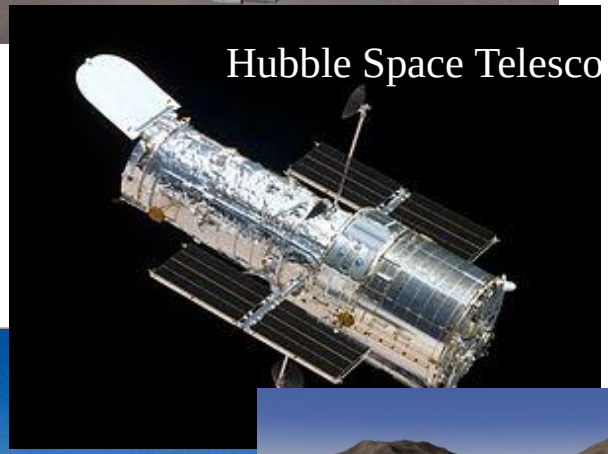

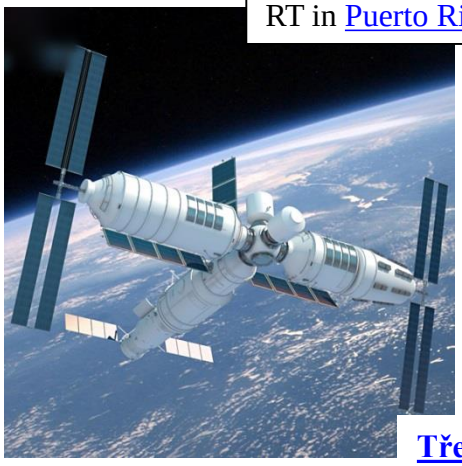

[Třetí nebeský palác]

Tiangong, officially the Tiangong space station

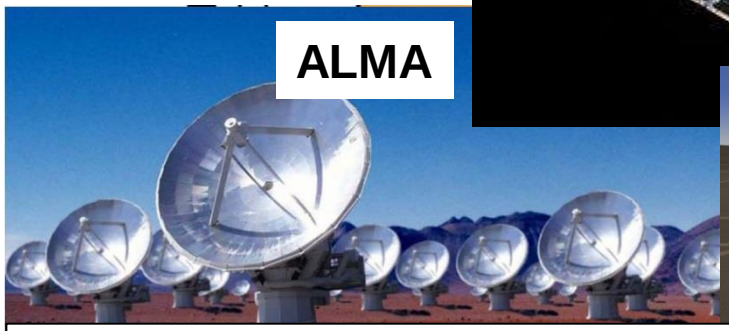

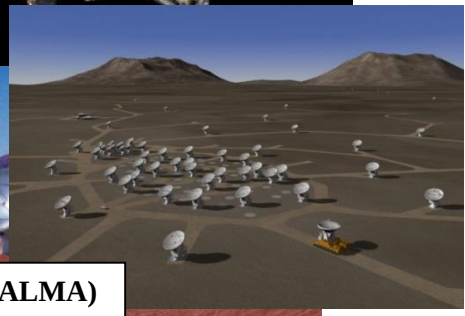

The Atacama Large Millimeter/sub-millimeter Array (ALMA)
astronomical interferometer of radio telescopes
Atacama desert of northern Chile

ISS

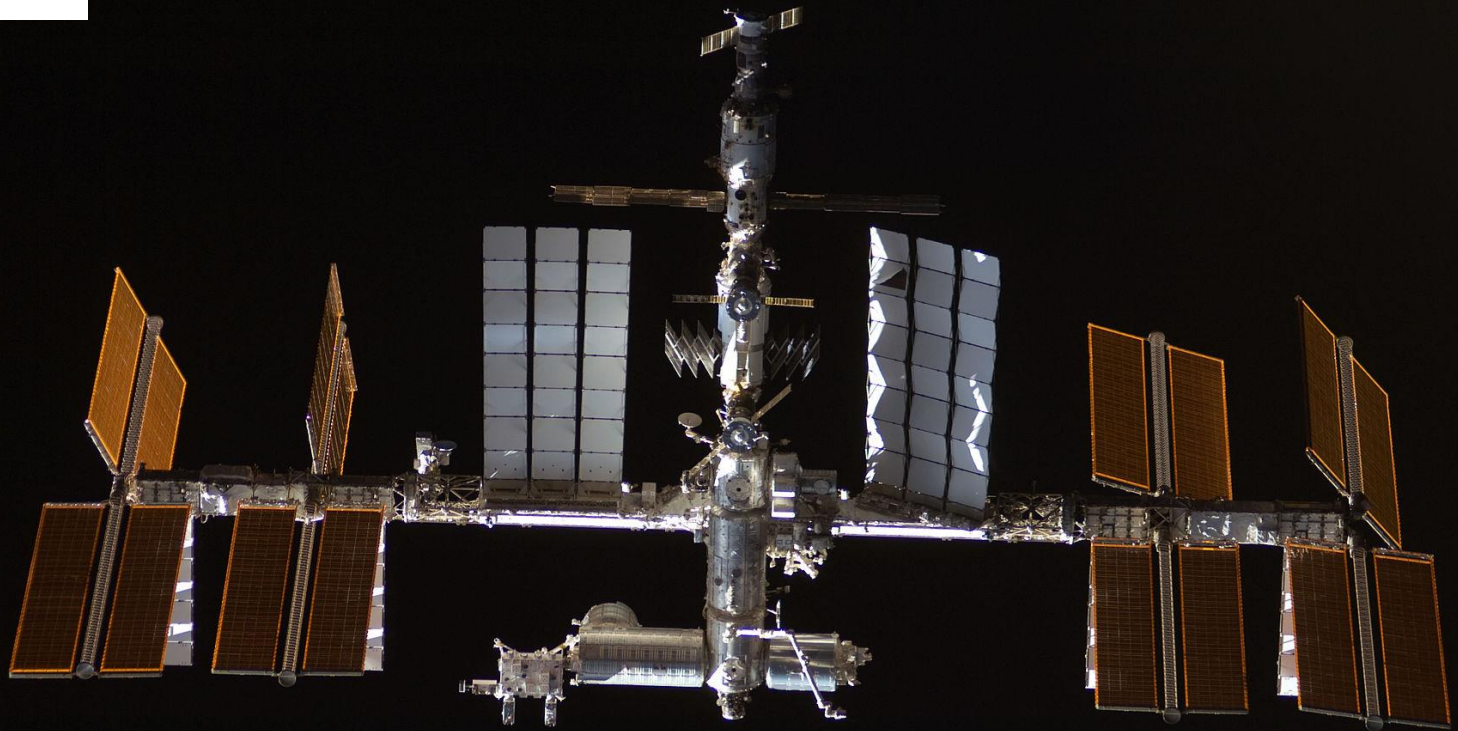

Not actualized, approximation

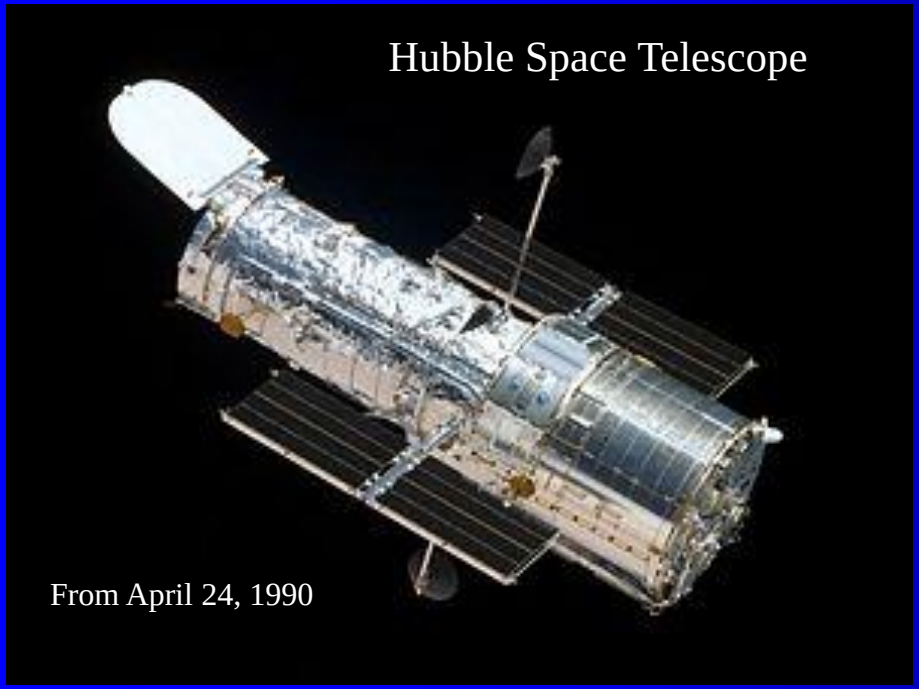

The Hubble Space Telescope is a space telescope that was launched into low Earth orbit in 1990 and remains in operation

The telescope is operating as of 2019,
and could last until 2030–2040.

Hubble is the only telescope designed to be maintained in space by astronauts. Five Space Shuttle missions have repaired, upgraded, and replaced systems on the telescope, including all five of the main instruments. The fifth mission was canceled on safety grounds following the *Columbia* disaster (2003), but NASA administrator Michael D. Griffin approved the fifth servicing mission which was completed in 2009. The telescope was still operating as of April 24, 2020, its 30th anniversary,[11] and could last until 2030–2040.[4] One successor to the Hubble telescope is the James Webb Space Telescope (JWST) which is scheduled to be launched in late 2021.[

Hubble má potíže, přestal fungovat čtvrtý gyroskop, který pomáhá s orientací teleskopu
08. 10. 2018
Hubble Teleskopy
V pátek se vesmírný teleskop Hubble přepnul do tzv. safe módu poté, co přestal fungovat jeden z gyroskopů, které teleskopu pomáhají udržet správnou orientaci při pozorování vzdálených cílů ve vesmíru. Hubble měl celkem 6 těchto gyroskopů a potřebuje nejméně tři pro optimální operace. Dva však už delší dobu nefungují a další nefunguje optimálně. Po odchodu čtvrtého tak zbývají pouze dva funkční gyroskopy. Operátoři mise nyní zkoumají možnosti, kterými uvést teleskop zpátky do plného provozu.

Pokud se nepodaří na dálku opravit porouchaný gyroskop, hodlají operátoři vyzkoušet onen třetí, který nefunguje optimálně. Aktuálně tak hledají cesty, jak teleskop na dálku opravit, pokud se to nepodaří, teleskop může pracovat dál se dvěma, nebo dokonce jedním gyroskopem. Je dokonce pravděpodobné, že pokud se oprava nepodaří, mise bude dále pokračovat pouze s jedním gyroskopem a druhý bude ponechán jako rezerva.

Všech šest gyroskopů teleskopu Hubble bylo vyměněno při poslední misi astronautů k teleskopu v roce 2009. Po dosloužení raketoplánů však teleskop nebyl astronauty navštíven a zatím se neplánuje žádná podobná mise s novými vesmírnými loděmi, které by NASA měla mít v následujících letech k dispozici. Hubble je ve vesmíru od roku 1990.

Vesmírný teleskop Hubble - teleskop Hubble obíhá Zemi od roku 1990 ve výšce asi 540 kilometrů.

en.wikipedia.org/wiki/Hubble_Space_Telescope

James Webb Space Telescope

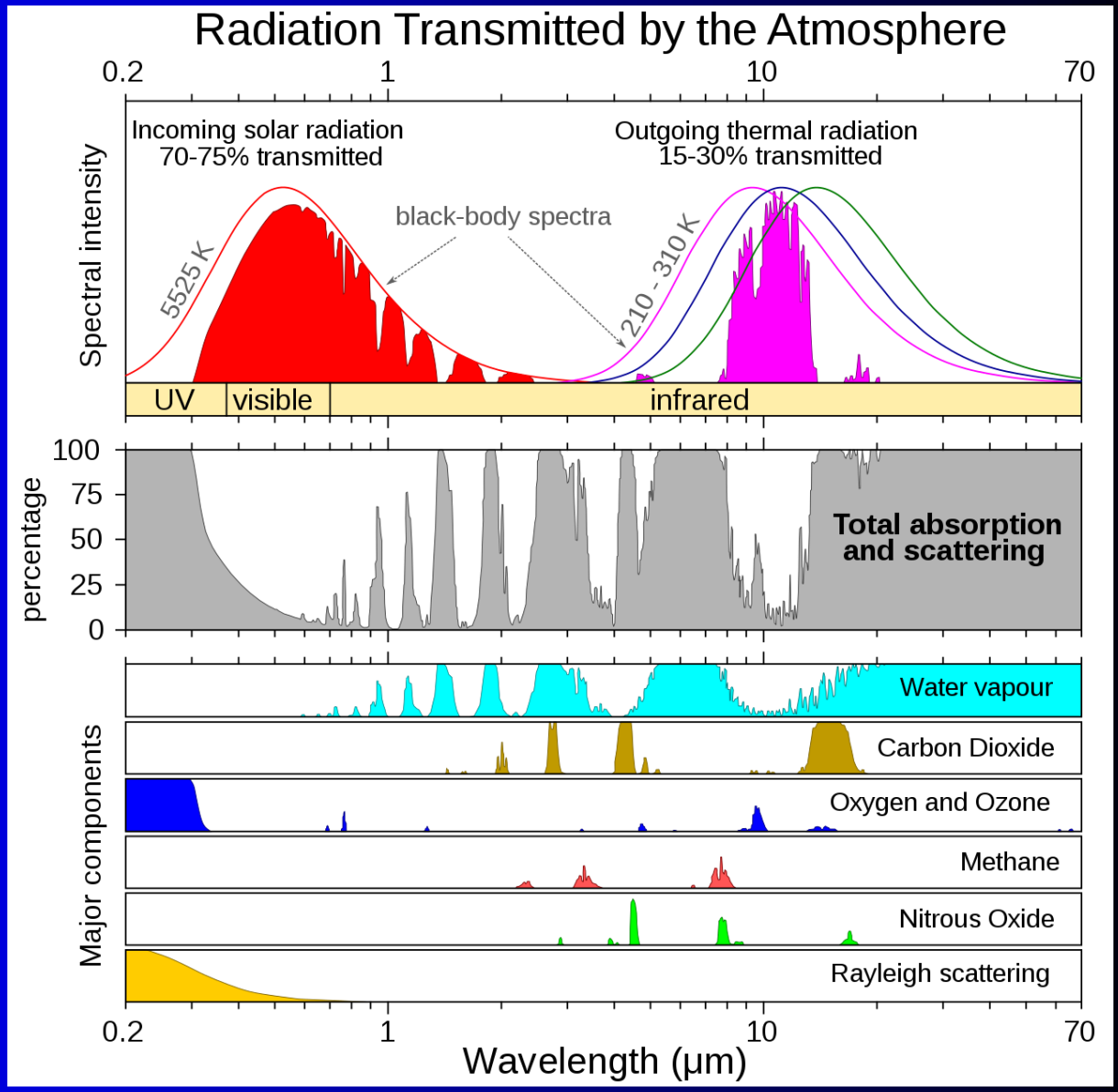

Atmospheric windows in the infrared: Much of this type of light is blocked when viewed from the Earth's surface. It would be like looking at a rainbow but only seeing one colour.

infrared astronomy

James Webb Space Telescope (JWST)

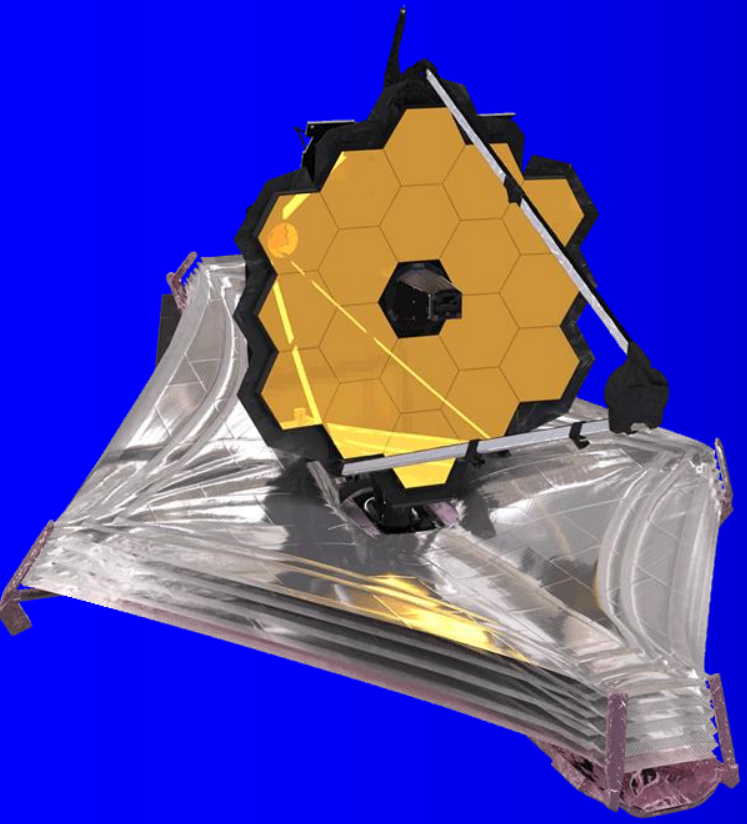

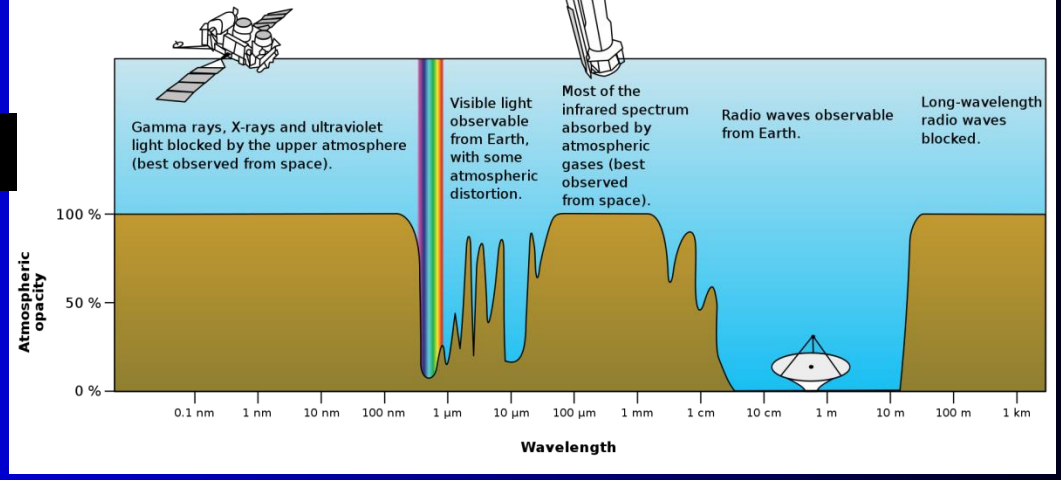

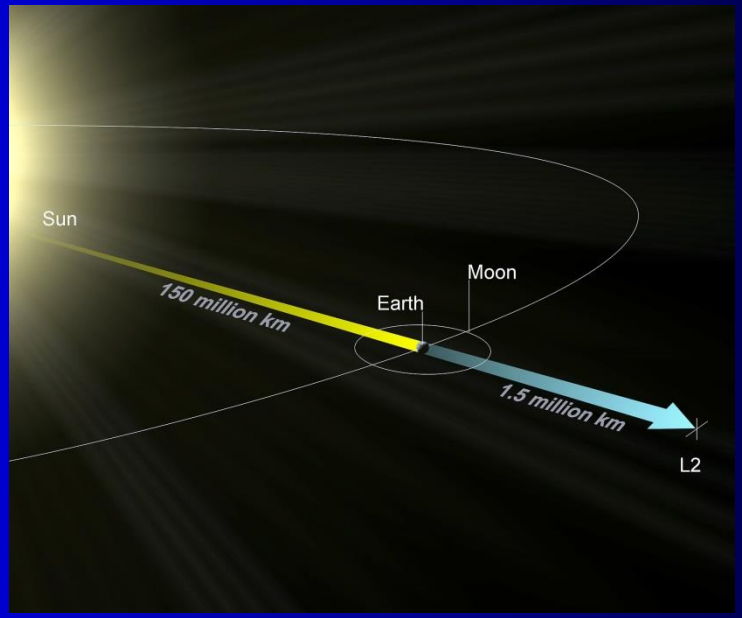

The **James Webb Space Telescope** (**JWST**) is a space telescope which conducts infrared astronomy. As the largest optical telescope in space, its high resolution and sensitivity allow it to view objects too old, distant, or faint for the Hubble Space Telescope. This will enable investigations across many fields of astronomy and cosmology, such as observation of the first stars, the formation of the first galaxies, and detailed atmospheric characterization of potentially habitable exoplanets.

~1/6 of mass is interstellar

~1/2 of interstellar matter is molecular!

Milky Way has ~10^{66} molecules!
Earth has only ~10^{50} molecules

Different views of the Milky Way (different wavelengths)

Hydrogen dominated plasma

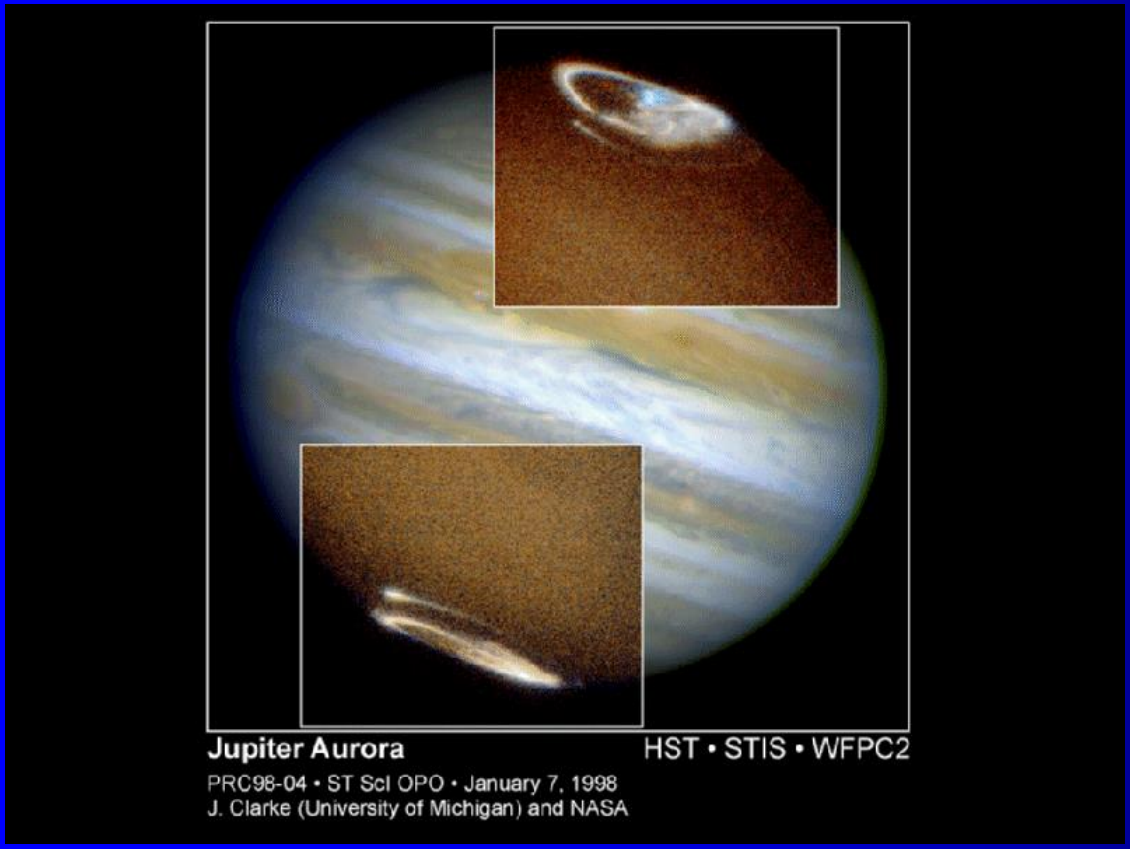

Hydrogen plasma in Jupiter Aurora

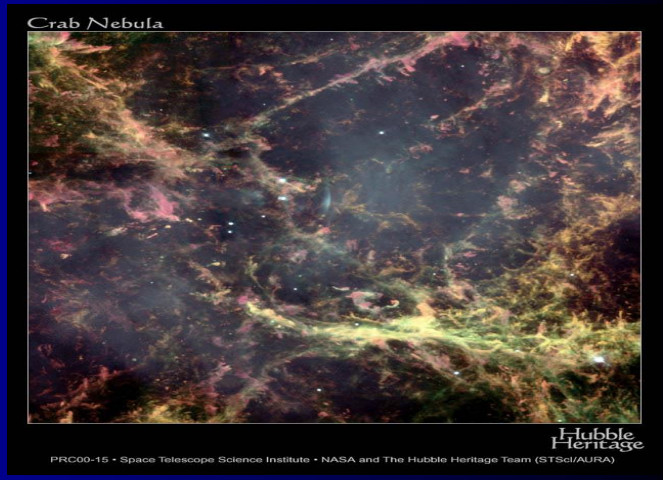

Crab Nebula

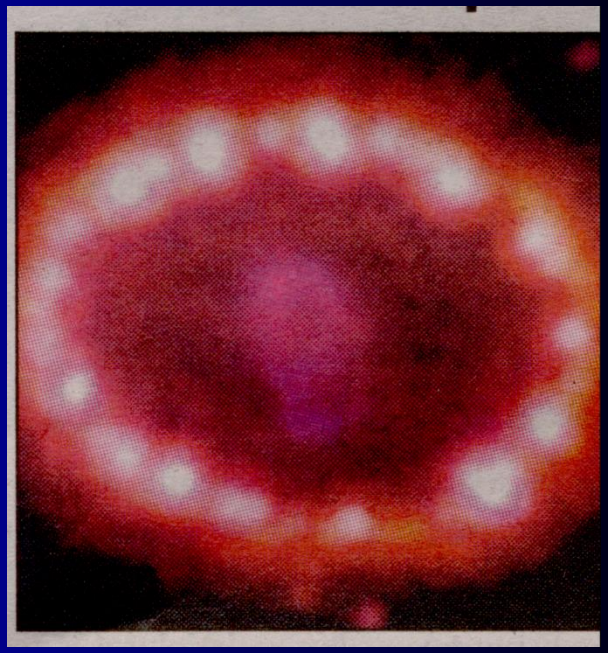

1994 -Supernova 1987A

Tvorba a zánik iontů v mezihvězdných oblacích, experimenty na Zemi

Formation of ions in interstellar space , laboratory astrophysics

$$H_2^+ + H_2 \rightarrow H_3^+ + H$$

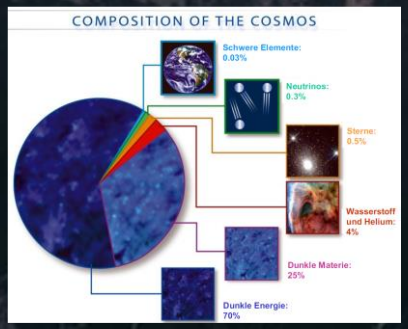

Richard Payne (Arizona Astrophotography)

Herschel

Herschel (red) and Hubble (blue) composite image of the Crab Nebula. *Credit: ESA/Herschel/PACS/MESS Key Programme Supernova Remnant Team; NASA, ESA and Allison Loll/Jeff Hester (Arizona State Uni)*

Hubble Space Telescope

The **Crab Nebula** is the remnant of a supernova explosion that was observed by Chinese astronomers in the year 1054.

ArH+

ArH+ ion in Crab nebula

ESA's Herschel Space Observatory

12 December 2013

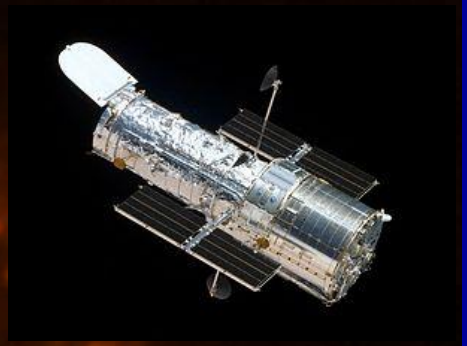

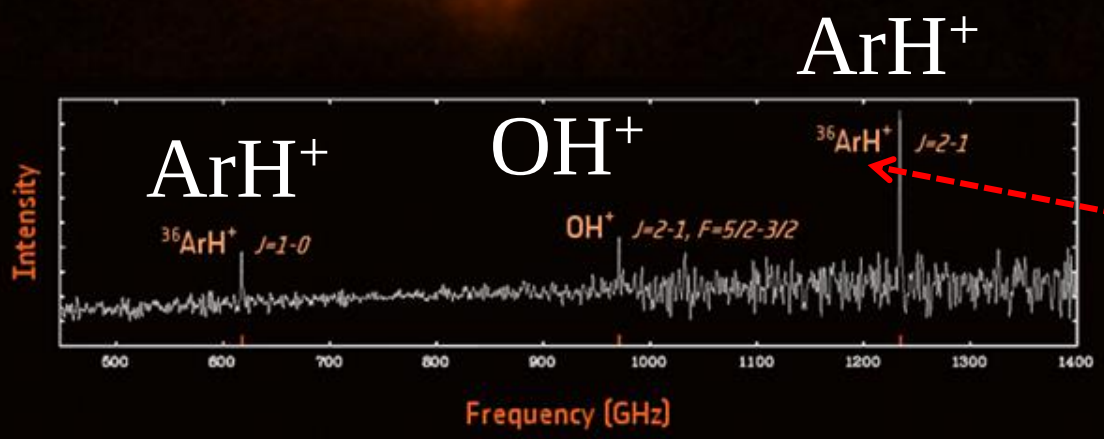

Using ESA's Herschel Space Observatory, a team of astronomers has found first evidence of a noble-gas based molecule in space. A compound of argon, the molecule was detected in the gaseous filaments of the Crab Nebula, one of the most famous supernova remnants in our Galaxy. While argon is a product of supernova explosions, the formation and survival of argon-based molecules in the harsh environment of a supernova remnant is an unforeseen surprise.

$^{36}ArH^{+}$

The results described in this article are reported in "***Detection of a Noble Gas Molecular Ion, $^{36}ArH^{+}$, in the Crab Nebula***", by M. J. Barlow et al., published in Science, 342, 6163, 1343-1345, 13 December 2013. DOI: 10.1126/science.124358213.

ArH+ ionty v Crab nebula

Using ESA's Herschel Space Observatory

12 December 2013

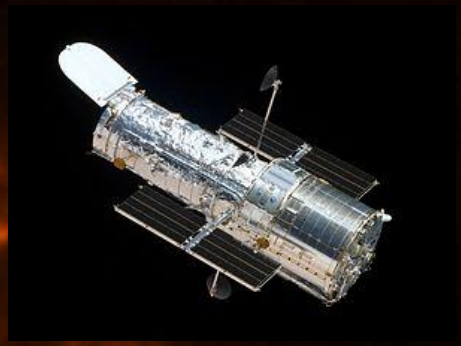

$^{36}ArH^+$ $^{36}ArH^+$

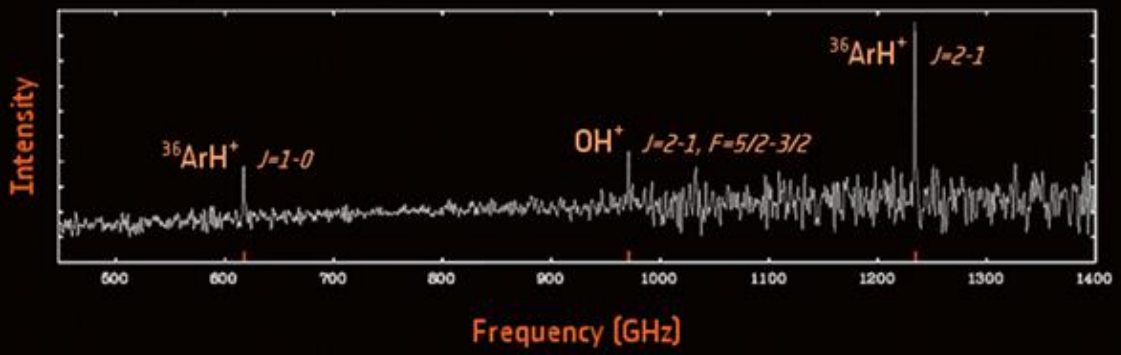

^{40}Ar

The argon isotope found in the Crab Nebula is different from the one that dominates in Earth's atmosphere, ^{40}Ar, which derives from the decay of a radioactive isotope of potassium (^{40}K) present in our planet's rocks.

^{36}Ar

The Herschel data indicate that the argon hydride found in the Crab Nebula is made up of the argon isotope ^{36}Ar. This is the first time that astronomers could identify the isotopic nature of an element in a supernova remnant.

"Finding that argon in the Crab Nebula consists of ^{36}Ar was not surprising because this is the dominant isotope of argon across the Universe.

"And it's also the main argon isotope to be synthesised in the nuclear reactions during supernova explosions, so its detection in the Crab Nebula confirms that this iconic nebula was created by the explosive death of a massive star," explains Barlow.

Multispectral Milky Way

LETTER

https://doi.org/10.1038/s41586-019-1090-x

18 APRIL 2019 | VOL 568 | NATURE

2019

Astrophysical detection of the helium hydride ion HeH^+

Rolf Güsten[1]*, Helmut Wiesemeyer[1], David Neufeld[2], Karl M. Menten[1], Urs U. Graf[3], Karl Jacobs[3], Bernd Klein[1,4], Oliver Ricken[1], Christophe Risacher[1,5] & Jürgen Stutzki[3]

During the dawn of chemistry[1,2], when the temperature of the young Universe had fallen below some 4,000 kelvin, the ions of the light elements produced in Big Bang nucleosynthesis recombined in reverse order of their ionization potential. With their higher ionization potentials, the helium ions He^{2+} and He^+ were the first to combine with free electrons, forming the first neutral atoms; the recombination of hydrogen followed. In this metal-free and low-density environment, neutral helium atoms formed the Universe's first molecular bond in the helium hydride ion HeH^+ through radiative association with protons. As recombination progressed, the destruction of HeH^+ created a path to the formation of molecular hydrogen. Despite its unquestioned importance in the evolution of the early Universe, the HeH^+ ion has so far eluded unequivocal detection in interstellar space. In the laboratory the ion was discovered[3] as long ago as 1925, but only in the late 1970s was the possibility that HeH^+ might exist in local astrophysical plasmas discussed[4–7]. In particular, the conditions in planetary nebulae were shown to be suitable for producing potentially detectable column densities of HeH^+. Here we report observations, based on advances in terahertz spectroscopy[8,9] and a high-altitude observatory[10], of the rotational ground-state transition of HeH^+ at a wavelength of 149.1 micrometres in the planetary nebula NGC 7027. This confirmation of the existence of HeH^+ in nearby interstellar space constrains our understanding of the chemical networks that control the formation of this molecular ion, in particular the rates of radiative association and dissociative recombination.

The deployment of the German Receiver for Astronomy at Terahertz Frequencies (GREAT)[9] heterodyne spectrometer on board the Stratospheric Observatory for Infrared Astronomy (SOFIA)[10] has now opened up new opportunities. Although the HeH^+ $J = 1–0$ transition at 149.137 μm (2010.183873 GHz; ref. [21]) cannot be observed from ground-based observatories, skies become transparent during high-altitude flights with SOFIA. The latest advances in terahertz technologies have

We then computed the equilibrium abundance of HeH^+, including the three reactions identified as being important in the layers in which HeH^+ is most abundant[7,13]:

$$He^+ + H \rightarrow HeH^+ + h\nu \quad (1)$$

$$HeH^+ + e^- \rightarrow He + H \quad (2)$$

$$HeH^+ + H \rightarrow H_2^+ + He \quad (3)$$

2019

Science REPORTS

Cite as: O. Novotný *et al.*, *Science* 10.1126/science.aax5921 (2019).

Quantum-state-selective electron recombination studies suggest enhanced abundance of primordial HeH^+

Oldřich Novotný[1]*, Patrick Wilhelm[1], Daniel Paul[1], Ábel Kálosi[1,2], Sunny Saurabh[1], Arno Becker[1], Klaus Blaum[1], Sebastian George[1,3], Jürgen Göck[1], Manfred Grieser[1], Florian Grussie[1], Robert von Hahn[1], Claude Krantz[1], Holger Kreckel[1], Christian Meyer[1], Preeti M. Mishra[1], Damian Muell[1], Felix Nuesslein[1], Dmitry A. Orlov[1], Marius Rimmler[1], Viviane C. Schmidt[1], Andrey Shornikov[1], Aleksandr S. Terekhov[4], Stephen Vogel[1], Daniel Zajfman[5], Andreas Wolf[1]

[1]Max-Planck-Institut für Kernphysik, Saupfercheckweg 1, 69117 Heidelberg, Germany. [2]Charles University, 18000 Praha, Czech Republic. [3]Universität Greifswald, Institut für Physik, 17487 Greifswald, Germany. [4]Rzhanov Institute of Semiconductor Physics, Novosibirsk 630090, Russia. [5]Weizmann Institute of Science, Rehovot 76100, Israel.

*Corresponding author. Email: oldrich.novotny@mpi-hd.mpg.de

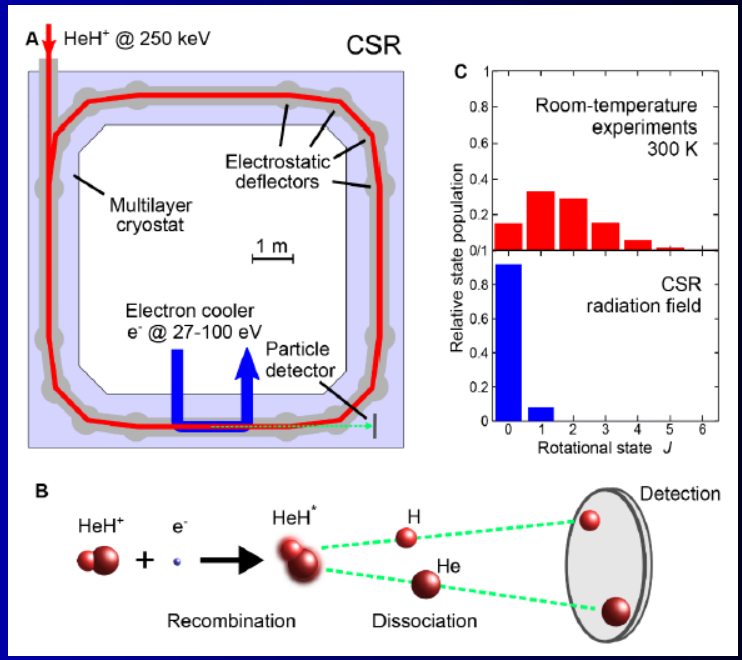

2020

PHYSICAL REVIEW LETTERS **124,** 043401 (2020)

Dissociative Recombination of Cold HeH^+ Ions

Roman Čurík*
J. Heyrovský Institute of Physical Chemistry, ASCR, Dolejškova 3, 18223 Prague, Czech Republic

Dávid Hvizdoš
J. Heyrovský Institute of Physical Chemistry, ASCR, Dolejškova 3, 18223 Prague, Czech Republic and Institute of Theoretical Physics, Faculty of Mathematics and Physics, Charles University in Prague, V Holešvičkách 2, 180 00 Prague, Czech Republic

Chris H. Greene
Department of Physics and Astronomy, Purdue University, West Lafayette, Indiana 47907, USA and Purdue Quantum Science and Engineering Institute, Purdue University, West Lafayette, Indiana 47907, USA

(Received 7 October 2019; revised manuscript received 27 November 2019; published 28 January 2020)

The Astrophysical Journal Supplement Series, 239:17 (48pp), 2018 December https://doi.org/10.3847/1538-4365/aae5d2

2018 Census of Interstellar, Circumstellar, Extragalactic, Protoplanetary Disk, and Exoplanetary Molecules

Brett A. McGuire[1,2,3]
[1] National Radio Astronomy Observatory, Charlottesville, VA 22903, USA
[2] Harvard-Smithsonian Center for Astrophysics, Cambridge, MA 02138, USA

Table 1
Commonly Used Facility Abbreviations

Abbreviation	Description
ALMA	Atacama Large Millimeter/submillimeter Array
APEX	Atacama Pathfinder Experiment
ARO	Arizona Radio Observatory
ATCA	Australian Telescope Compact Array
BIMA	Berkeley-Illinois-Maryland Array
CSO	Caltech Submillimeter Observatory
FCRAO	Five College Radio Astronomy Observatory
FUSE	*Far Ultraviolet Spectroscopic Explorer*
GBT	Green Bank Telescope
IRAM	Institut de Radioastronomie Millimétrique
IRTF	Infrared Radio Telescope Facility
ISO	*Infrared Space Observatory*
KPNO	Kitt Peak National Observatory
MWO	Millimeter-wave Observatory
NRAO	National Radio Astronomy Observatory
OVRO	Owens Valley Radio Observatory
PdBI	Plateau de Bure Interferometer
SEST	Swedish-ESO Submillimeter Telescope
SMA	Sub-millimeter Array
SMT	Sub-millimeter Telescope
SOFIA	*Stratospheric Observatory for Infrared Astronomy*
UKIRT	United Kingdom Infrared Telescope

3. Known Interstellar Molecules

Two-atom Molecules

3.1. CH (Methylidyne)

Swings & Rosenfeld (1937) suggested that an observed line at $\lambda = 4300$ Å by Dunham (1937) using the Mount Wilson Observatory in diffuse gas toward a number of supergiant B stars might have been due to the $^2\Delta \leftarrow {}^2\Pi$ transition of CH, reported in the laboratory by Jevons (1932). McKellar (1940) later identified several additional transitions in observational data. The first radio identification was reported by Rydbeck et al. (1973) at 3335 MHz with the Onsala telescope toward more than a dozen sources using estimated fundamental rotational transition frequencies from Shklovskii (1953), Goss (1966), and Baird & Bredohl (1971). The first direct measurement of the CH rotational spectrum was reported by Brazier & Brown (1983).

3.64. H_3^+

First suggested as a possible interstellar molecule in Martin et al. (1961), H_3^+ was detected 35 years later in absorption toward GL 2136 and W33A by Geballe & Oka (1996) using UKIRT to observe three transitions of the ν_2 fundamental band near 3.7 μm. The laboratory work was performed by Oka (1980).

Molecules in interstellar space

Not actualized, approximation

3	4	5	6	7	8	9	10	11	13
H_2	C_3	c-C_3H	C_5	C_5H	C_6H	CH_3C_3N	CH_3C_4H	CH_3C_5N?	HC_9N	$HC_{11}N$
AlF	C_2H	l-C_3H	C_4H	l-H_2C_4	CH_2CHCN	$HCOOCH_3$	CH_3CH_2CN	$(CH_3)_2CO$		
AlCl	C_2O	C_3N	C_4Si	C_2H_4	CH_3C_2H	CH_3COOH?	$(CH_3)_2O$	NH_2CH_2COOH?		
C_2	C_2S	C_3O	l-C_3H_2	CH_3CN	HC_5N	C_7H	CH_3CH_2OH			
CH	CH_2	C_3S	c-C_3H_2	CH_3NC	$HCOCH_3$	H_2C_6	HC_7N			
CH^+	HCN	C_2H_2	CH_2CN	CH_3OH	NH_2CH_3	CH_2OHCHO	C_8H			
CN	HCO	**CH_2D^+?**	CH_4	CH_3SH	c-C_2H_4O					
CO	**HCO^+**	HCCN	HC_3N	**HC_3NH^+**	CH_2CHOH					
CO^+	**HCS^+**	**$HCNH^+$**	HC2NC	HC_2CHO						
CP	**HOC^+**	HNCO	HCOOH	NH_2CHO						
CSi	H_2O	HNCS	H2CHN	C_5N						
HCl	H_2S	**$HOCO^+$**	H_2C_2O							
KCl	HNC	H_2CO	H_2NCN							
NH	HNO	H2CN	HNC_3							
NO	MgCN	H_2CS	SiH_4							
NS	MgNC	**H_3O^+**	**H_2COH^+**							
NaCl	**N_2H^+**	NH_3								
OH	N_2O	SiC_3								
PN	NaCN									
SO	OCS									
SO^+	SO_2									
SiN	c-SiC_2									
SiO	CO_2									
SiS	NH_2									
CS	**H_3^+**									
HF	SiCN									
SH	AlNC									
FeO?										

~2015

16 JULY 2015 | VOL 523 | NATURE | 323

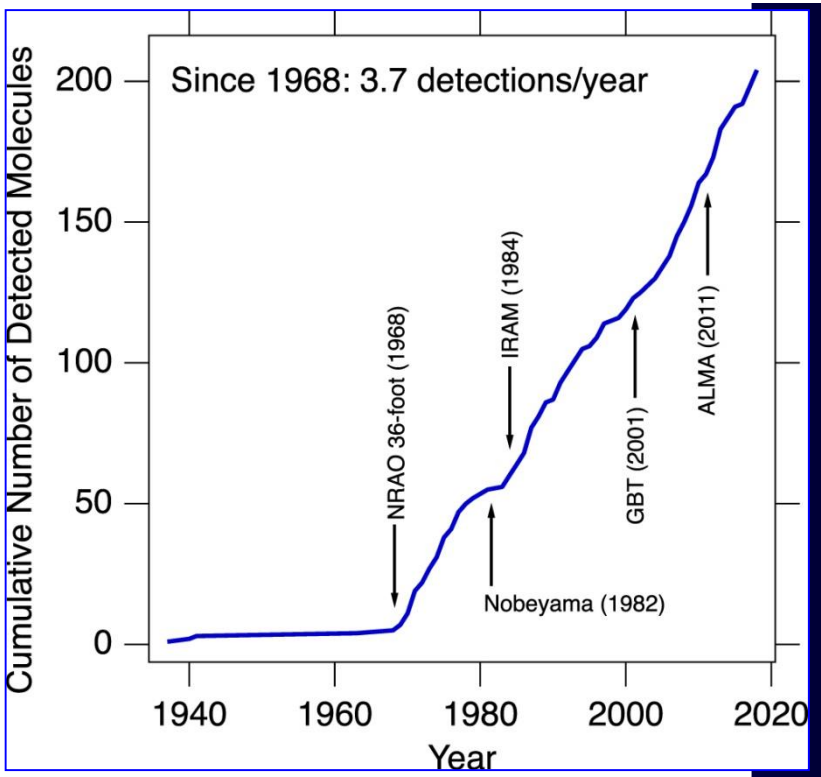

Cumulative number of known interstellar molecules over time. Commissioning dates of major contributing facilities are noted with arrows. [McGuire 2018]

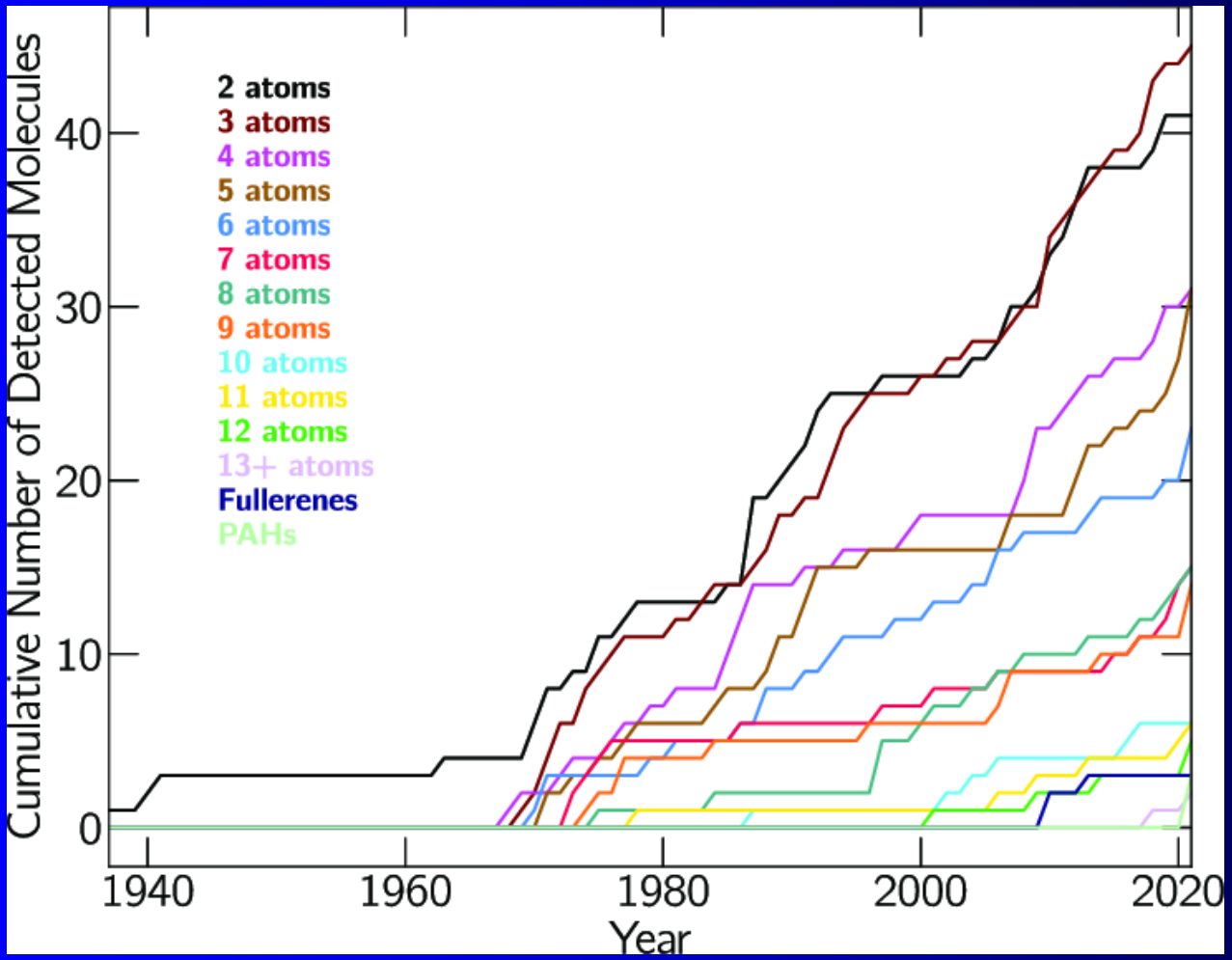

Cumulative number of known interstellar molecules with 2-13 atoms, as well as fullerene molecules, as a function of time. The traces are color coded by number of atoms and labeled on the right.

Molecules in interstellar space

Not actualized, approximation

16 JULY 2015 | VOL 523 | NATURE | 323

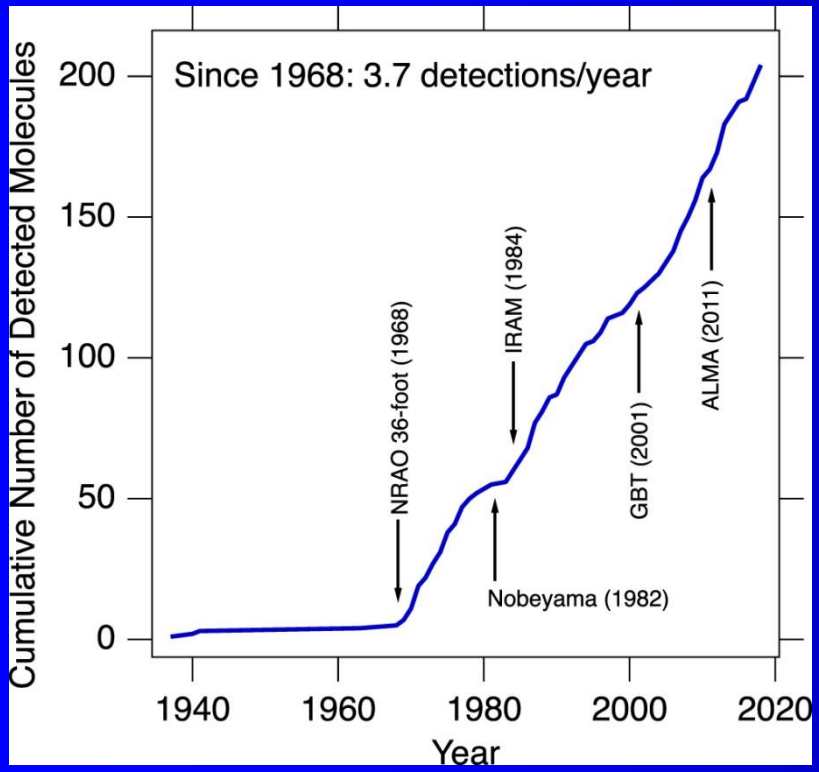

Cumulative number of known interstellar molecules over time. Commissioning dates of major contributing facilities are noted with arrows. [McGuire 2018]

actualized, approximation **2021**

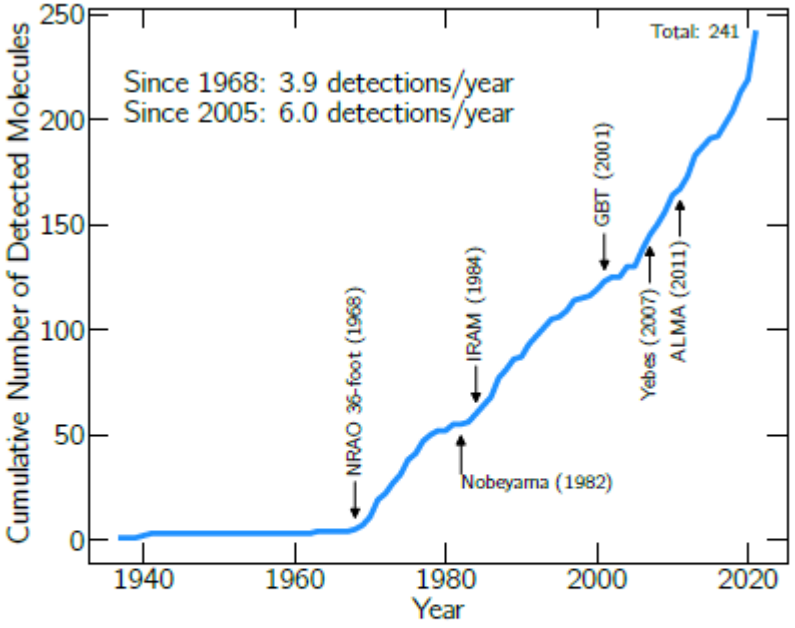

Figure 1. Cumulative number of known interstellar molecules over time. After the birth of molecular radio astronomy in the 1960s, there have been on average 3.9 new detections per year. The commissioning dates of several major contributing facilities are noted with arrows.

Draft version October 1, 2021
Typeset using LaTeX **twocolumn** style in AASTeX631

2021 Census of Interstellar, Circumstellar, Extragalactic, Protoplanetary Disk, and Exoplanetary Molecules

Brett A. McGuire[1, 2, 3]

[1] *Department of Chemistry, Massachusetts Institute of Technology, Cambridge, MA 02139, USA*
[2] *National Radio Astronomy Observatory, Charlottesville, VA 22903, USA*
[3] *Harvard-Smithsonian Center for Astrophysics, Cambridge, MA 02138, USA*

Not actualized, approximation (2018)

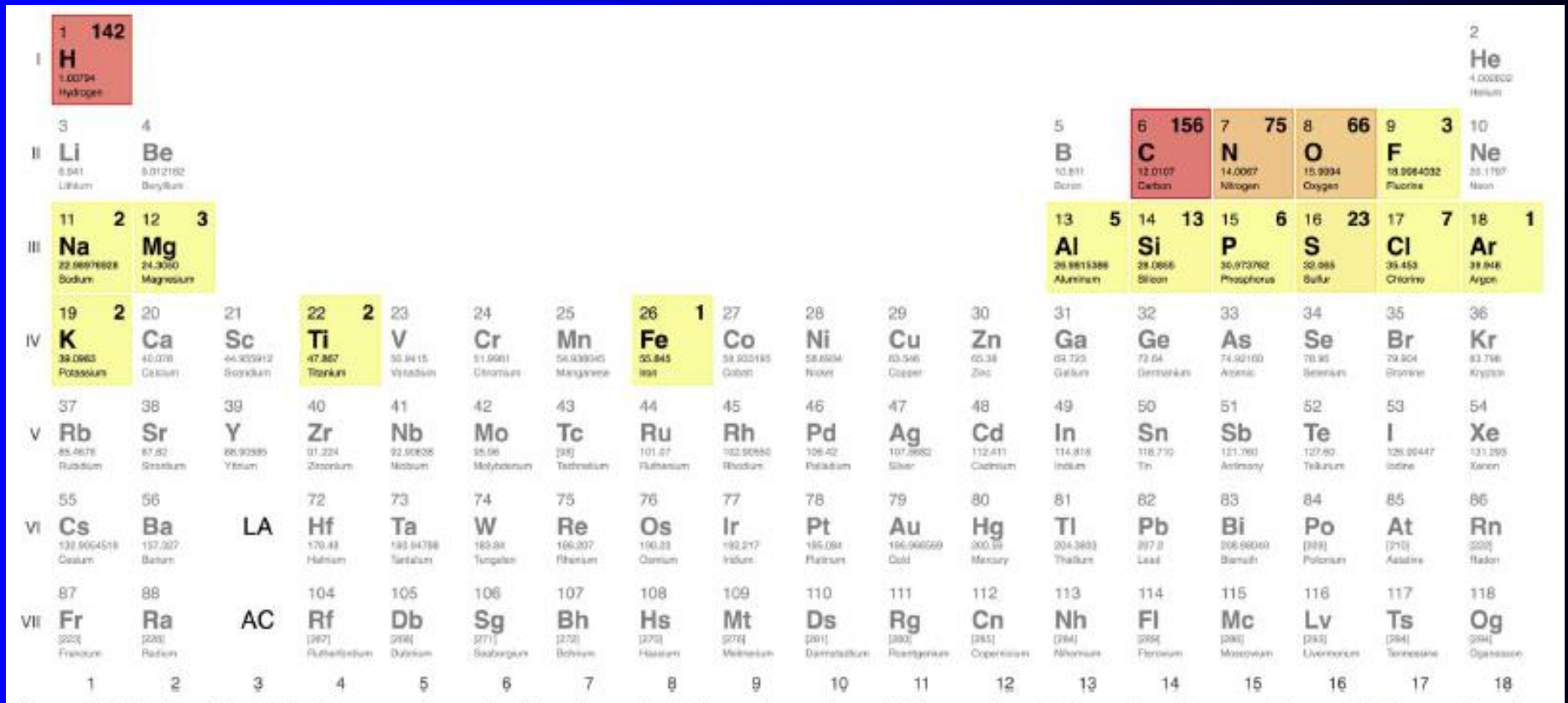

Figure 6. Periodic table of the elements, absent the lathanide and actinide series, color-coded by number of detected species containing each element. For those elements with detected ISM molecules, that number is displayed in the upper right of each cell.

The Astrophysical Journal Supplement Series, 239:17 (48pp), 2018 December https://doi.org/10.3847/1538-4365/aae5d2

2018 Census of Interstellar, Circumstellar, Extragalactic, Protoplanetary Disk, and Exoplanetary Molecules

Brett A. McGuire[1,2,3]
[1] National Radio Astronomy Observatory, Charlottesville, VA 22903, USA
[2] Harvard-Smithsonian Center for Astrophysics, Cambridge, MA 02138, USA
Received 2018 May 27; revised 2018 September 20; accepted 2018 September 20; published 2018 November 26

actualized, approximation (2021)

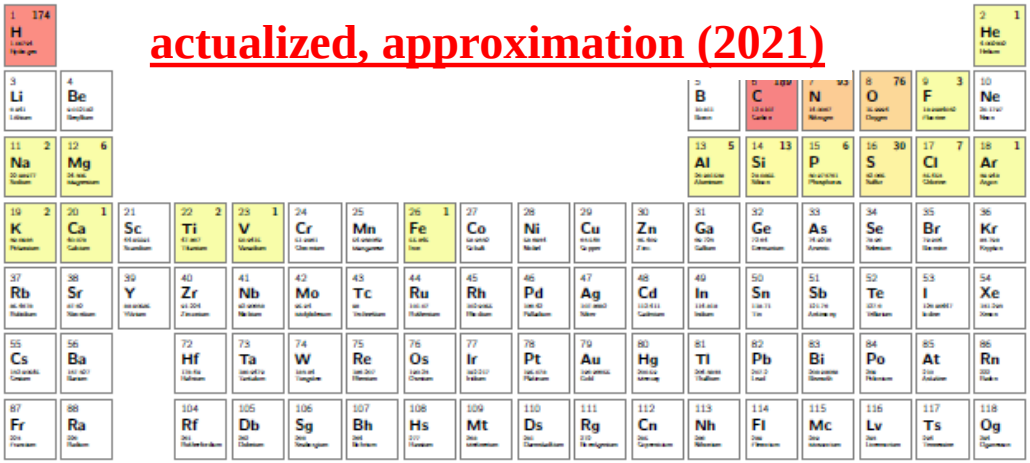

Figure 6. Periodic table of the elements, absent the lathanide and actinide series, colored by number of detected species containing each element. For those elements with detected ISM molecules, that number is displayed in the upper right of each cell.

Figure 10. Percentage of known interstellar molecules that are neutral, cationic, anionic, radical species, or cyclic. Many molecules fall into more than one of these categories (e.g. most radical species have a net neutral charge).

Draft version October 1, 2021
Typeset using LaTeX **twocolumn** style in AASTeX631

2021 Census of Interstellar, Circumstellar, Extragalactic, Protoplanetary Disk, and Exoplanetary Molecules

Brett A. McGuire[1, 2, 3]

[1] *Department of Chemistry, Massachusetts Institute of Technology, Cambridge, MA 02139, USA*
[2] *National Radio Astronomy Observatory, Charlottesville, VA 22903, USA*
[3] *Harvard-Smithsonian Center for Astrophysics, Cambridge, MA 02138, USA*

Interstellar medium

92.1% of nucleons in the universe are protons
7.8% are helium nuclei !
0.1%……C,N,O,S,Si….

Cosmic abundance

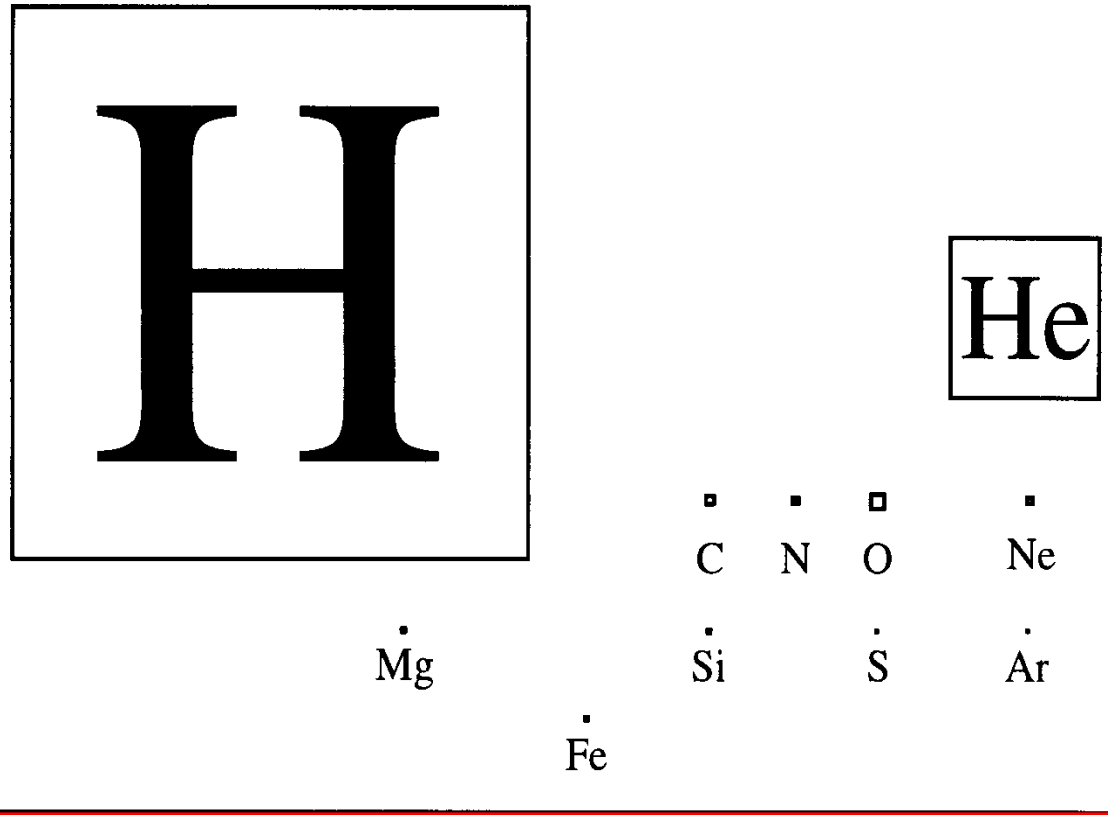

~0.005%……D

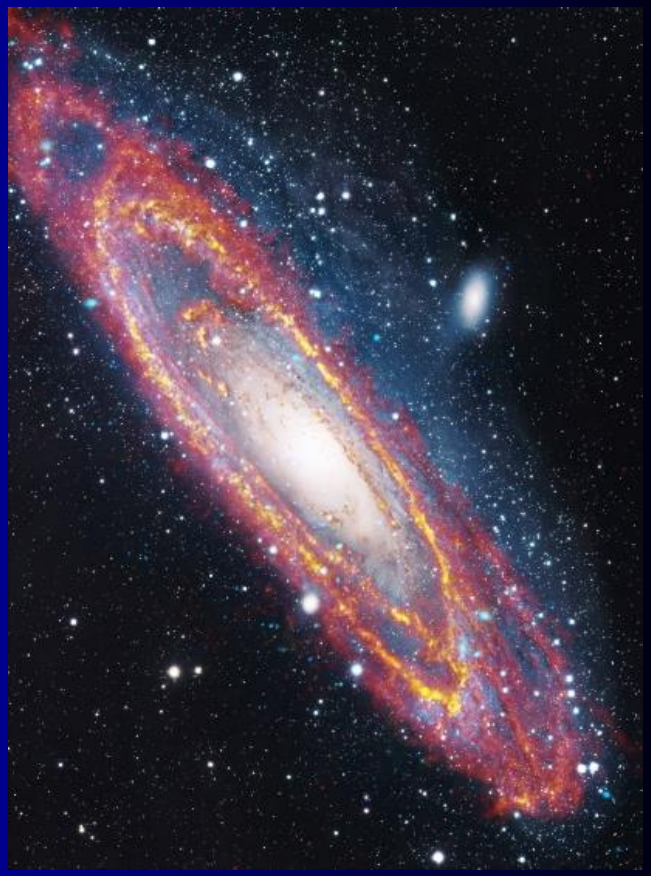

Andromeda composite

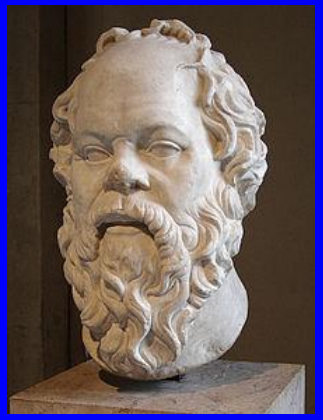

Scio me nihil scire

The astrochemistry game plan

Laboratory astrophysics and related theory

- Spectroscopy
- Collisional excitation rate coefficients
- Bimolecular reaction rate coefficients
- Grain surface reactions
- Photoionization and photodissociation cross-sections

Observations of astrophysical molecules

- Emission line luminosities
- Absorption line optical depths

Astrochemical modeling of …

- Diffuse IS cloud
- Dense IS clouds
- Photodissociation regions
- Circumstellar outflows
- X-irradiated regions
- Excitation and radiative transfer

Information of general astrophysical interest

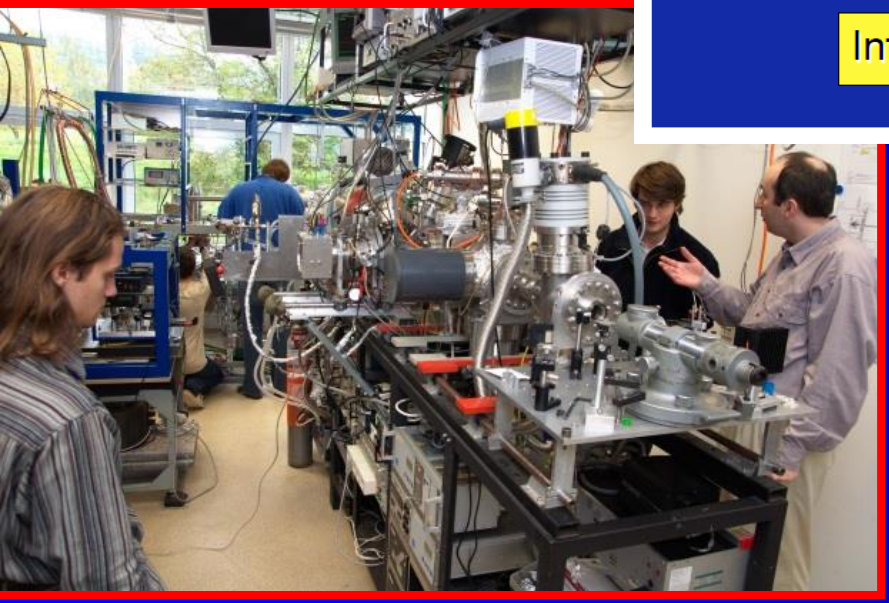

Plasma physics laboratory

KFPP MFF UK

Načo chodiť do školy

THE ASTROPHYSICAL JOURNAL, 787:44 (10pp), 2014 May 20 doi:10.1088/0004-637X/787/1/44

2014

FIRST TIME-DEPENDENT STUDY OF H_2 AND H_3^+ *ORTHO–PARA* CHEMISTRY IN THE DIFFUSE INTERSTELLAR MEDIUM: OBSERVATIONS MEET THEORETICAL PREDICTIONS*

T. ALBERTSSON[1], N. INDRIOLO[2], H. KRECKEL[3], D. SEMENOV[1], K. N. CRABTREE[4], AND TH. HENNING[1]
[1] Max-Planck-Institut für Astronomie, Königstuhl 17, D-69117 Heidelberg, Germany
[2] Department of Physics and Astronomy, Johns Hopkins University, Baltimore, MD 21218, USA
[3] Max-Planck-Institut für Kernphysik, D-69117 Heidelberg, Germany
[4] Harvard–Smithsonian Center for Astrophysics, 60 Garden Street, Cambridge, MA 02138, USA
Received 2013 December 4; accepted 2014 March 28; published 2014 May 2

The chemistry in the diffuse interstellar medium (ISM)

THE ASTROPHYSICAL JOURNAL, 787:44 (10pp), 2014 May 20

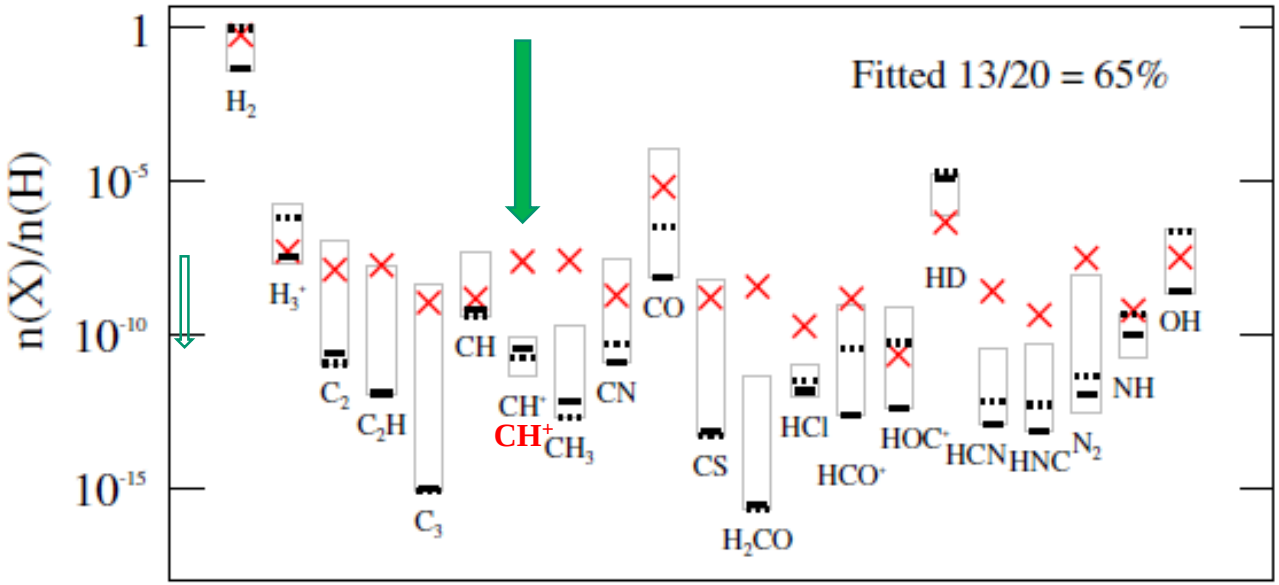

Figure 6. Comparison of observed abundances (red crosses) to modeled values of key species in diffuse clouds. Gray boxes show the range of abundances calculated from the considered models (Table 2) and black lines show abundances from the best-fit model "2X+C15" (30 K, solid line, and 90 K, dotted line).

(A color version of this figure is available in the online journal.)

Temperature scale should be logarithmic

Far Infrared Absolute Spectrophotometer (FIRAS)

cosmic microwave background

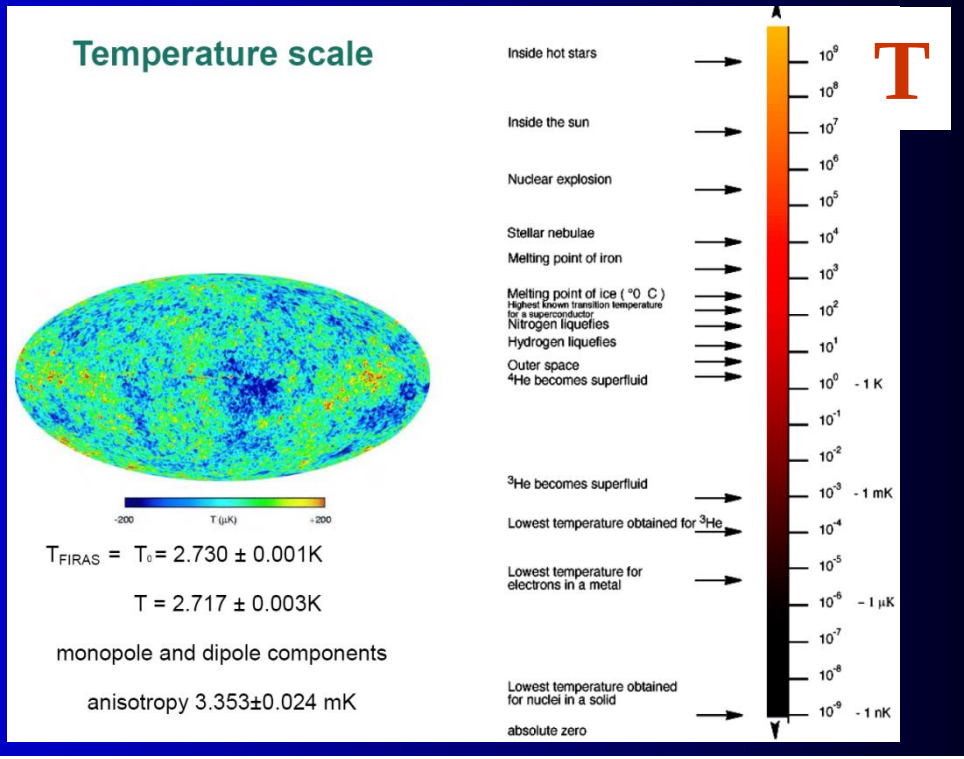

The **cosmic microwave background** (**CMB, CMBR**), Big Bang cosmology, is electromagnetic radiation which is a remnant from an early stage of the universe, also known as "relic radiation". The CMB is faint cosmic background radiation filling all space. It is an important source of data on the early universe because it is the oldest electromagnetic radiation in the universe, dating to the epoch of recombination. With a traditional optical telescope, the space between stars and galaxies (the *background*) is completely dark. However, a sufficiently sensitive radio telescope shows a faint background noise, or glow, almost isotropic, that is not associated with any star, galaxy, or other object. This glow is strongest in the microwave region of the radio spectrum. The accidental discovery of the CMB in 1965 by American radio astronomers Arno Penzias and Robert Wilson[1][2] was the culmination of work initiated in the 1940s, and earned the discoverers the 1978 Nobel Prize in Physics.

Plasma

Pla

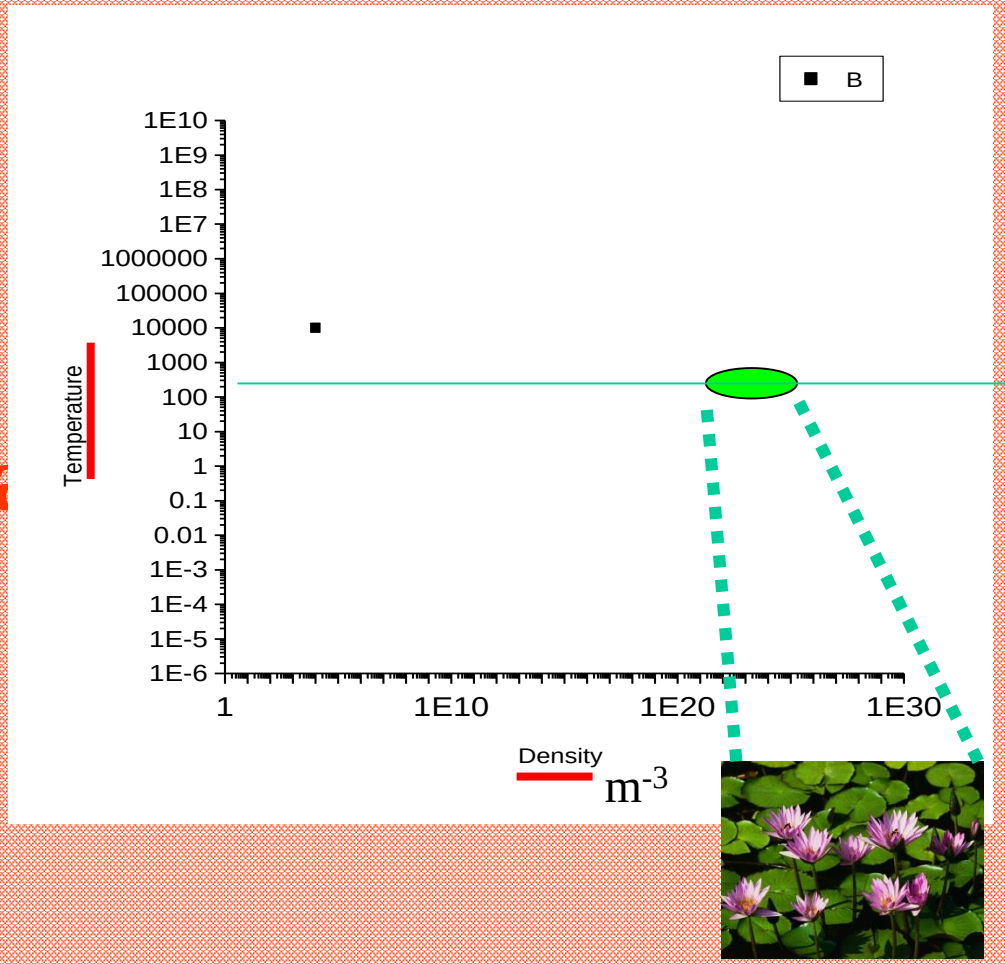
B
1E10
1E9
1E8
1E7
1000000
100000
10000
1000
100
10
1
0.1
0.01
1E-3
1E-4
1E-5
1E-6
Temperature
1
1E10
1E20
1E30
Density
m-3

Not actualized, approximation

Plazma ….n_e …T_e …. T

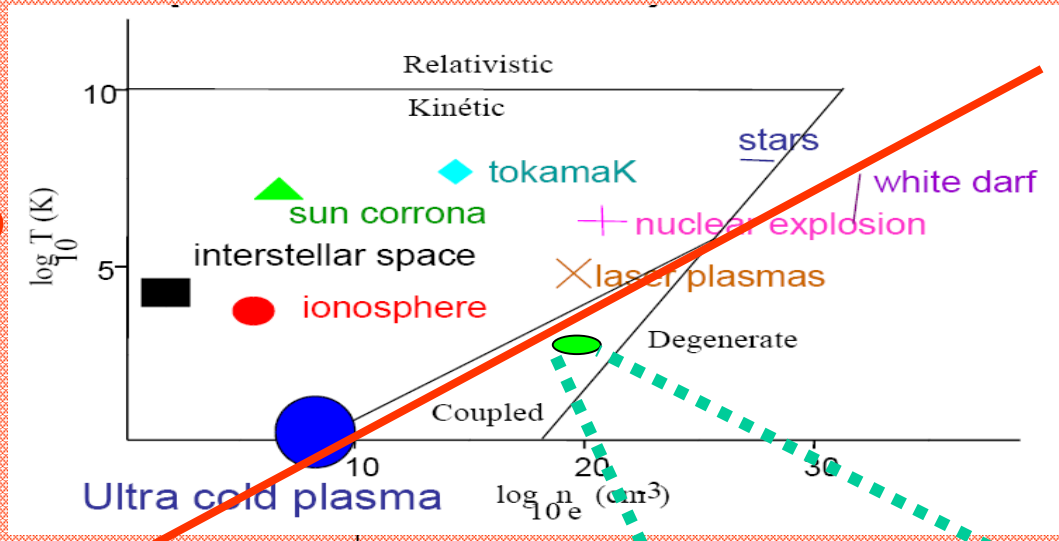

P

$n_0 = 2{,}686\ 781\ 1(15)\times 10^{25}\ \mathrm{m}^{-3}$.

$$W_{kin} \sim W_{Pot..elektrost}$$

$$\frac{3}{2}kT \sim \frac{e^2}{\varepsilon a} \sim \frac{e^2}{\varepsilon N^{-1/3}}$$

$$T \sim \frac{10^{-38}}{k\varepsilon} N^{1/3}$$

$$T_K = 1K \Rightarrow N_K = 10^9\, m^{-3}$$

Temperatures and energies

$E \leftrightarrow kT$

1eV ~ 11 604.505 K

1K ~ 9×10^{-5}eV

$\log T_e$ (K)

PLASMA AS A STATE OF MATTER

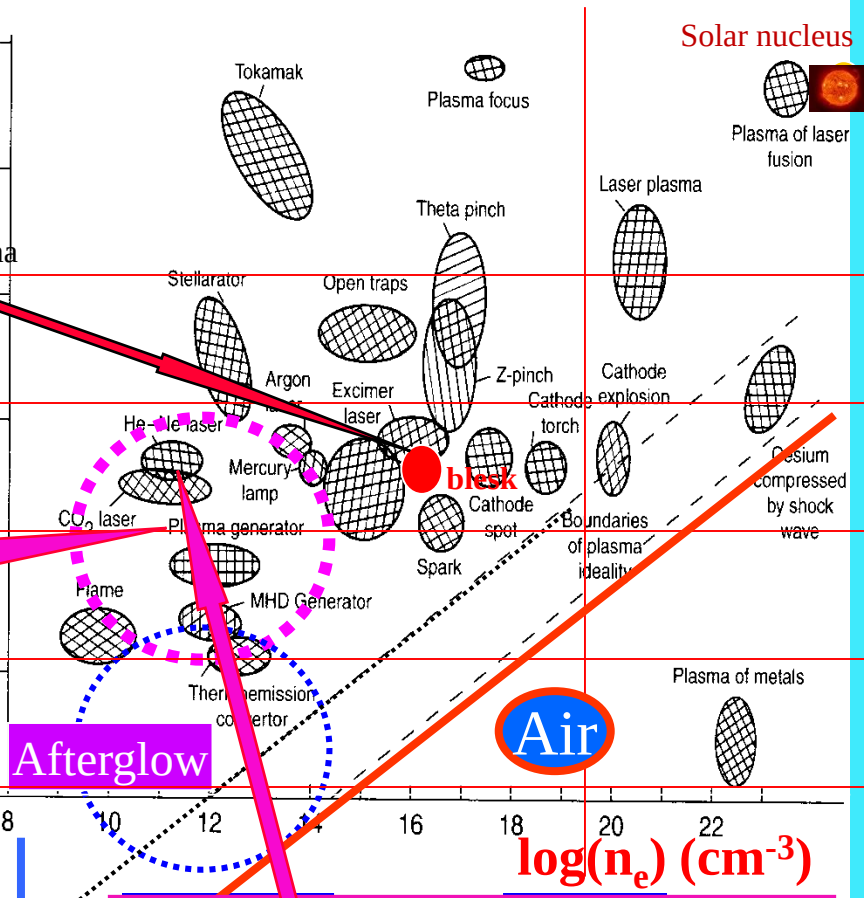

Plasma in earth's magnetosphere

Solar corona

100eV 10^6 K

10eV 10^5 K

Solar wind near the Earth

1eV 10^4 K

Ionosféra

0.1eV 1000 K F_2 F_1

D E

0.01eV 100 K

Afterglow

Air

ISM

1meV 10 K

ATHENA

4 K

ATRAP

4 K

0.1meV 1 K

e^+, p

$\log(n_e)$ (cm^{-3})

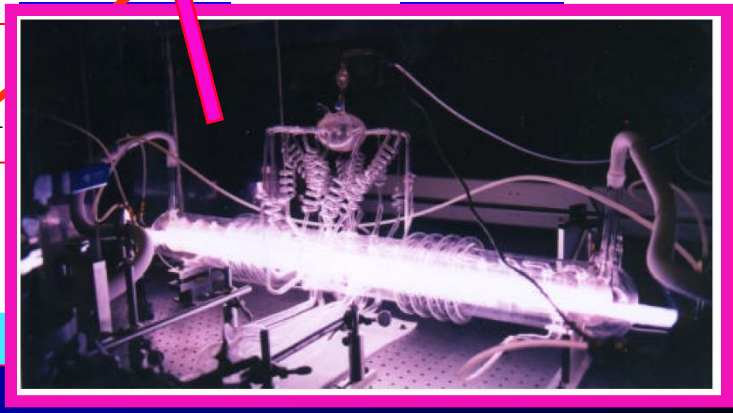

Not actualized, approximation

Parameters of laboratory plasmas

Not actualized, approximation

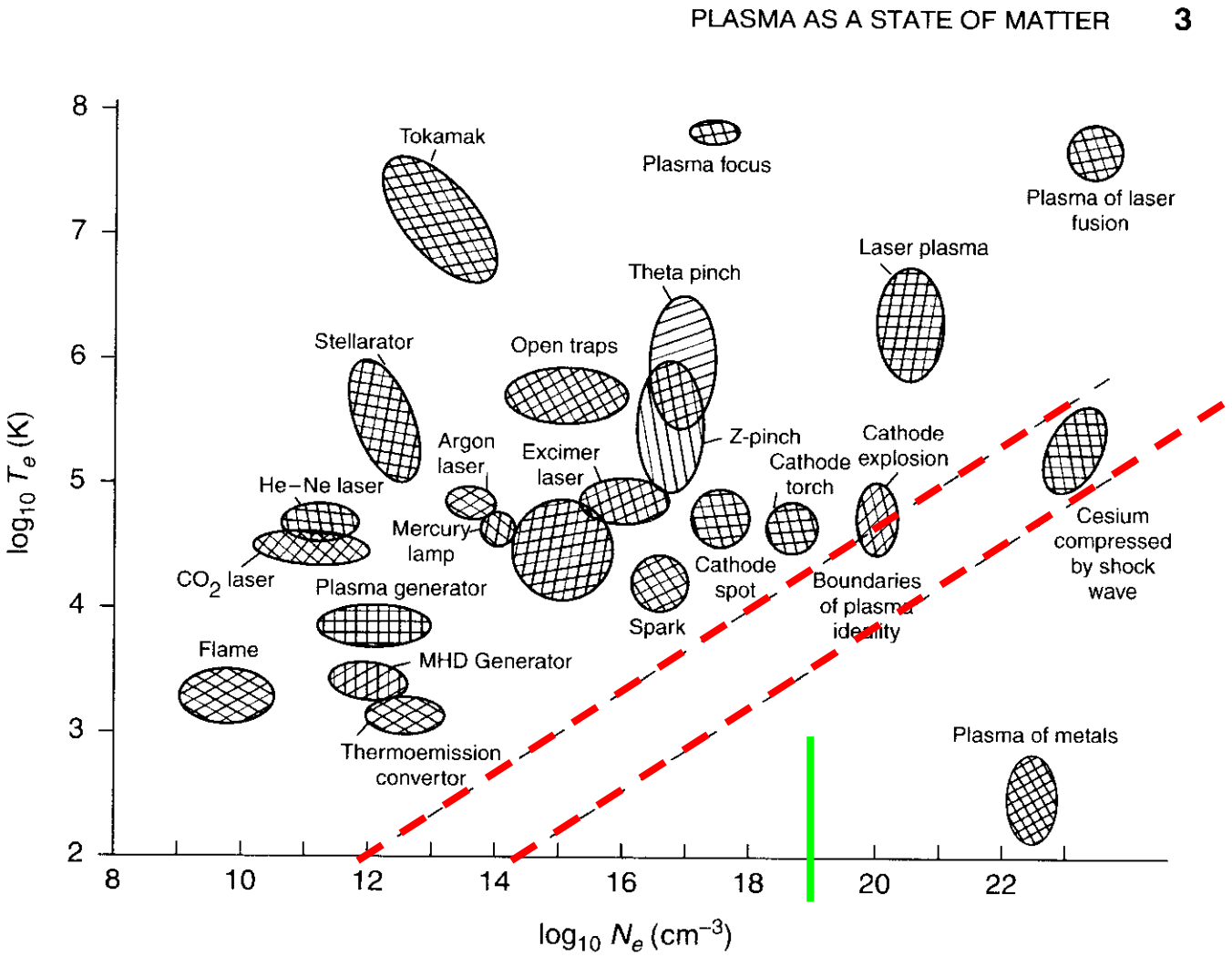

Figure 1.1 Parameters of laboratory plasmas.

Physics of Ionized Gases
Boris M. Smirnov
John Wiley&Sons 2001

Electron temperature and electron number density - PLASMA

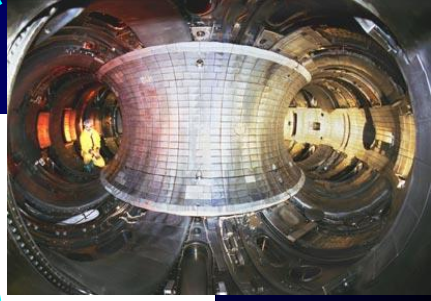

Relativistic

Kinétic

10

5

$\log_{10} T$ (K)

stars

tokamaK

white darf

sun corrona

nuclear explosion

interstellar space

laser plasmas

ionosphere

300 K

Degenerate

Coupled

10

20

30

Ultra cold plasma

$\log_{10} n_e$ (cm^{-3})

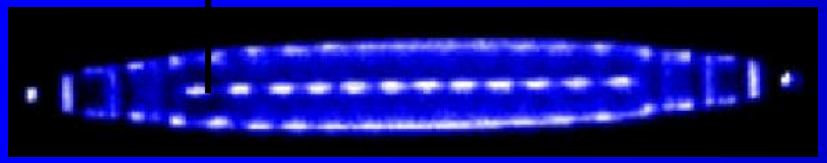

Neutral 1 atm

life

Experiment: T ~ 6 mK

Parameters of plasmas found in nature

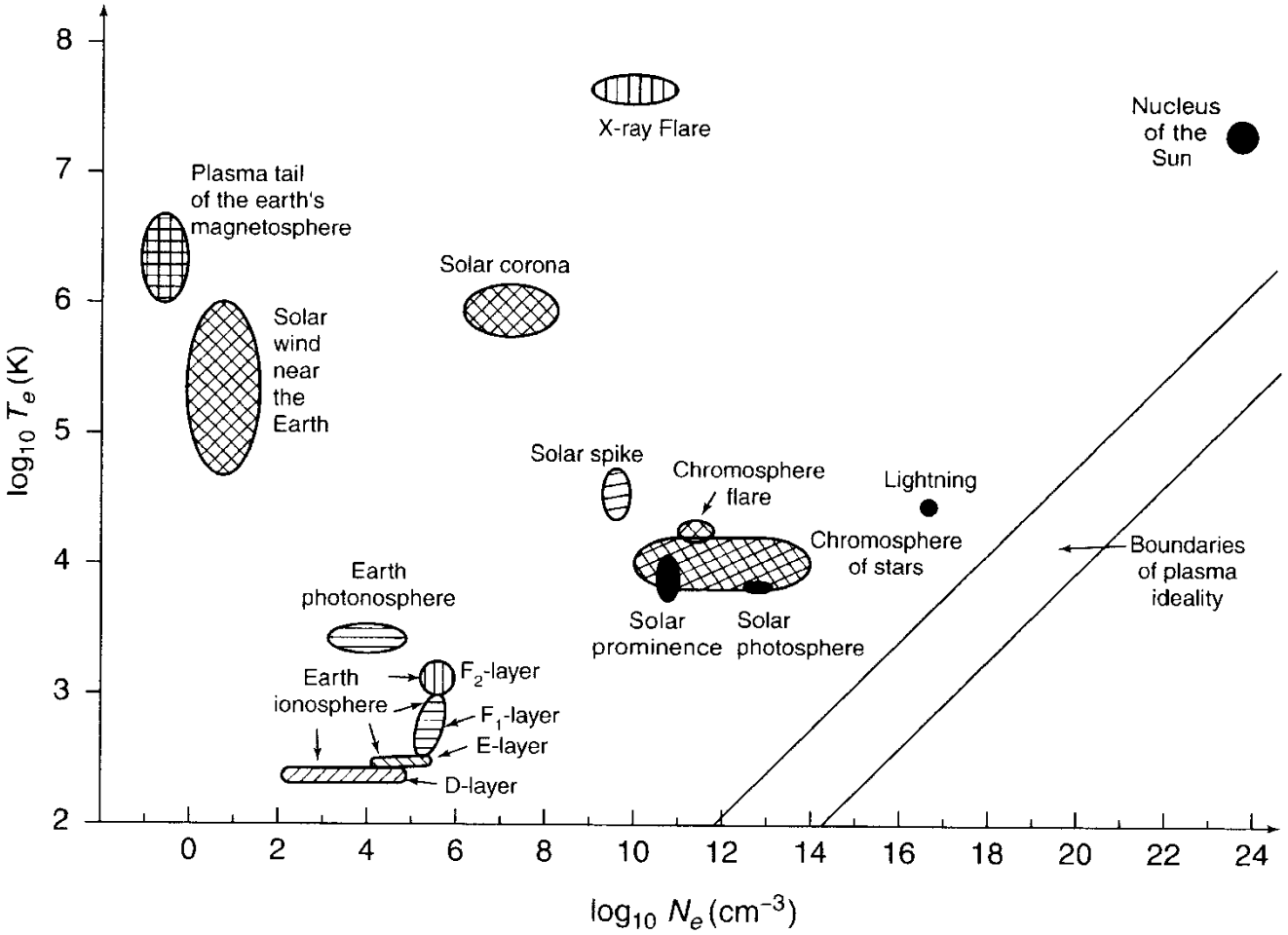

Figure 1.2 Parameters of plasmas found in nature.

Electron and gas temperatures in plasmas

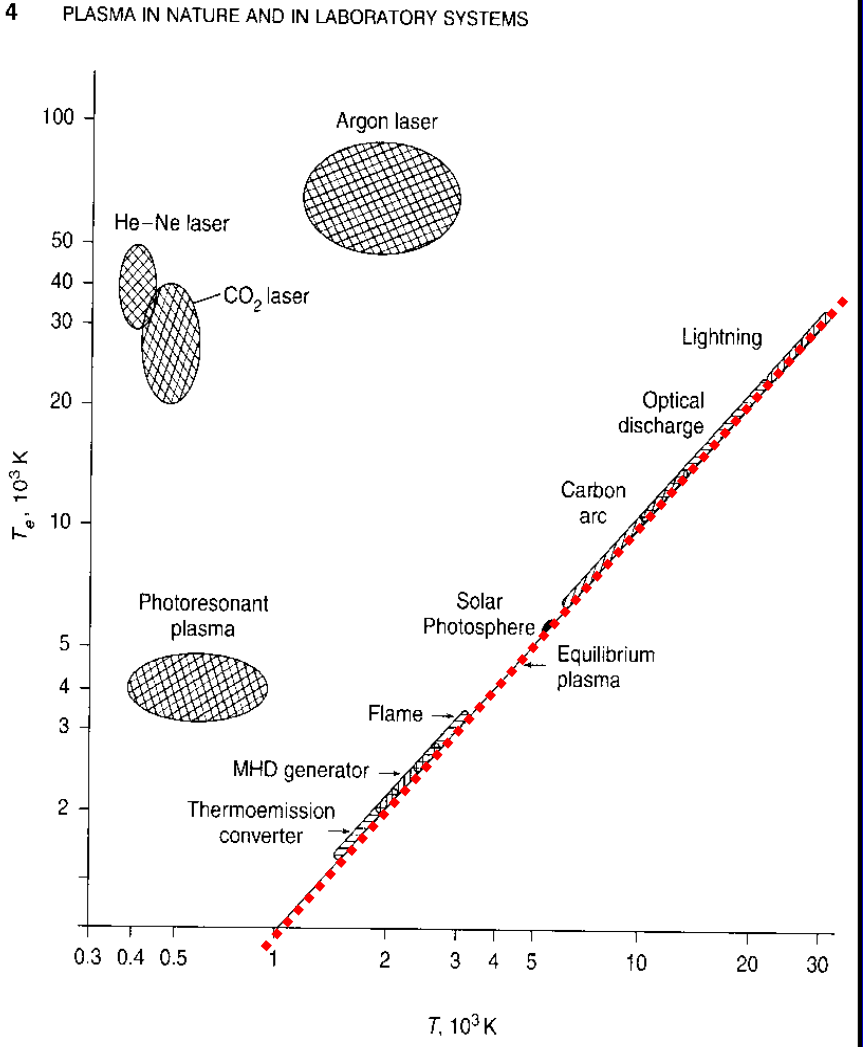

Figure 1.3 Electron and gas temperatures of laboratory plasmas. The straight line corresponds to the equilibrium plasma whose electron and gas temperatures are the same.

Difference in electron, ion and neutral gas temperature in plasma

Equilibrium; relaxation time,

Probability of interactions…

Collisional frequency, Energy transfer

cross section

Temperature in the ionosphere

Temperatures in the ionosphere

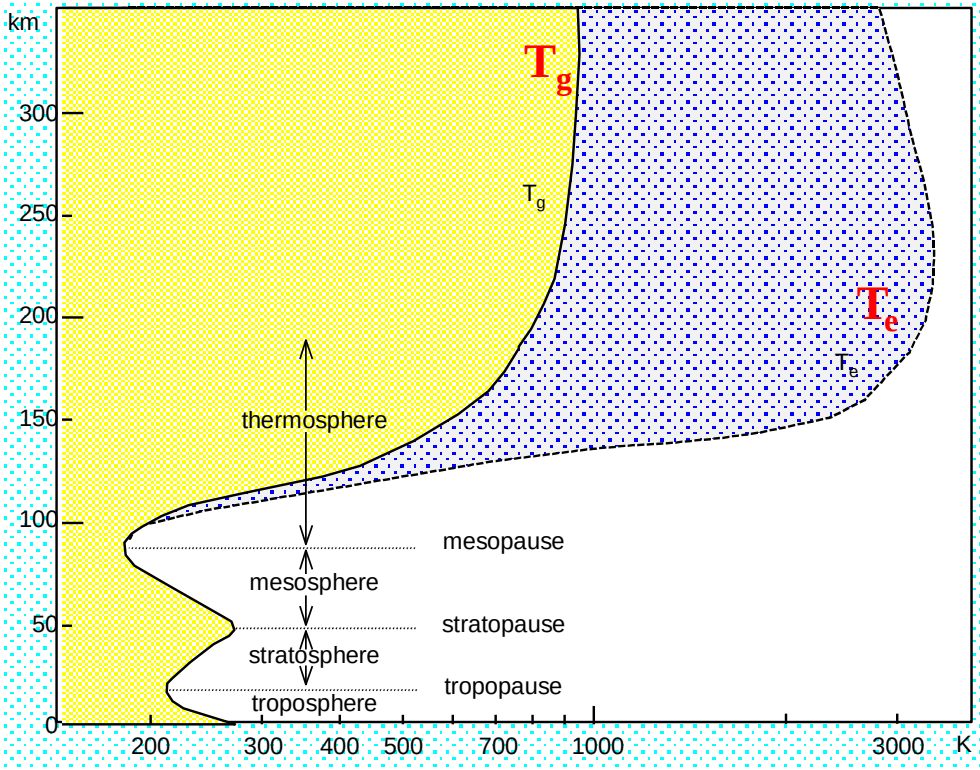

Ions chemistry

n_0 = 2,686 781 1(15)×10^{19} cm^{-3}.

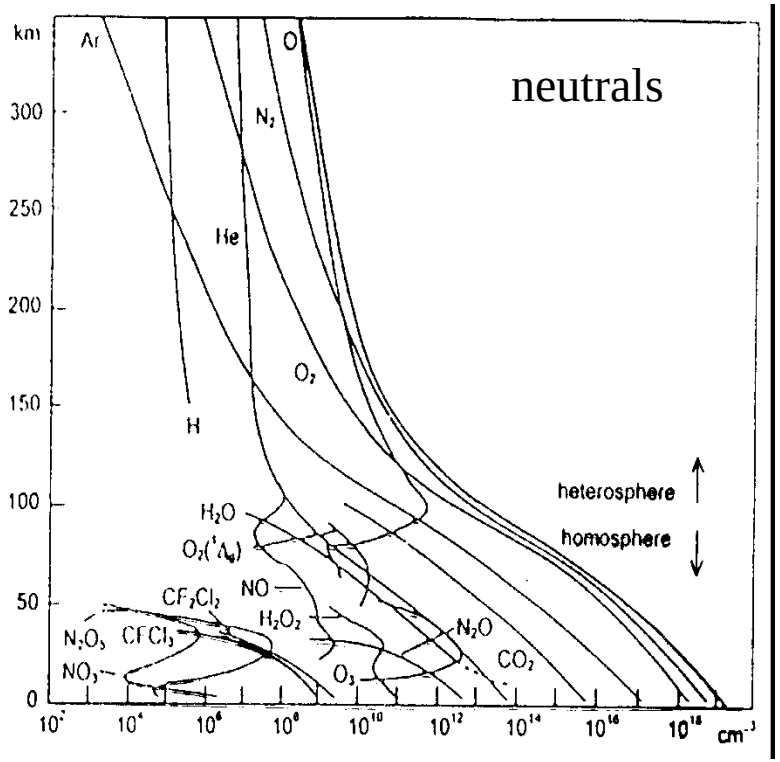

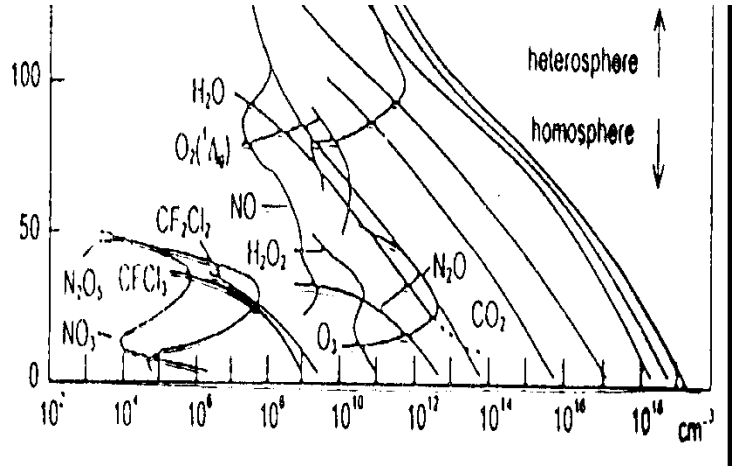

Ions in the terrestrial atmosphere

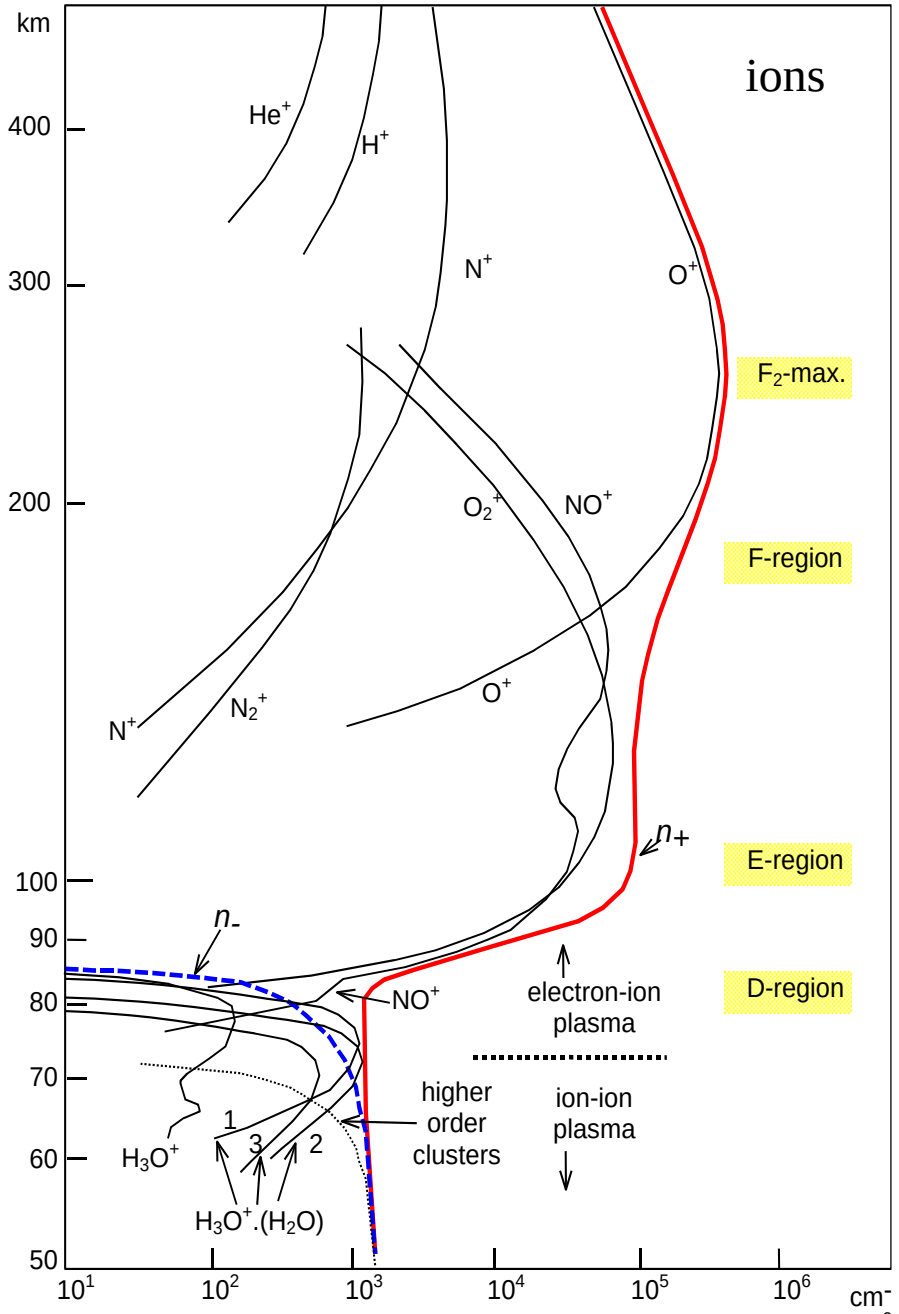

Ions in the terrestrial atmosphere

Temperatures in the ionosphere

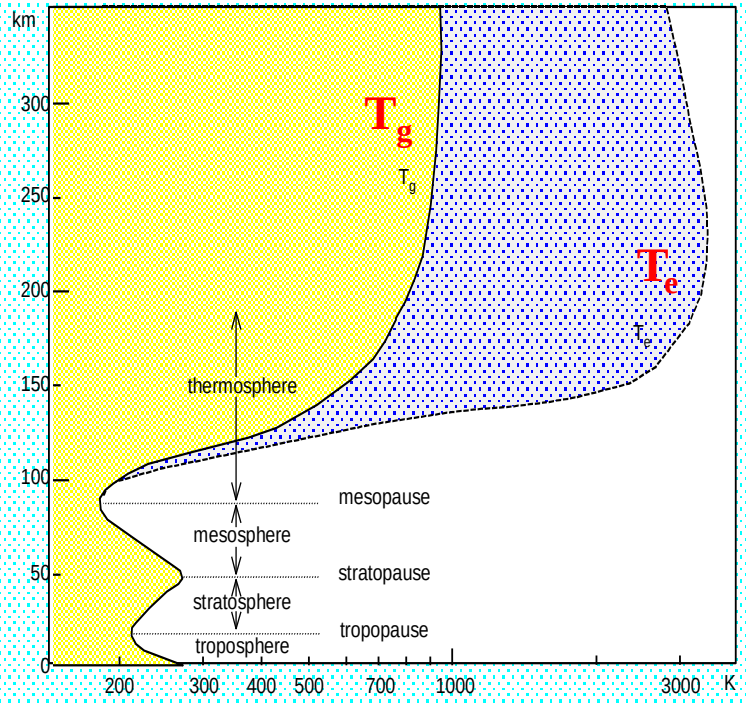

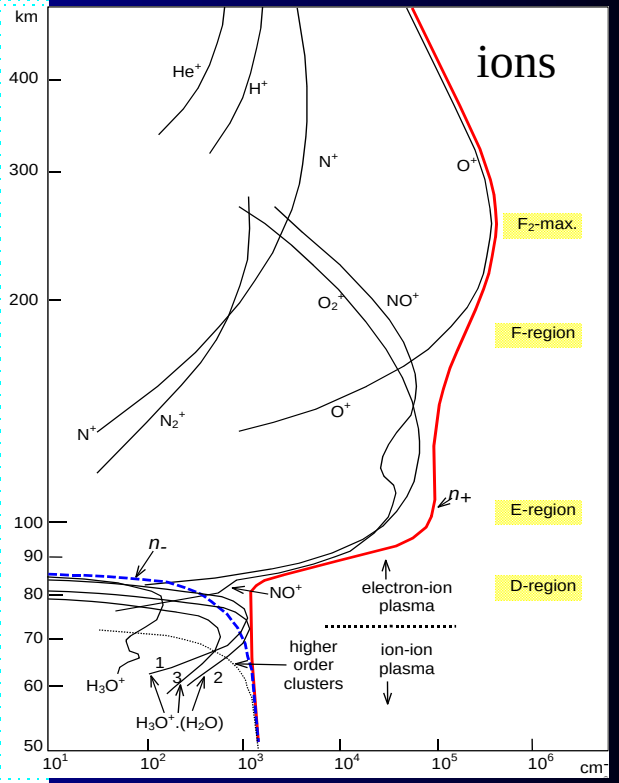

Recombination?? $\alpha(T)$

Crab Nebula

ISM

Hydrogen only??

Ions chemistry

Electron – ion interactions

Negative ions ??

….. ??

Scio me nihil scire

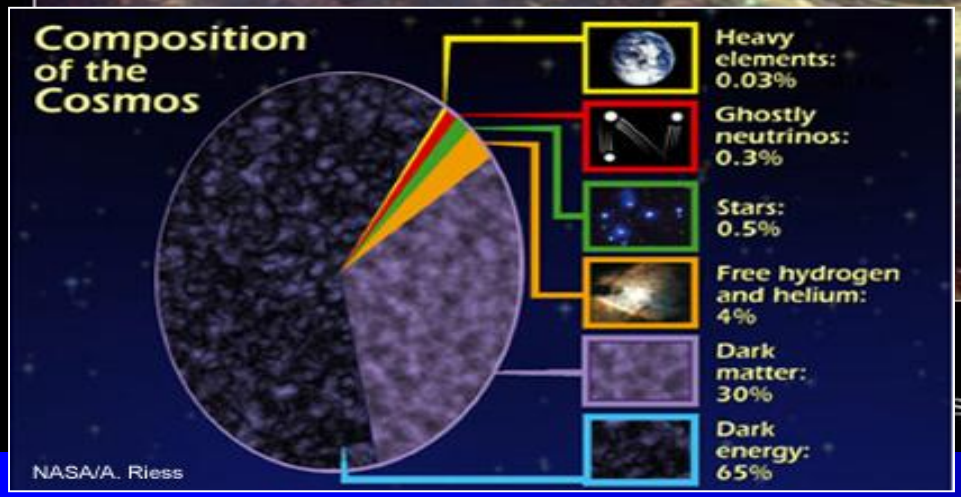

Hubble Heritage

SA and The Hubble Heritage Team (STScI/AURA)

Interstellar medium

92.1% of nucleons in the universe are protons
7.8% are helium nuclei !

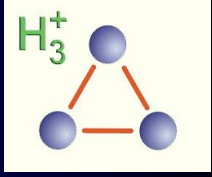

Hydrogen only??

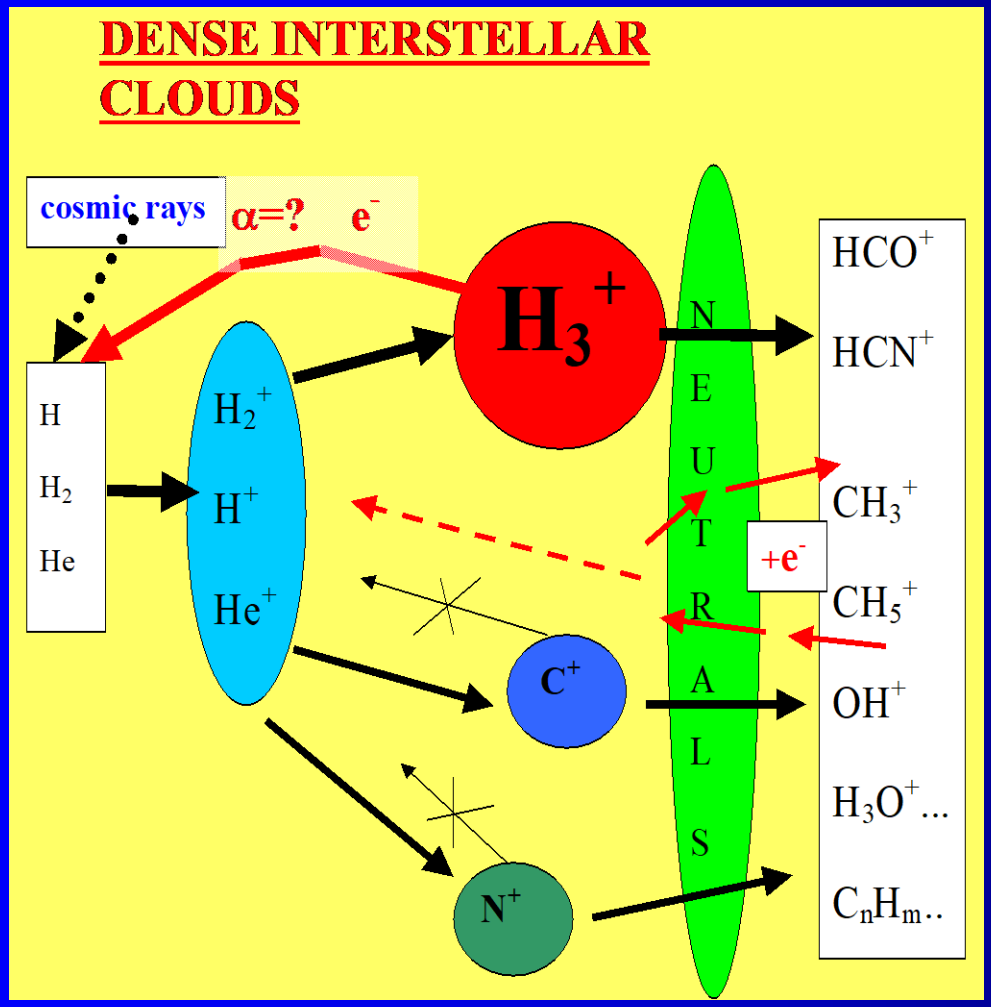

α=?
T~ 10-50K

$$H_3^+ + e^- \Rightarrow H + H_2, 3H$$

Interstellar medium, HD role

@ 10-50K

92.1% of nucleons in the universe are protons
7.8% are helium nuclei !
0.1%……C,N,O,S,Si….

Cosmic abundance

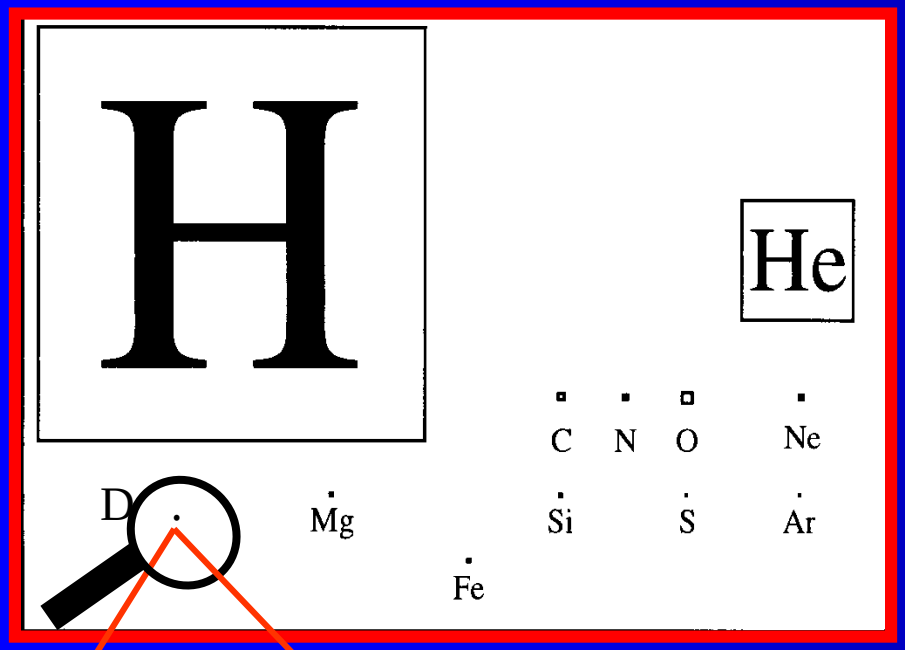

D/H ratio ~ 10^{-5}

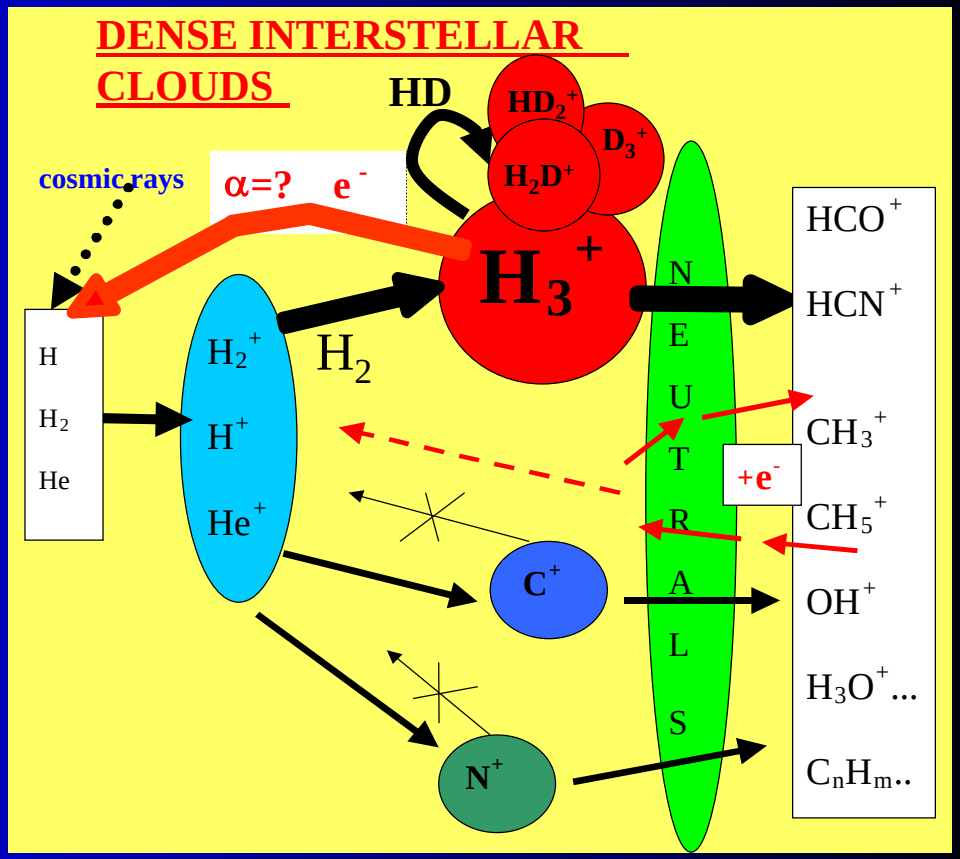

$$H_3^+ + e^- \xrightarrow{\alpha} \text{neutral products}$$

α (10 K) = ???? **k (10 K) = ????**

$$H_3^+ \xrightarrow{HD} H_2D^+ \xrightarrow{HD} HD_2^+ \xrightarrow{HD} D_3^+$$

H_3^+ in interstellar space

$$H_2 \xrightarrow{\text{cosmicray}} H_2^+ + e^-$$

$$H_2 + H_2^+ \rightarrow H_3^+ + H$$

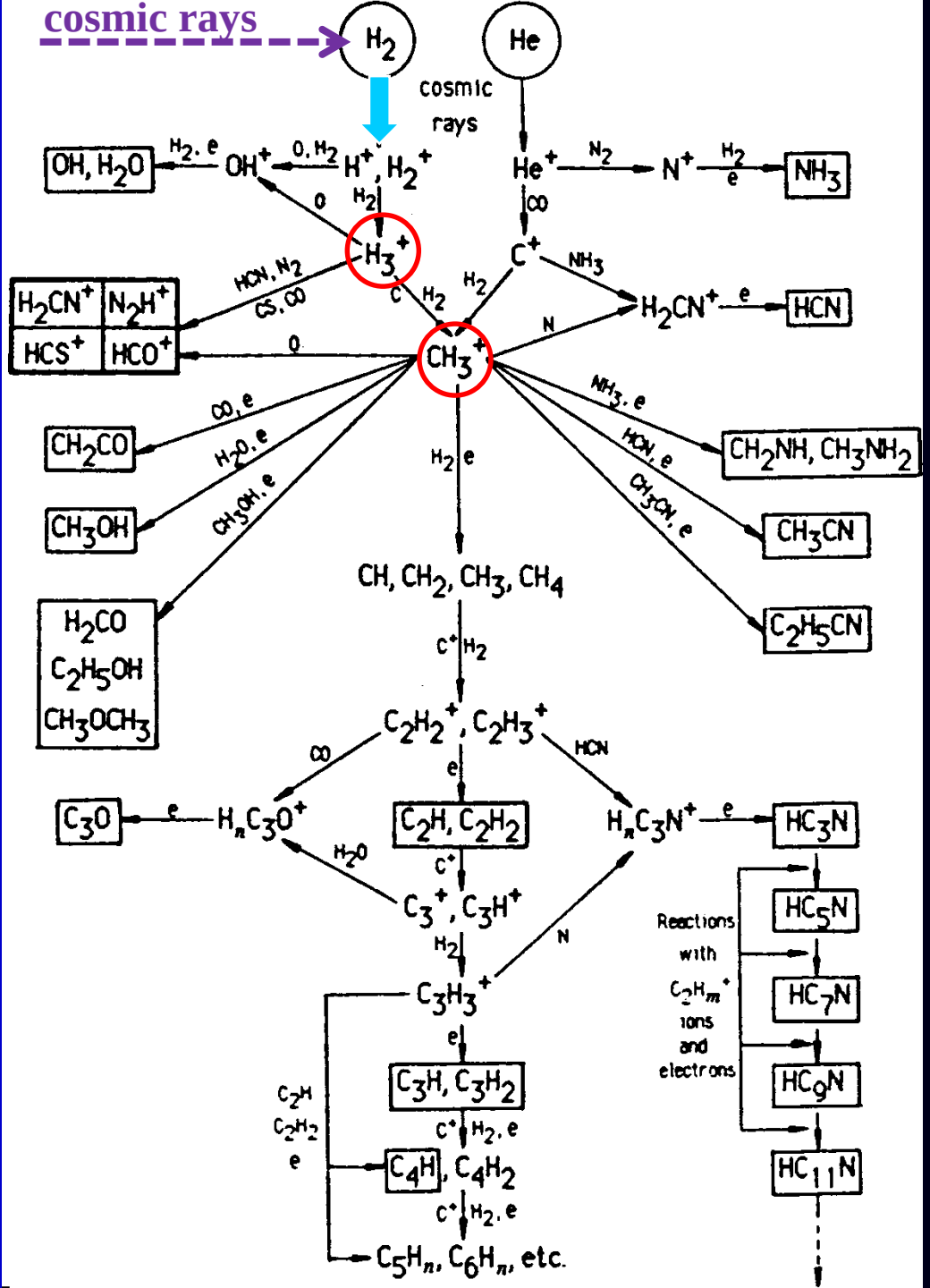

Observation of high population of deuterated molecules

The first detection of deuterated molecules were made in the early 1970s……. Observed enhancement of D in molecules

H_2D	Stark	(1999)	1_{10}–1_{11} transition of ortho- emission from young stellar object NGC 1333 IRAS4A.
H_2D^+	Caselli	(2003)	detected towards L1544.
HD_2^+	Vastel	(2004)	the first detection
CH_2DOH…	Parise	(2003, 2004)	have detected 4 isotopomers of deuterated methanol
NHD_2/NH_3	Roueff	(2000)	
	Loinard	(2001)	is 0.005 in the cold cloud L134N and 0.03 in the low-mass protostar 16293 E
D_2CO/H_2CO	Loinard	(2002)	
	Bacmann	(2003)	is between 0.01 and 0.4 in a low-mass protostars and prestellar cores
NH_2D/NH_3	J. Hatchell	(2003)	high ratios~4–33% in protostellar cores
ND_3/NH_3	Lis	(2002)	ratio ~10^{-3} cold dense Barnard 1cloud
	Tak	(2002)	Class 0 protostar NGC 1333 IRAS4A

Observed ratio ~10^{-3}

statistical ratio ~ $(D/H)^3$ ≈ 10^{-14} ➔Enhancement of 10^{11}

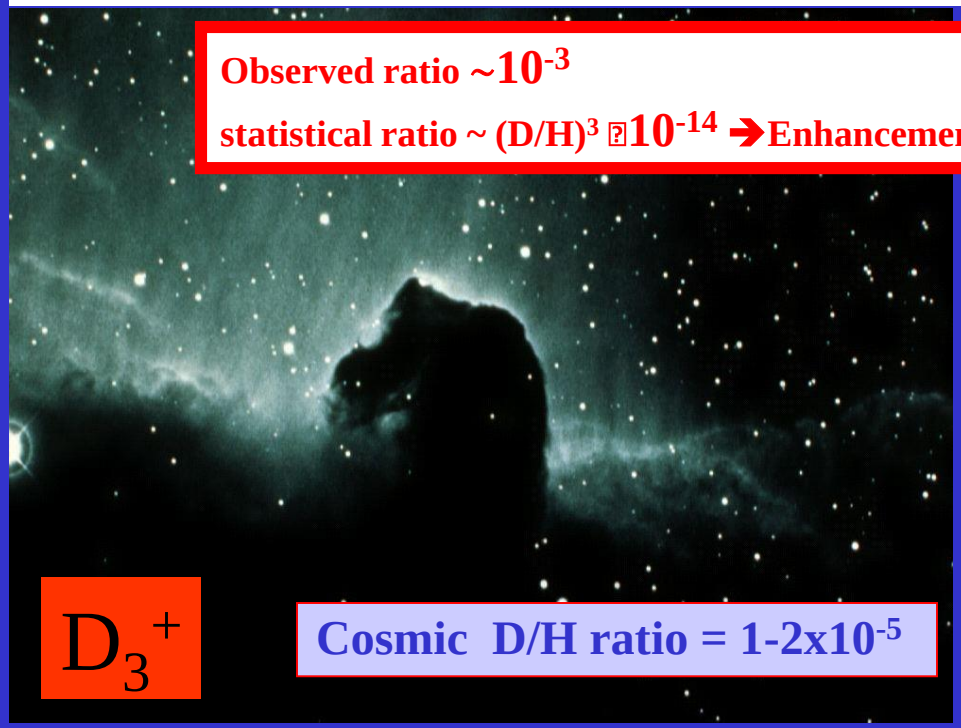

D_3^+

Cosmic D/H ratio = 1-2x10^{-5}

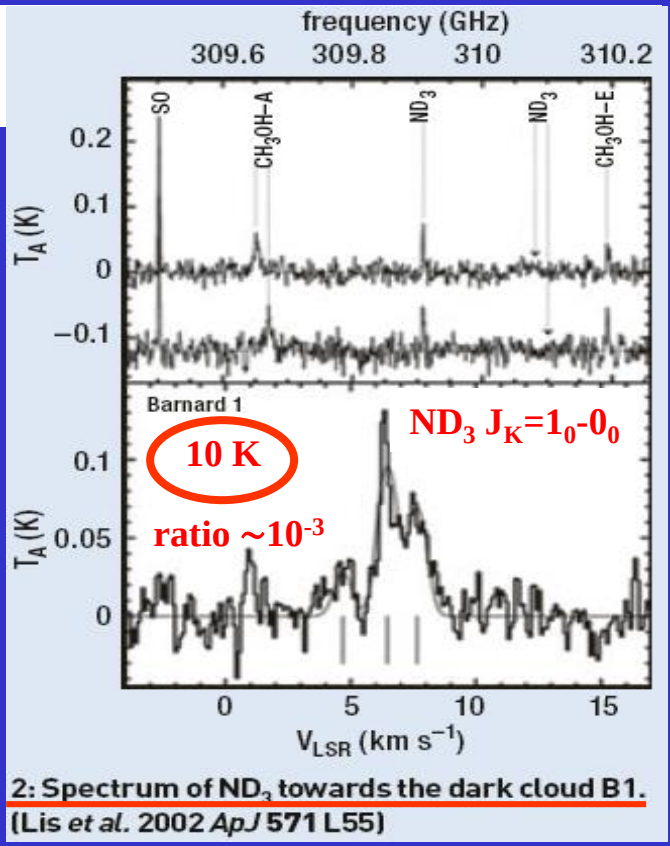

2: Spectrum of ND_3 towards the dark cloud B1. (Lis *et al.* 2002 *ApJ* **571** L55)

High population of deuterated molecules

Cosmic D/H ≈ 10^{-5}

XD/XH ≈ 10^{-1}-10^{-3}

XD_2 / XH_2 ≈ 10^{-2}

XD_3 / XH_3 ≈ 10^{-3}

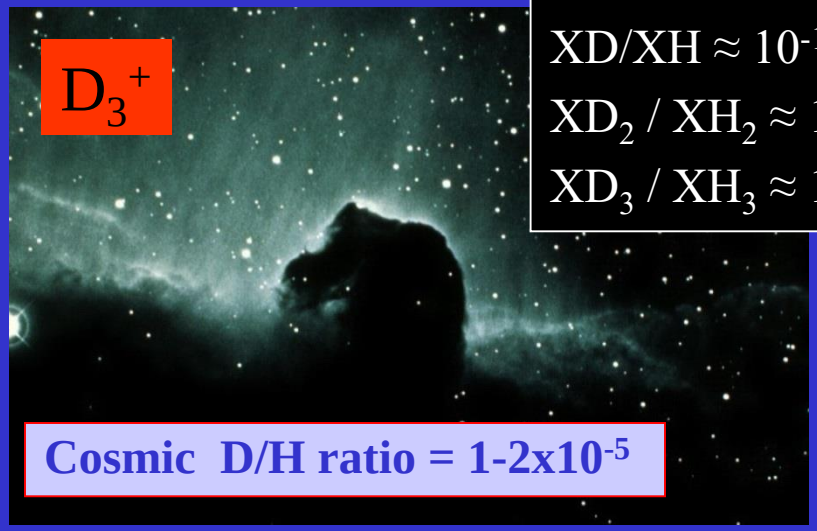

Cosmic D/H ratio = 1-2x10^{-5}

Species	Observed ratio
NH_2D/NH_3	0.01
$HDCO/H_2CO$	0.005-0.11
DCN/HCN	0.023
DNC/HNC	0.015
C_2D/C_2H	0.01
DCO^+/HCO^+	0.02
N_2D^+/N_2H^+	0.08
DC_3N/HC_3N	0.03-0.1
$HDCS/H_2CS$	0.02

	H_3^+	D_3^+
HD	H_2D^+	D_2H^+
N_2D^+	DCO^+	DCN
DNC	HDCS	D_2CS
HDO	DC_3N	DC_5N
C_3HD	HDCO	D_2CO
CH_3OD	CH_2DOH	CHD_2OH
CD_3OH	CH_2DCN	NH_2D
NHD_2	ND_3	CHD_2CCH
CH_3CCD	C_2D	C_4D
HDS	D_2S	

Deuterated molecules that have been detected in interstellar clouds as of February 2005.

Gas phase reactions,

ion-molecule reactions,
recombination

Grain surface reactions

Physics of condensation and evaporation from grain surface

Deuterated gas phase molecules in space

HD * #	HDCO	H_2D^+ *	D_2CO
HDO *	HDCS	DCO^+ *	ND_2H
DCN *	DC_3N	N_2D^+	CHD_2OH
DNC	CH_2DOH		D_2S
HDS	CH3OD		ND_3
C_2D	DC_5N		CD_3OH
C_4D	CH_2DCCH		D_2CS
C_3HD	CH_2DCN		
NH_2D	CH_3D		

Planets
Comets
CS disks
ISM
Extragalactic #

Cosmic D/H ≈ 10^{-5}

XD/XH ≈ 10^{-1}-10^{-3}

XD_2 / XH_2 ≈ 10^{-2}

XD_3 / XH_3 ≈ 10^{-3}

HD

$$H_3^+ + HD \Leftrightarrow H_2D^+ + H_2$$

$$H_2D^+ + HD \Leftrightarrow HD_2^+ + H_2$$

$$HD_2^+ + HD \Leftrightarrow D_3^+ + H_2$$

Energy

Small differences in zero point energies for deuterated molecules

$\Delta H / k = -232\ K$

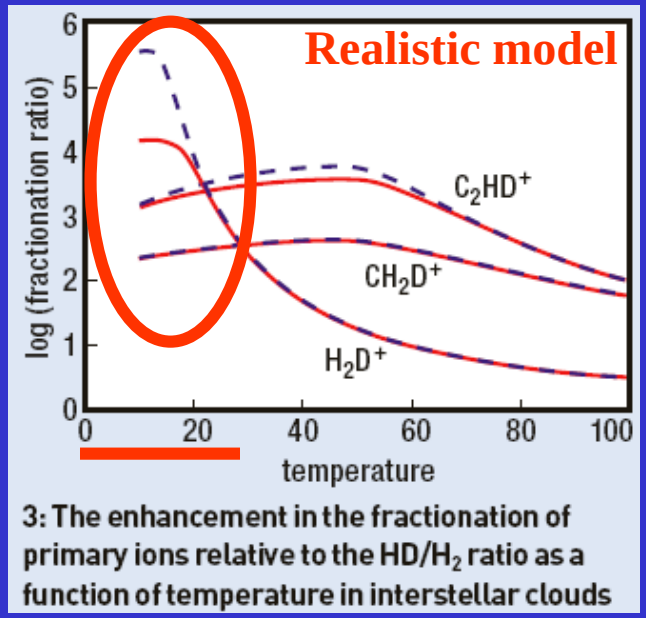

3: The enhancement in the fractionation of primary ions relative to the HD/H_2 ratio as a function of temperature in interstellar clouds

$$H_3^+ + HD \underset{k_r}{\overset{k_f}{\rightleftharpoons}} H_2D^+ + H_2$$

$$k_r / k_f \sim \exp(\Delta H / kT) \sim \exp(-232\ /T)$$

In equilibrium $\quad \dfrac{H_3^+}{H_2D^+} = \dfrac{H_2}{HD}\dfrac{k_r}{k_f}$

$$@300\ K \quad k_r / k_f \sim \exp(-1) \sim 0.4$$

k_f ⇀ ↽ k_r

$$@10\ K \quad k_r / k_f \sim \exp(-23) \sim 10^{-10}$$

k_f ⇀ ✗ ↽ k_r

$$@10\ K \quad \frac{H_3^+}{H_2D^+} = \frac{H_2}{HD}\frac{k_r}{k_f} \sim 10^5 \cdot 10^{-10} = 10^{-5}$$

ONLY PARTLY !!!???

	$-\Delta H / k$
$H_2D^+ + HD \Leftrightarrow HD_2^+ + H_2$	$187\,K$
$HD_2^+ + HD \Leftrightarrow D_3^+ + H_2$	$234K$

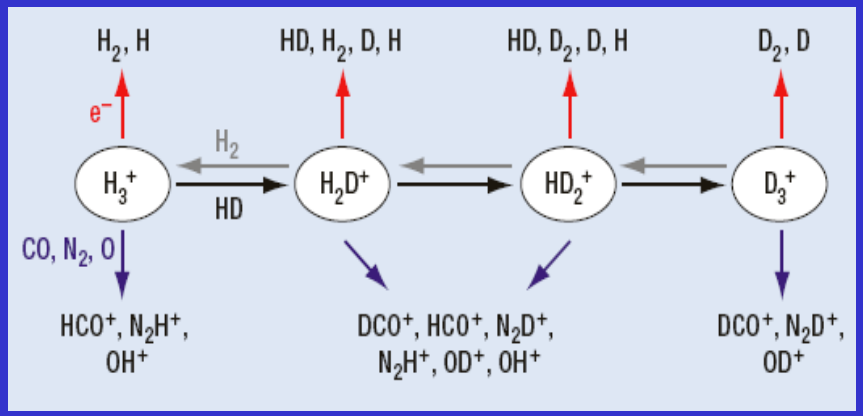

Molecules in interstellar space

DIBs - diffuse bands

1919-1922

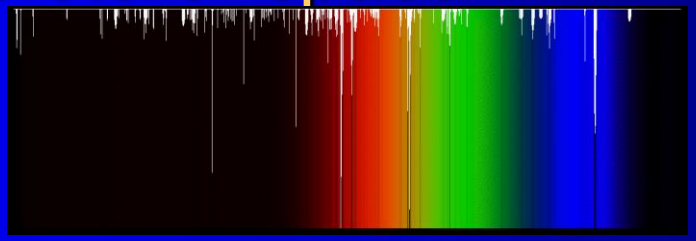

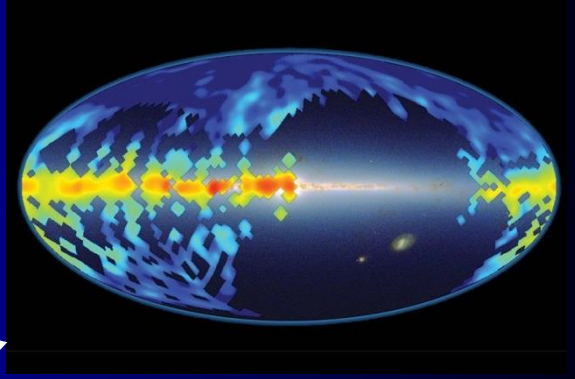

1919-1922 Heger discovers the DIBs

Nearly 100 years ago Mary Lea Heger discovered diffuse bands in the spectra of stars due to some sort of material maybe molecules in the space between stars and Earth. A map of the data from the Sloan Digital Sky Survey, by a team from Johns Hopkins produced this map. **Red indicates areas with the most abundant DIB molecules, blue the least.**

Molecules in interstellar space

DIBs - diffuse bands

1919-1922

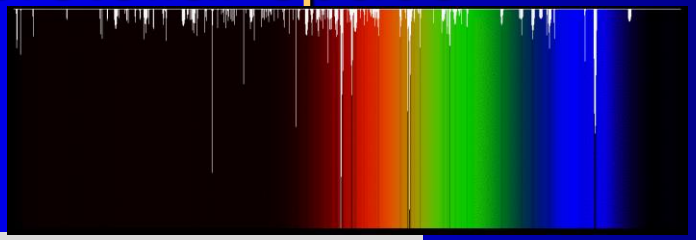

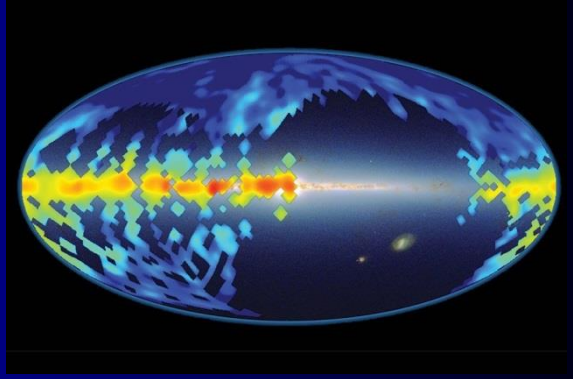

1919-1922 Heger discovers the DIBs

Nearly 100 years ago Mary Lea Heger discovered diffuse bands in the spectra of stars due to some sort of material maybe molecules in the space between stars and Earth. A map of the data from the Sloan Digital Sky Survey, by a team from Johns Hopkins produced this map. Red indicates areas with the most abundant DIB molecules, blue the least.

16 JULY 2015 | VOL 523 | NATURE | 323

LETTER **2015**

doi:10.1038/nature14566

Laboratory confirmation of C_{60}^+ as the carrier of two diffuse interstellar bands

E. K. Campbell[1], M. Holz[1], D. Gerlich[2] & J. P. Maier[1]

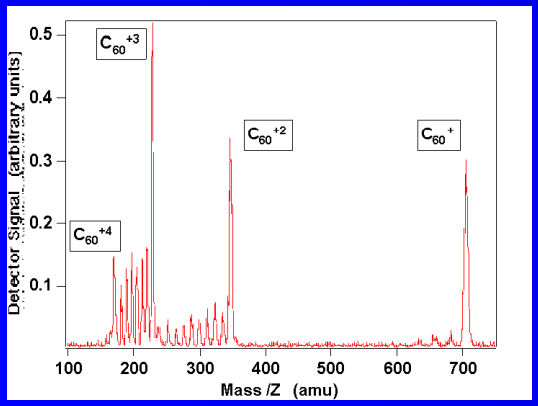

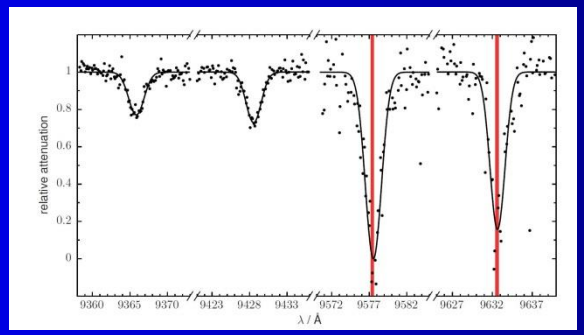

RESEARCH NEWS & VIEWS

ASTROCHEMISTRY

Fullerene solves an interstellar puzzle

Laboratory measurements confirm that a 'buckyball' ion is responsible for two near-infrared absorption features found in spectra of the interstellar medium, casting light on a century-old astrochemical mystery. SEE LETTER P.322

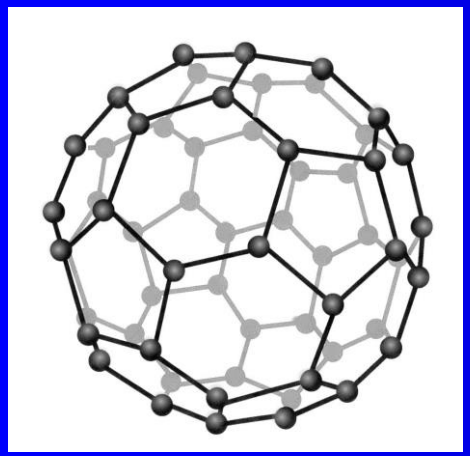

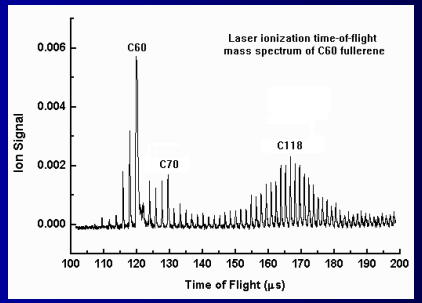

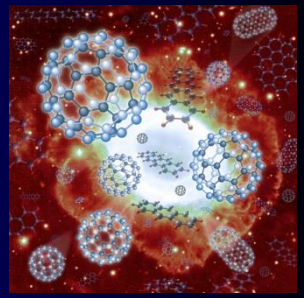

Observation of H_2O^+

A&A 550, A25 (2013)
DOI: 10.1051/0004-6361/201220466

2013

Astronomy & Astrophysics

Excited OH^+, H_2O^+, and H_3O^+ in NGC 4418 and Arp 220⋆

E. González-Alfonso[1], J. Fischer[2], S. Bruderer[3], H. S. P. Müller[4], J. Graciá-Carpio[3], E. Sturm[3], D. Lutz[3], A. Poglitsch[3], H. Feuchtgruber[3], S. Veilleux[5,6], A. Contursi[3], A. Sternberg[7], S. Hailey-Dunsheath[8], A. Verma[9], N. Christopher[9], R. Davies[3], R. Genzel[3], and L. Tacconi[3]

⋆ *Herschel* is an ESA space observatory with science instruments provided by European-led Principal Investigator consortia and with important participation from NASA.

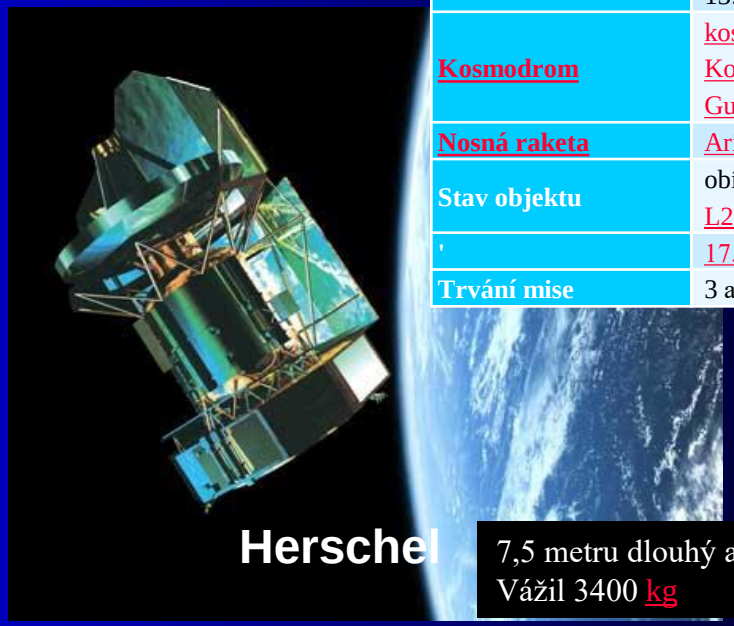

Start	14. května 2009 v 13:12:02 UTC
Kosmodrom	kosmodrom v Kourou, Francouzská Guyana[1]
Nosná raketa	Ariane 5[1]
Stav objektu	obíhala Librační bod L2[1]
'	17. června 2013
Trvání mise	3 až 4 roky[1]

7,5 metru dlouhý a 4 m široký. Vážil 3400 kg

ABSTRACT

We report on *Herschel*/PACS observations of absorption lines of OH^+, H_2O^+ and H_3O^+ in NGC 4418 and Arp 220. Excited lines of OH^+ and H_2O^+ with E_{lower} of at least 285 and ~200 K, respectively, are detected in both sources, indicating radiative pumping and location in the high radiation density environment of the nuclear regions. Abundance ratios OH^+/H_2O^+ of 1–2.5 are estimated in the nuclei of both sources. The inferred OH^+ column and abundance relative to H nuclei are $(0.5–1)\times10^{16}$ cm^{-2} and $\sim2\times10^{-8}$, respectively. Additionally, in Arp 220, an extended low excitation component around the nuclear region is found to have $OH^+/H_2O^+ \sim 5–10$. H_3O^+ is detected in both sources with $N(H_3O^+) \sim (0.5–2)\times10^{16}$ cm^{-2}, and in Arp 220 the pure inversion, metastable lines indicate a high rotational temperature of ~500 K, indicative of formation pumping and/or hot gas. Simple chemical models favor an ionization sequence dominated by $H^+ \rightarrow O^+ \rightarrow OH^+ \rightarrow H_2O^+ \rightarrow H_3O^+$, and we also argue that the H^+ production is most likely dominated by X-ray/cosmic ray ionization. The full set of observations and models leads us to propose that the molecular ions arise in a relatively low density ($\gtrsim10^4$ cm^{-3}) interclump medium, in which case the ionization rate per H nucleus (including secondary ionizations) is $\zeta > 10^{-13}$ s^{-1}, a lower limit that is several $\times 10^2$ times the highest current rate estimates for Galactic regions. In Arp 220, our lower limit for ζ is compatible with estimates for the cosmic ray energy density inferred previously from the supernova rate and synchrotron radio emission, and also with the expected ionization rate produced by X-rays. In NGC 4418, we argue that X-ray ionization due to an active galactic nucleus is responsible for the molecular ion production.

Modeling observations of the interstellar medium (ISM)

David Neufeld
Johns Hopkins University

Recent discoveries of molecules in the diffuse ISM

OH^+	Wyrowski et al. 2010	APEX
SH^+	Menten et al. 2011	APEX
H_2O^+	Gerin et al. 2010	Herschel
HF	Neufeld et al. 2010	Herschel
HCl^+	de Luca et al. 2013	Herschel
H_2Cl^+	Lis et al. 2010	Herschel
SH	Neufeld et al. 2012	SOFIA
ArH^+	Schilke et al. 2014	Herschel

All hydrides with high frequency rotational transitions that are unobservable from the ground or observable only from superb submillimeter sites

Measuring the cosmic-ray ionization rate with OH^+ and H_2O^+

Unlike C^+ and S^+, O^+ does react with H_2 at low temperature. But O is not ionized by UV radiation longward of the Lyman limit, so OH^+ and H_2O^+ formation must be initiated by cosmic ray ionization

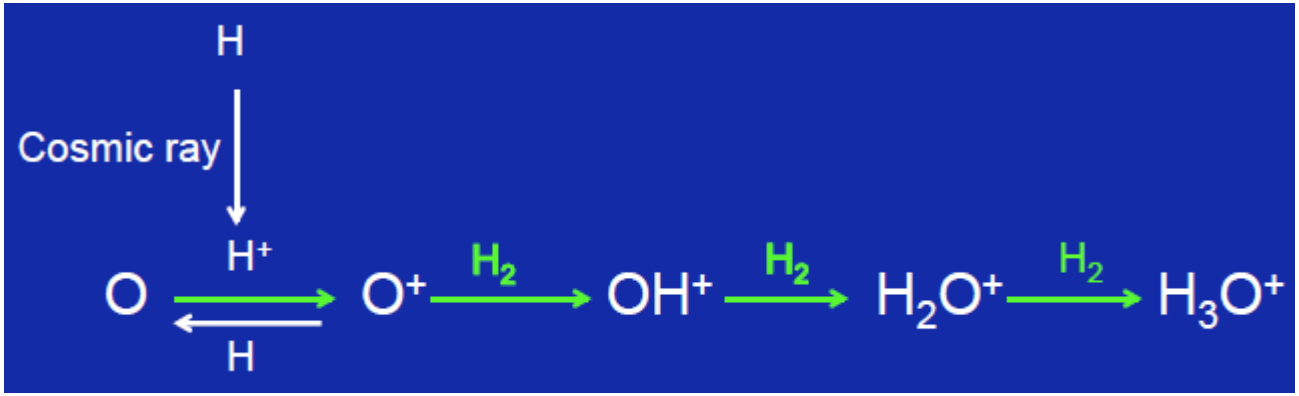

Determining the molecular fraction in the diffuse ISM

The OH^+/H_2O^+ ratio reflects a competition between reaction of OH^+ with H_2 and reaction with electrons

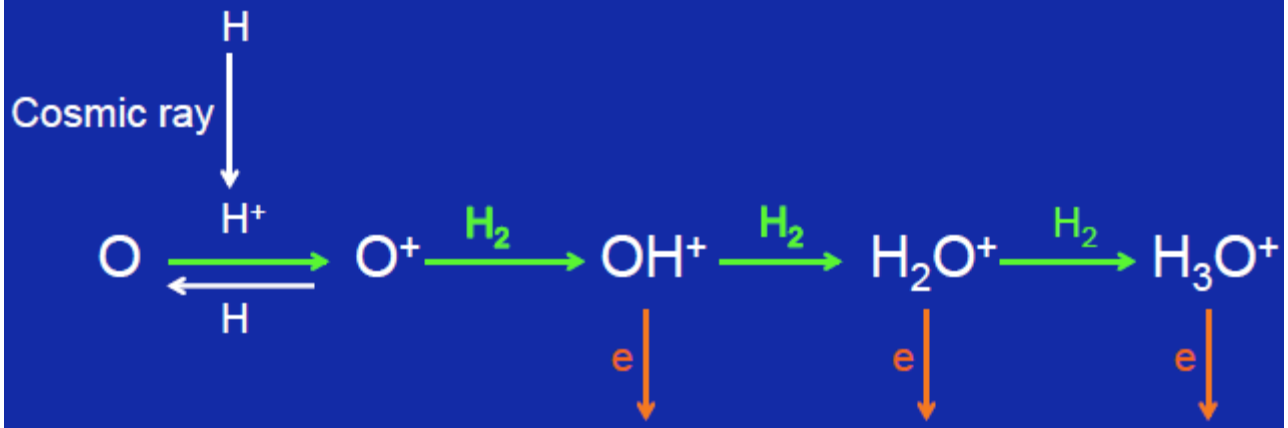

Observed OH^+/H_2O^+ ratios ~ 3 to 15 imply that only 2 – 10 % of the H is typically in H_2

The Astrophysical Journal, 856:100 (6pp), 2018 April 1 https://doi.org/10.3847/1538-4357/aab106

2018

OH^+ Formation in the Low-temperature $O^+(^4S) + H_2$ Reaction

Artem Kovalenko, Thuy Dung Tran, Serhiy Rednyk, Štěpán Roučka, Petr Dohnal, Radek Plašil, Dieter Gerlich, and Juraj Glosík
Department of Surface and Plasma Science, Faculty of Mathematics and Physics, Charles University, Prague, Czech Republic; radek.plasil@mff.cuni.cz
Received 2017 December 18; revised 2018 February 7; accepted 2018 February 18; published 2018 March 28

$$O^+(^4S) + H_2 \xrightarrow{k_{O+}} OH^+ + H; \quad \Delta H = -0.54\ \text{eV}.$$

The Astrophysical Journal, 854:25 (5pp), 2018 February 10 https://doi.org/10.3847/1538-4357/aaa0d8

2018

Formation of H_2O^+ and H_3O^+ Cations in Reactions of OH^+ and H_2O^+ with H_2: Experimental Studies of the Reaction Rate Coefficients from $T = 15$ to 300 K

Thuy Dung Tran, Serhiy Rednyk, Artem Kovalenko, Štěpán Roučka, Petr Dohnal, Radek Plašil, Dieter Gerlich, and Juraj Glosík
Department of Surface and Plasma Science, Faculty of Mathematics and Physics, Charles University, V Holešovičkách 2, Prague, 180 00, Czech Republic; stepan.roucka@mff.cuni.cz
Received 2017 October 24; revised 2017 December 8; accepted 2017 December 8; published 2018 February 7

$$OH^+ + H_2 \xrightarrow{k_{OH^+}} H_2O^+ + H, \quad \Delta H = -1.02\ \text{eV},$$

$$H_2O^+ + H_2 \xrightarrow{k_{H_2O^+}} H_3O^+ + H, \quad \Delta H = -1.7\ \text{eV},$$

$$H \xrightarrow{CR} H^+ \xrightarrow{O} O^+ \xrightarrow{H_2} OH^+ \xrightarrow{H_2} H_2O^+ \xrightarrow{H_2} H_3O^+.$$

$$H_2 \xrightarrow{CR} H_2^+ \xrightarrow{H_2} H_3^+ \xrightarrow{O} OH^+ \xrightarrow{H_2} H_2O^+ \xrightarrow{H_2} H_3O^+.$$

2018

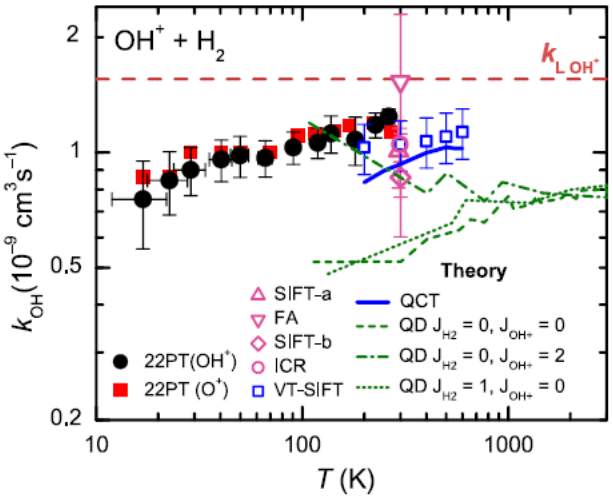

Figure 4. Temperature dependence of the rate coefficient k_{OH^+} of the reaction of OH^+ with normal hydrogen. The averaged data obtained in experiments with OH^+ and O^+ ions injected into the trap are indicated by full circles and squares, respectively. The systematic error due to pressure measurement is 20%. The dashed horizontal line ($k_{L\ OH^+}$) indicates the Langevin collisional rate coefficient. The previous results at 300 K are FA (Fehsenfeld et al. 1967), ICR (Kim et al. 1975), SIFT-a (Jones et al. 1981), and SIFT-b (Shul et al. 1988). The temperature dependencies of k_{OH^+} calculated (QCT) and measured (VT-SIFT) by Martinez et al. (2015) are indicated by the full line and open squares, respectively. The dashed, dotted, and dash-dotted lines represent the phenomenological rate coefficients ($v\sigma$) derived from the theoretical QD cross-sections (Song et al. 2016a) corresponding to different rotational states of reactants as indicated in the legend.

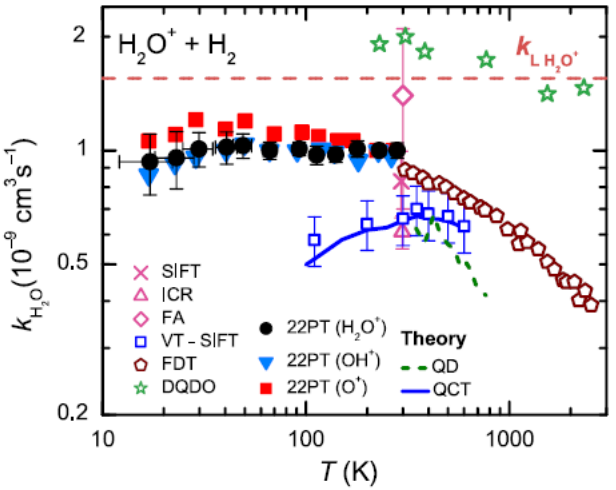

Figure 5. Temperature dependence of the reaction rate coefficient $k_{H_2O^+}$ of the reaction of H_2O^+ with normal hydrogen. The averaged data obtained in experiments with H_2O^+, OH^+, and O^+ ions injected into the trap are indicated by full circles, triangles, and squares, respectively. The systematic error due to pressure determination is 20%. The dashed horizontal line ($k_{L\ H_2O^+}$) indicates the Langevin collisional rate coefficient. The previous results at 300 K are FA (Fehsenfeld et al. 1967), ICR (Kim et al. 1975), FDT (Dotan et al. 1980), and SIFT (Jones et al. 1981). The values measured (VT-SIFT) and calculated (QCT) by Ard et al. (2014) are indicated by the open squares and by the full line (QCT), respectively. The dashed line and stars represent the phenomenological rate coefficients ($v\sigma$) derived from the theoretical QD, and experimental DQDO cross-sections (Song et al. 2016b). The uncertainty of the DQDO results is 50%.

Interstellar Hydrides

Maryvonne Gerin,[1,2] David A. Neufeld,[3,4] and Javier R. Goicoechea[5]

Annu. Rev. Astron. Astrophys. 2016. 54:181–225

First published online as a Review in Advance on July 22, 2016

The *Annual Review of Astronomy and Astrophysics* is online at astro.annualreviews.org

2016

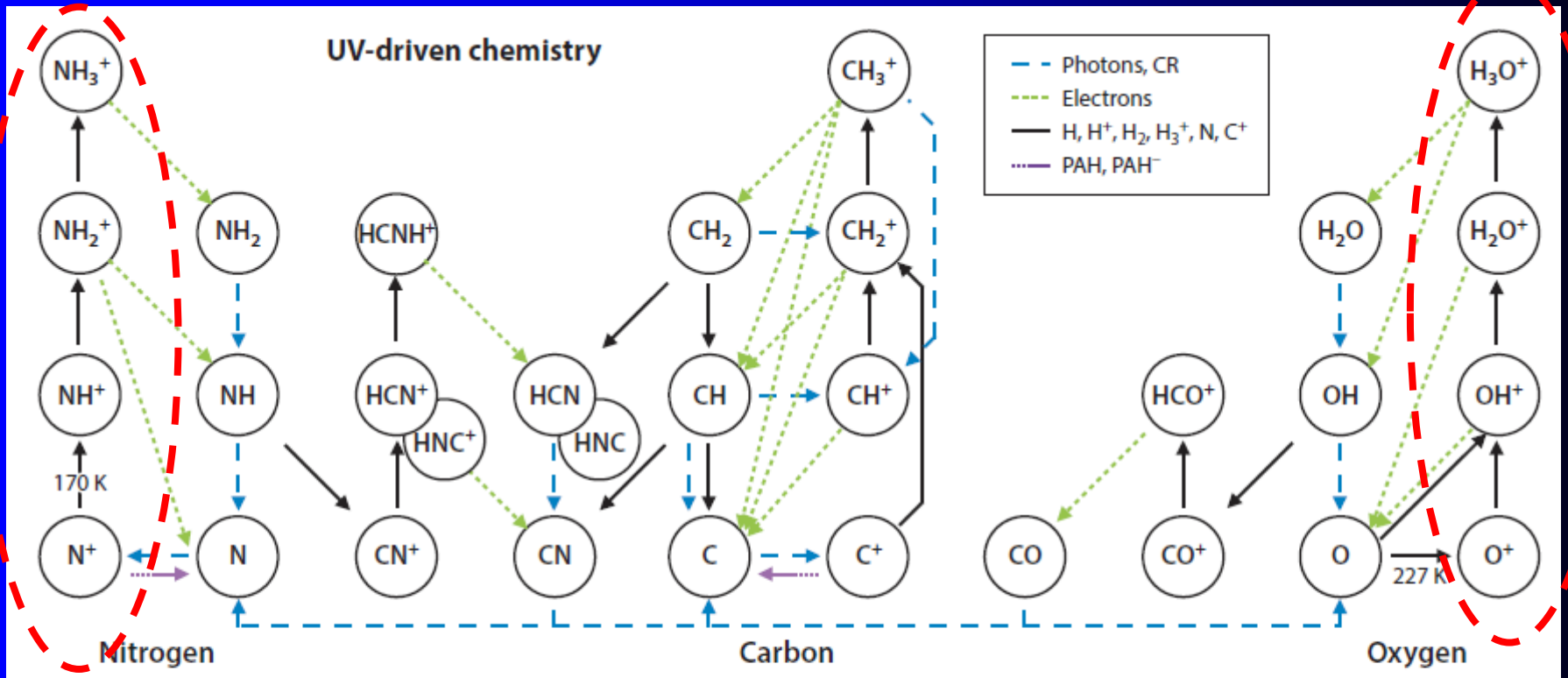

Figure 3

Illustration of the chemical network initiating the carbon, oxygen, and nitrogen chemistry in diffuse cloud conditions ($n_H = 50$ cm^3, $A_V = 0.4$ mag, $\chi = 1$). The black arrows show the reactions with H, H^+, H_2, H_3^+, C^+, and N, with values of the endothermicity for the reaction between N^+ and H_2 and for the charge exchange reaction between O and H^+. Note that CH_2^+ is formed in the slow radiative association reaction between C^+ and H_2. The dashed blue arrows indicate the reactions induced by FUV photons or cosmic rays (CR). Dissociative recombination reactions with electrons are shown with green dotted arrows. Purple arrows show the neutralization reactions on dust grains and polycyclic aromatic hydrocarbons (PAHs). Adapted from Godard et al. (2014) with permission.

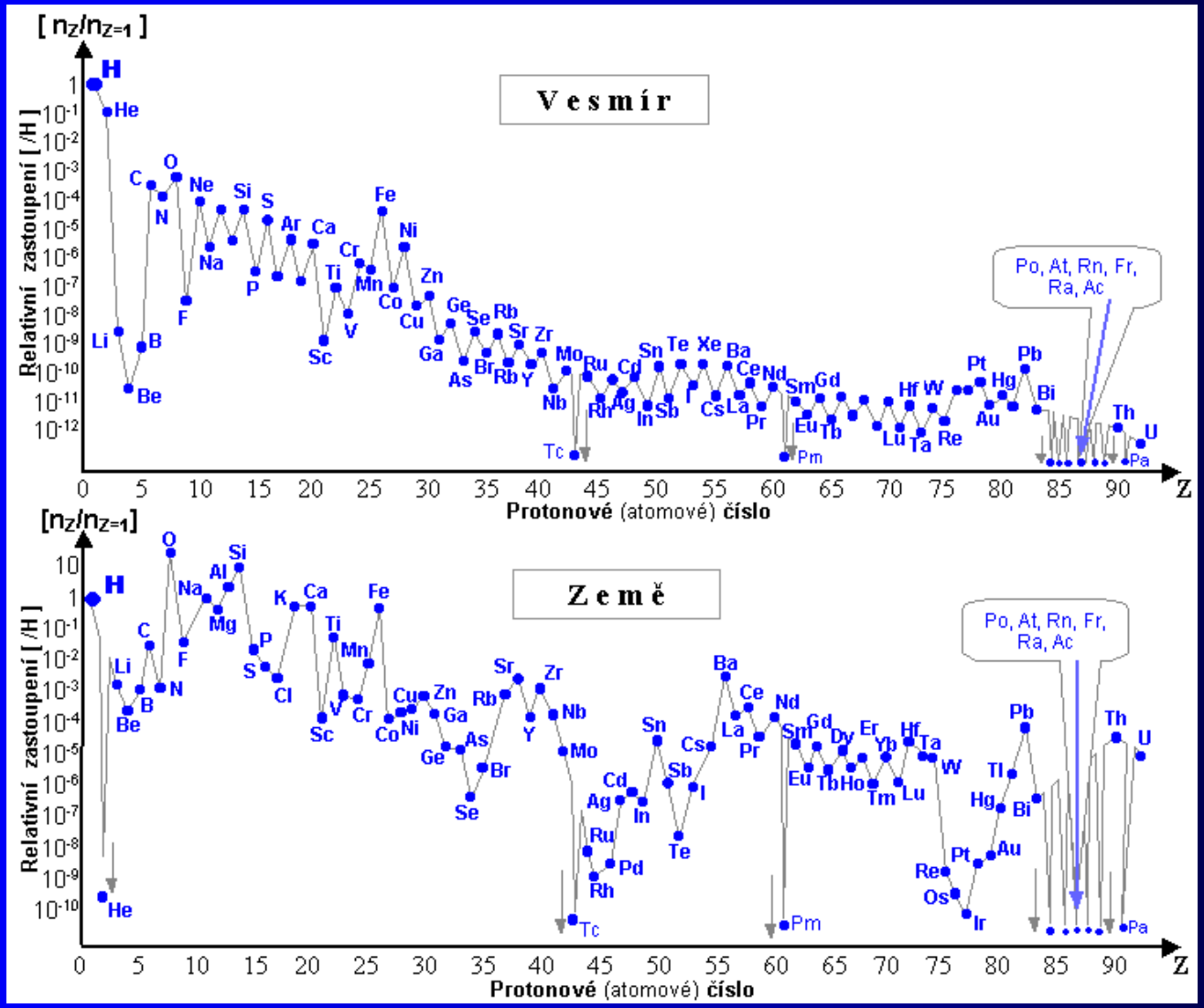

Relativní zastoupení prvků v přírodě v závislosti na jejich protonovém (atomovém) čísle Z, vztažené k vodíku Z=1.
Nahoře: Nynější průměrné zastoupení prvků ve vesmíru. **Dole:** Výskyt prvků na Zemi (v zemské kůře) a terestrických planetách.
Vzhledem k velkému rozpětí hodnot je relativní zastoupení prvků (vztažené k vodíku Z=1) na svislé ose vyneseno v logaritmickém měřítku; to ale může zvláště na horním grafu opticky zkreslit velký rozdíl v zastoupení vodíku a hélia oproti těžším prvkům..